CHARACTERIZATION AND APPLICATIONS OF LIPOSOMES MICROENCAPSULATED BY A NOVEL SUPERCRITICAL FLUID PROCESS

A dissertation

Presented to the faculty of the Graduate School

of Cornell University

In partially Fulfillment of the Requirements for the Degree of

Doctor of Philosophy

by

Wen-Chyan Tsai

August 2015

Characterization and applications of liposomes microencapsulated by a novel supercritical fluid process

Wen-Chyan Tsai, Ph.D.

Cornell University 2015

A novel supercritical fluid (SCF) process, composed of SCF extraction, rapid expansion of a supercritical solution, and vacuum-driven cargo loading based on the Bernoulli principle, was successfully developed for liposomal microencapsulation. It aimed to be a non-toxic and continuous process based on the flow-through design and without usage of any organic solvent. Soy lecithin and cholesterol in a 10:1 mass ratio were dissolved in SC-CO_2 at 20 ± 0.5 MPa and 60 ^{o}C. The phospholipids/cholesterol-laden SC-CO_2 was then passed through a 1000-micron nozzle and immediately mixed with the cargo solution to form liposomes. Liposome size, zeta potential, and encapsulation efficiency (EE) were characterized as functions of the operating parameters. The results showed that the average liposome size varied from 400-500 nm to 900-1200 nm when the pressure was increased from 8.27 to 16.55 MPa. For the liposomal microencapsulation of 0.2 M glucose solution, it was found that the highest EE of 31.6 % was reached at 12.41 MPa, 90 ^{o}C, and 0.25 ml/second of cargo loading rate. Under a confocal laser scanning microscope, the large unilamellar vesicles (LUVs) and multivesicular vesicles (MVVs) accounted for a majority of the liposomal emulsion produced by this novel SCF technique.

Simultaneous microencapsulation of hydrophilic and lipophilic compounds in the integrated liposomes were also conducted for versatile applications of this novel SCF process. The liposomal microencapsulation was run via a 1000-micron jetting nozzle at 12.41 MPa, 90 ^{o}C, and 0.25 ml/second of the cargo loading rate. Vitamins C and E were used as model hydrophilic and

lipophilic compounds, respectively, for characterization and storage-stability evaluation of the SCF-based liposomes. The average vesicle size of vitamins C and E microencapsulated liposomes was 951.02 nm with a zeta potential of -51.87 mV. The EE for vitamin C was 32.97 %, and EE for vitamin E was 99.32 %. During 20 days of storage at 4 ^{o}C, the EEs were found to slightly decrease by 1.76 % and 0.88 %, for vitamins C and E, respectively. The simultaneous microencapsulation of hydrophilic and lipophilic compounds in the liposomes was successfully demonstrated using this SCF process.

BIOGRAPHICAL SKETCH

Wen-Chyan Tsai was born in Taiwan. He earned his bachelor degree in Animal Science, National Taiwan University. During his undergraduate study, he was very interested in the development of new dairy and meat products. After his two-year military service, he applied for Food Science in Cornell University and got enrolled in M.S/Ph.D program. He chose Food Engineering as his major field with Food Chemistry and Hotel Administration as his minor fields. After he passed the exam of doctoral candidacy in 2010, he took a temporary leave back to Taiwan and worked as a R&D manager in Quaker Oats Company. During the time, he also got married and has a son. In the 2012 summer, he resumed his doctoral research in Food Science, Cornell University. His study has focused on development of a novel and nontoxic supercritical fluid process for liposomal microencapsulation.

ACKNOWLEDGEMENTS

I would like to thank my advisor, Professor Syed S. H. Rizvi, for his patience and careful instruction during my doctoral research. This has been a precious experience to me. Creating a new technology is challenging. However, I feel so fulfilled and confident to have overcome many of the difficulties and limits inherent in such undertakings with sufficient help from my advisor.

I also would like to thank my Special Committee members, Professor Rui Hai Liu and Professor Mary H. Tabacchi. I have undergone a diversified study at Cornell University with the help of their knowledgeable guidance and instructions.

I do appreciate the full support from my lab colleagues and Food Science Department. I could achieve my goals because of your encouragement.

Last but not least, I would like to thank my family. With your unconditional love, I could finish my study. I am grateful for my parents' selfless support during my doctoral study. Especially to my wife and son, thank you so much for giving me such a wonderful life in Ithaca. We will bond together and steadily sail to the unknown future.

TABLE OF CONTENTS

LIST OF FIGURES

LIST OF TABLES

Chapter 1: Literature review-liposomal microencapsulation using the conventional methods and novel supercritical fluid processes

1.1. Abstract

Liposomes are spherical vesicles consisting of one or multiple phospholipid bilayers separating an inner aqueous core from the outer aqueous medium. They possess the versatility to encapsulate hydrophilic compounds in the core and lipophilic compounds inside the phospholipid bilayers. Organic solvent residue has always been a concern in liposomal microencapsulation produced by conventional methods, such as thin film hydration, reverse phase evaporation, and membrane extrusion. Dense gas techniques using supercritical carbon dioxide as the phospholipid-dissolving agent can provide an eco-friendly solution for the reduction or avoidance of organic solvent use. In this introduction, conventional and innovative dense gas processes of liposomal microencapsulation are described and compared. Comprehensively understanding the current progress of the supercritical fluid techniques for liposomal microencapsulation will be helpful for the development of a non-toxic continuous process of liposomal formation in the pharmaceutical and related industries where harm from toxicity of organic solvents is always a concern.

Keywords: Supercritical carbon dioxide, Supercritical fluids, Rapid expansion of supercritical solutions, Liposomes, Microencapsulation, Drug delivery

1.2. Introduction

Liposomes are self-assembled spherical vesicles with one or more phospholipid bilayers separating the inner aqueous environment from the outer aqueous medium. It has long been used as a model for biological membrane study due to its similarity to real cell membrane. The compound of interest was securely encapsulated in the inner aqueous core surrounded with one or more phospholipid bilayers [1-3]. Based on the size and lamellarity, liposomes can be categorized into four types: small unilamellar vesicles (SUV), large unilamellar vesicles (LUV), multilamellar vesicles (MLV) and multivesicular vesicles (MVV), as shown in Figure 1.1. The liposomal size of SUVs varies from 20 to c.a. 100 nm. The sizes of LUVs, MLVs, and MVVs range from a few hundred nanometers to microns. The thickness of one phospholipid bilayer has been reported to be approximately 4 to 5 nm [4].

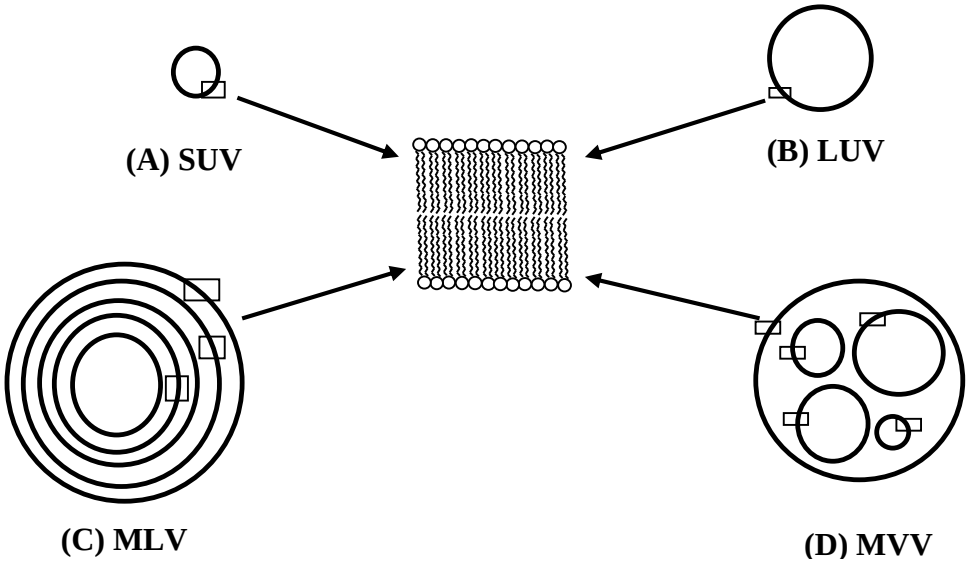

Figure 1.1 Different types and lamellarity of liposomes.
SUV: small unilamellar vesicles; LUV: large unilamellar vesicles; MLV: multilamellar vesicles; MVV: multivesicular vesicles.

Interest in liposomes is greatest in the pharmaceutical industry, due to the solubility improvement, controlled release and targeted delivery of the drugs [5-9]. Liposomal microencapsulation has recently been applied in food industry for the antioxidant, enzyme and nutraceutical encapsulations [2, 10, 11]. LUV is always preferred due to its higher encapsulation efficiency, simpler process and better stability [12]. By adding cholesterol, surfactants, or carbohydrates into the phospholipid bilayer, the rigidity, fluidity and permeability can be modified for specific purposes [13-15].

Traditionally, liposomes are prepared by thin-film hydration (TFH, the Bangham method), reverse phase evaporation vesicles (REV), and membrane extrusion. Nowadays, due to the concern of organic solvent toxicity, several new techniques have been attempted to reduce or even completely avoid the use of organic solvents in the liposomal microencapsulation, including microfluidics, rapid expansion of supercritical solutions (RESS), supercritical reverse phase evaporation (SCRPE) and several dense gas processes [16-22].

The salient features of different liposomal microencapsulation methods are summarized in Table 1.1. Supercritical carbon dioxide (SC-CO_2) is a non-toxic density-adjustable fluid with similar solvent behavior to hexane [23, 24]. Its moderate critical pressure (7.4 MPa) and low critical temperature (31.1 ^{o}C) make SC-CO_2 an ideal candidate for biomaterial processing. The conventional and innovative techniques of liposomal formation will be compared and described in this review.

Table 1.1. Comparison of conventional and innovative methods of liposomal microencapsulation

Methods	Organic solvent	Process time	Process type	Liposomal size
Conventional				
TFH	Yes	> 1 hour	Batch	Variable
REV	Yes	2 - 3 hours	Batch	Variable
Membrane extrusion	Yes	1 - 2 hours	Batch	Variable
Innovative				
Microfluidics	Yes	15 - 30 minutes	Semi-continuous	50 - 100 µm
Dense gas				
RESS-cosolvent	10-20 %	15 - 30 minutes	Semi-continuous	200 - 250 nm
Improved RESS	Yes	30 minutes	Batch	< 1 µm
SCRPE	No	2-3 hours	Batch	200 nm
DESAM	Yes	45 - 60 minutes	Continuous	100 - 400 nm
CFN	Yes	20 - 40 minutes	Batch	300 nm
CAS	Yes	45 - 60 minutes	Continuous	10 - 100 µm
PGSS	Yes	60 minutes	Continuous	1 - 5 µm
DELOS-SUSP	Yes	30 - 60 minutes	Batch	100 – 150 nm

Notes:
TFH: thin film hydration
REV: reverse phase evaporation vesicles
SCRPE: supercritical reverse phase evaporation
DESAM: depressurization of an expanded solution into aqueous media
CFN: critical fluid nanosome
CAS: continuous antisolvent process
PGSS: particles from gas saturated solutions
DELOS-SUSP: depressurization of an expanded liquid organic solution-suspension

1.3. Conventional methods of liposomal microencapsulation

1.3.1. Thin film hydration

Thin film hydration (TFH; the Bangham method) was created as a simplified liposomal microencapsulation technique [25]. Basically, an appropriate quantity of the pure or mixed phospholipids with other lipophilic compounds is dissolved in chloroform followed by the organic

solvent evaporation in a rotary vacuum evaporator or nitrogen blowing. After the thin lipid film is formed on the bottom of the evaporation flask, a certain quantity of the hydrophilic cargo solution is then added into the flask and mixed with the phospholipid film by vortex shaking or sonication to form liposomal microcapsules. Liposomes prepared by the Bangham method are usually mutilamellar vesicles (MLVs) with relatively low encapsulation efficiency compared to the large unilamellar vesicles (LUVs) made by membrane extrusion [26] and reverse phase evaporation [27].

Some membrane modifications created a structural change on the liposomal bilayers produced with the Bangham method [14]. It was found that the liposomes prepared with dipalmitoylphosphatidylcholine (DPPC) / stearylamine (SA) in the ratio of 9.5 to 0.5 converted the MLVs into LUVs. The encapsulation efficiency of the resulting LUVs consisting of the DPPC / SA phospholipid bilayer was ten times higher than that of the MLVs assembled by the DPPC multilayers [14].

1.3.2. Reverse phase evaporation vesicles

Reverse phase evaporation vesicles (REV) was first reported by Szoka and Papahadjopoulos in 1978. In the REV process, phospholipids are first dissolved in an organic solvent with a low boiling point, such as chloroform, diethyl ether, or methanol [13, 28]. An aqueous solution containing the active compounds is added into the organic phase to form an emulsion by vortex shaking or low energy sonication. At this step, the emulsion stays in the water-in-oil or reversed micellar system. The hydrophilic domain of the polar lipids attaches to the inner aqueous droplet containing the targeted compound while the fatty acid chains interact with the continuous organic phase. During the evaporation under vacuum, the organic solvent is gradually removed and the continuous phase is converted from the oil phase to the water phase. Eventually, the double

emulsion (water in oil in water, W/O/W) is formed as the desired liposome. Although the encapsulation efficiency is relatively high compared to the other methods, a complete removal of the organic solvent is often challenging [27].

The calcium cations were encapsulated in liposomes prepared with egg phosphatidyl choline (EPC) by the REV method [29]. The liposomes were LUVs with the droplet size ranging from 0.25 to 1.8 μm and 63% encapsulation efficiency. These calcium-encapsulated liposomes were then used as meat tenderizer. The effect of the liposomal protection of β-D-glucosidase against the cupric ion was evaluated [30]. The liposomes composed of L-α-dimyristoyl-phosphatidylcholine (DMPC) / cholesterol / diacetyl phosphate (DCP) in the ratio of 7:2:1 were prepared with the REV method. β-D-glucosidase encapsulated in the REV liposome reached 20% encapsulation efficiency and presented 2 to 3 fold higher enzymatic activity than the unencapsulated glucosidase during 20 days of storage .

1.3.3. Membrane extrusion

Membrane extrusion is a homogenization process used to narrow the size distribution of the final liposomal emulsion. Sometimes, it is a follow-up process after the liposomes are prepared by thin film hydration or REV to selectively obtain the resulting liposome with the desired size. The dispersed phase containing large liposomes is forced to pass through a membrane or filter with a uniform pore size, generating a homogenous population of small vesicles. This is because the forced passage through the pores of the membrane or filter exerts sheer force that causes a rupture of the liposomal bilayers, followed by a rapid resealing to form the smaller liposomal sizes [12].

The hemoglobin (Hb)-encapsulated liposome (LEHb) was produced to evaluate its feasibility as an oxygen-carrying blood substitute [31]. The lipid film consisted of 5% dimyristoyl-

phosphatidylcholine (DMPC), 42% dimyristoylphosphatidylglycerol (DMPG), 40% cholesterol, 2% α-tocopherol, 10% PEG-DSPE-2000, and 1% K^+ ionophore. The plain Hb solution (30 g / dL) and the mixed solution containing the actin (1 mg / mL) and Hb (30 g / dL) were respectively used in the extruded microencapsulation. The liposomes were extruded 25 times through the polycarbonate membranes with the pore sizes of 400 and 600 nm, respectively. The thin disk-shaped liposomes containing the actin / hemoglobin solution were observed in sizes ranging from 136 to 140 nm, while the spherical liposomes containing the plain hemoglobin were found in sizes varying from 115 to 142 nm. Both of the liposomal types showed similar oxygen affinity and c.a. 30% encapsulation efficiency.

1.3.4. Sonication

Sonication is also used widely for the preparation of liposomes. This is usually a secondary process after TFH, REV and membrane extrusion for better uniformity of the liposomal size distribution. Lipid suspensions are mixed using acoustic energy from a bath or a probe tip sonicator. The induced pressure breaks up the larger multilamellar vesicles into smaller vesicles that may be either unilamellar or multilamellar in configuration [32]. Bath sonication is preferably chosen for preparation of SUVs [33]. Frequency, power input and sonication time are the main factors that control the size distribution of the final product.

Size distribution of the liposomes prepared with L-α-dilauroyl phosphatidylcholine (DLPC) was evaluated for the effects of frequency and power input of the bath sonication [34]. 43, 133 and 480 KHz of frequencies and 8 and 18 W of the powers were employed for the size characterization of the DLPC liposomes. Their results suggested that lower frequencies (43, 133 KHz) could reduce the liposomal size faster than higher frequency (480 KHz). The short-time and high-power

sonication was found to be more efficient on the liposomal size reduction than the long-time and low-power sonication. 50 to 70 nm of the liposomal size distribution was reached in the optimal condition.

1.4. Innovative methods of liposomal microencapsulation

1.4.1. Microfluidic microencapsulation

Liposomal monodisperse, double emulsions generated from a glass microcapillary device was proposed by Shum *et al*. (2008), as shown in Figure 1.2 [20, 35]. In Figure 1.2 (A), the device assembled with a round 1-mm O.D. glass capillary tube from the left side coaxially nested within a 1-mm I.D. square glass tube. A tapered cylindrical capillary tube with a tip (40 to 60 μm I.D.) was coaxially inserted from the right side into the left round tube. The inner aqueous fluid containing 0.02% (w / v) of 1 μm yellow green sulfate-modified microspheres was pumped into the tapered capillary tube and through the tip from the right side. The middle fluid containing 5-10 mg / ml of 1,2-dipalmitoyl-sn-glycerol-3-phosphocholine (DPPC) dissolved in toluene and chloroform (1.8 : 1 of volume ratio) was pumped alongside the outer tapered capillary tube in the same direction as the inner fluid from the right side. Both solutions began to mix at the exit orifice inside the round glass tube to form the liposomes. The outer fluid of the aqueous buffer was coaxially pumped through the area between the round glass capillary and square tube from the left side. These three fluids were forced to mix with each other around the exit orifice for the final emulsion.

By adjusting the flow-rate ratio of the inner and middle fluids to 4:1, it was observed that the uniformed monodisperse liposomes were formed within the sizes ranging from 20 to 150 μm. It was also found that the orifice diameter of the left round capillary tube ranging from 20 to 200

μm could supportively control the uniformity of liposomal droplet size [20, 35]. Figure 1.2 (B) demonstrates the microfluidic microencapsulation of liposomes. The morphology of the monodisperse liposomes observed under a confocal laser scanning microscope (CLSM) is presented in Figure 1.2 (C).

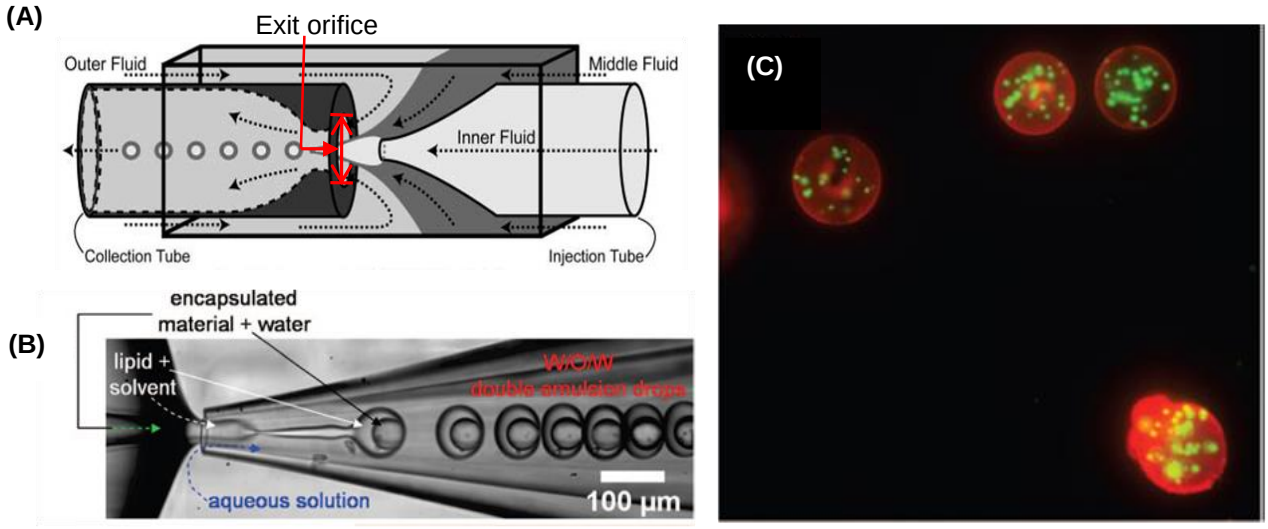

Figure 1.2. Liposomal formation conducted in the microfluidic microencapsulation (Utada et al., 2005; Shum et al., 2008): (A) The configuration of a glass microcapillary device; (B) The process of making the W/O/W double emulsion; (C) CLSM images of the DPPC liposomes encapsulating fluorescent latex microspheres.

The liposomal bilayers were stained with 0.02 mol % Texas red and emitted red fluorescence at 615 nm of emission wavelength. The microspheres displayed yellow green color in the cores of the liposomes surrounded by red phospholipid layers. This method was claimed by the authors to have improved size control during liposomal formation and reduced usage of organic solvents.

1.4.2. Dense gas techniques of liposomal microencapsulation

Dense gas techniques of liposomal microencapsulation are derived from rapid expansion of supercritical solutions (RESS). The principles and applications of the RESS process are briefly

described in Figure 1.3. Supercritical fluids (SCFs) are chosen as the phospholipid-dissolving medium in the dense gas methods for liposomal formation, in order to reduce or avoid the usage of organic solvents. SC-CO_2 is extensively chosen due to its nontoxicity, incombustibility, low critical temperature (31.1 ^oC) and moderate critical pressure (7.4 MPa). It is ideal for heat labile compounds to prevent from oxidative damage during thermal processing. This technique was first demonstrated in 1996 [16] and improved later [36]. When SC-CO_2 containing phospholipids is released through a small orifice and simultaneously mixed with an aqueous cargo solution, rapid pressure drop results in the desolvation of the phospholipids from CO_2, forming one or several phospholipid layers around the aqueous droplets. Depending on the process parameters, such as the pre-expansion pressure, orifice size, solubilities of the coating materials in SC-CO_2, it is feasible to control the uniformity of the final liposomal size. 5 to 10% of ethanol may be added into the supercritical solution to improve the solubility of phospholipids in SC-CO_2.

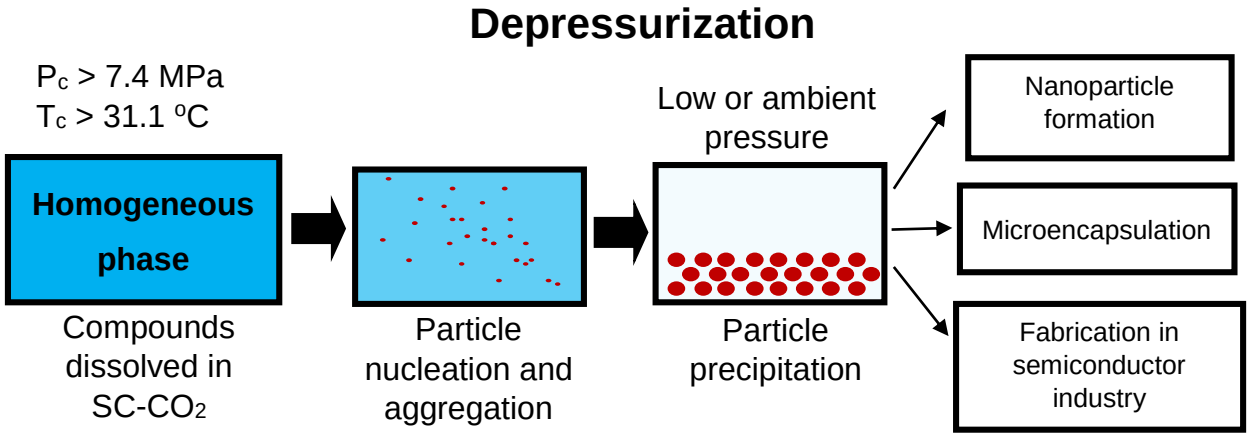

Figure 1.3. Principles and applications of a typical rapid expansion of supercritical solutions (RESS). P_c: critical pressure; T_c: critical temperature.

Liposomes ranging from the submicron to micron levels can be produced with different shapes, such as sphere and ellipsoid, as shown in Figure 1.4 [37]. The issue of solvent residue in the conventional liposomal microencapsulation can be addressed by the SCF techniques,

because SC-CO_2 completely evaporates from the final emulsion into the air at the ambient pressure and temperature. Adopting dense gas methods in the liposomal microencapsulation is limited due to the high fragility of the liposomes and low encapsulation efficiency. However, no toxic residue is the most desirable benefit of these processes. The current progress includes RESS-related techniques, supercritical reverse phase evaporation (SCREP), and critical fluid nanosome (CFN) process. Several other promising dense gas methods for liposomal microencapsulation are also described in this review.

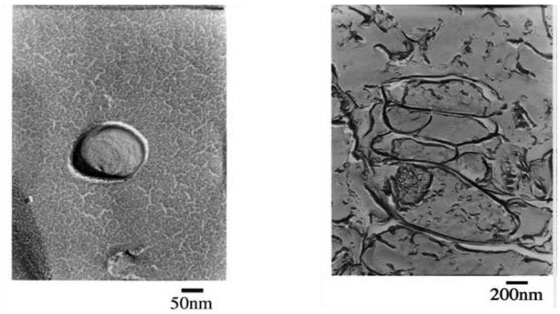

Figure 1.4. Structural images of liposomes produced using the supercritical reverse phase evaporation (SCRPE) method (Imura et al., 2002).

1.4.2.1. The RESS-coslovent method

The RESS-coslovent technique was attempted for liposomal microencapsulation of the water soluble fluorescein isothiocyanate (FITC)-dextran [17]. The schematic diagram is shown in Figure 1.5. 1-palmitoyl-2-oleoylphosphatidylcholine (POPC) and cholesterol in the molar ratio of 7 to 3 were weighed in the cartridge guard column. SC-CO_2 was introduced into the high pressure recycling system up to 25 MPa at 60 ^oC, with 4.8% (v /v) addition of absolute ethanol as co-solvent. Ethanol and SC-CO_2 were homogenously mixed by the dynamic mixer before entering the recycling system. Without this ethanol addition, it was observed that no liposome was formed due

to very low solubility of POPC in SC-CO_2. 30 minutes of the recycling period was required to reach the saturated solubilities of POPC and cholesterol in SC-CO_2.

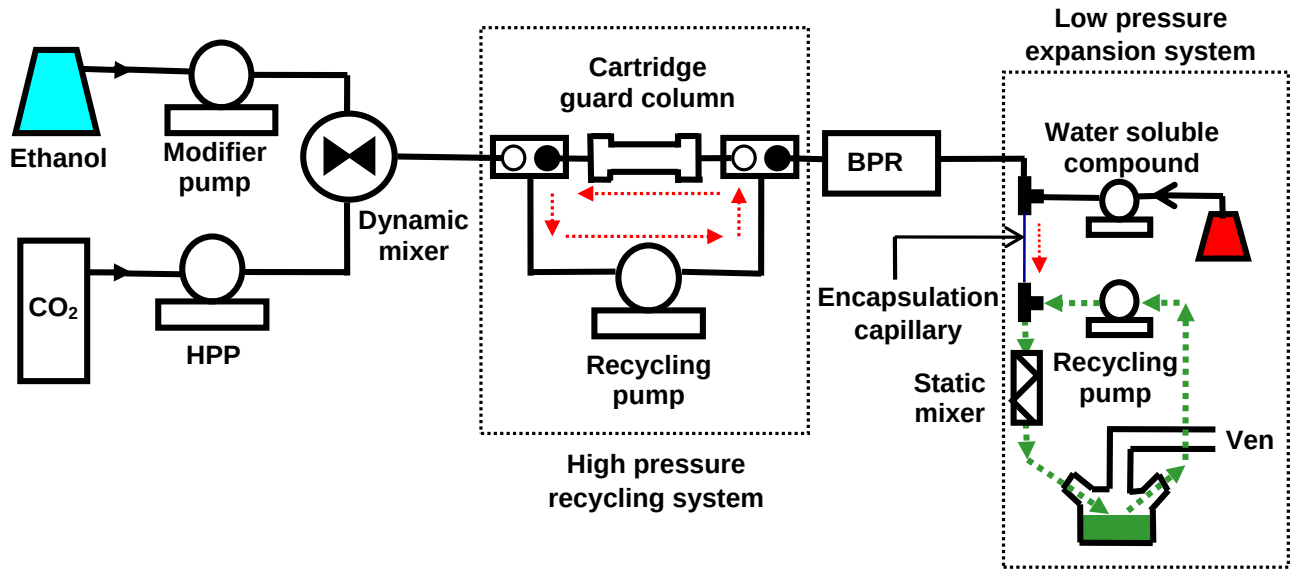

Figure 1.5. Schematic diagram of the RESS-coslovent process (Frederiksen et al., 1997).

The SC-CO_2 containing POPC and cholesterol was introduced into the lower pressure expansion system by a back pressure regulator (BPR) controlling the flow rate at 5 ml per min. The FITC-dextran solution was pumped into encapsulation capillary (0.5 mm I.D.) at 40 µl per min.

The results indicated only 1% encapsulation efficiency. However, the encapsulation efficiency was significantly raised to 15% when the capillary inner diameter was reduced from 0.5 mm to 0.25 mm. A static mixer was inserted between the capillary and collection flask to suppress foam formation in the liposomal emulsion. The final emulsion in the expansion system was recycled through the static mixer to completely recover all liposomes. The multilamellar liposomes produced in this condition had the size distribution between180 and 200 nm with medium polydispersity.

1.4.2.2. The improved RESS process

The liposomal microencapsulation of atractylone was conducted using the improved RESS process [38]. Atractylone was extracted from a Chinese herb, Baizhu, which is claimed to suppress tumor growth and protect the liver and lung. Generally, the liposome is applied to secure hydrophilic compounds in the inner aqueous core. In their study, the lipophilic atractylone was incorporated in the phospholipid bilayers of the liposomes. The schematic diagram of the improved RESS system is shown in Figure 1.6. The system mainly includes a high pressure pump, reactor and collector.

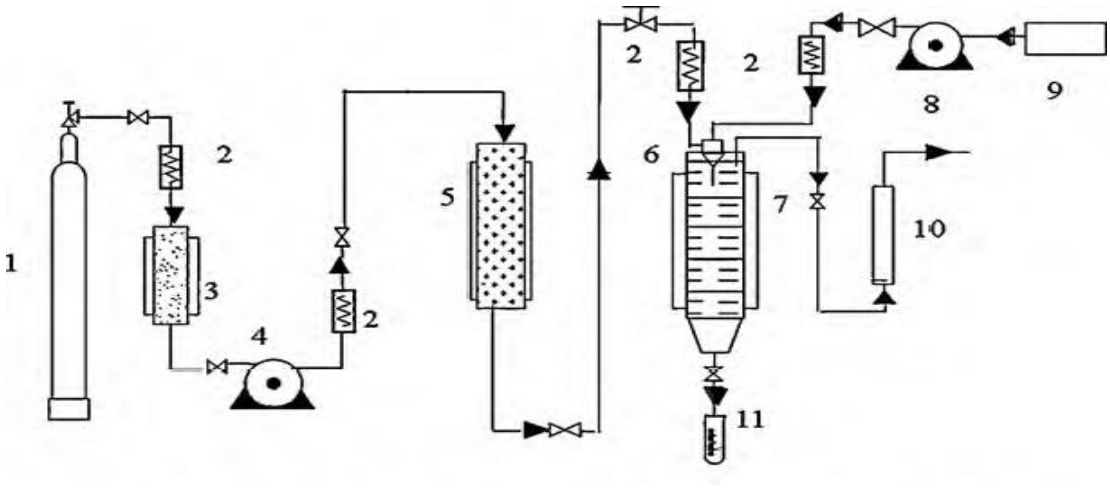

Figure 1.6. Schematic diagram of liposomal microencapsulation by the improved RESS process (Wen et al., 2010). 1-cylinder; 2-heat exchanger; 3-refrigerating machine; 4,8-syringe pump; 5-reactor; 6-coaxial injector; 7-collector; 9-storage tank; 10-rotameter; 11-volumetric cylinder.

For liposome preparation, phosphatidylcholine (PC) was mixed with cholesterol in a 3:1 ratio. Then the coating material was blended with atractylone in a 20:1 ratio. The mixture was dissolved in ethanol and placed in the reactor. SC-CO_2 was then introduced into the reactor. Two hours of phase equilibrium at desired conditions were required for this microencapsulation. SC-CO_2 containing the PC / cholesterol / atractylone mixture was sprayed into the PBS buffer (pH 7.2) in

the collector by a coaxial injector to produce liposomes. It was found that 83.1% of the highest encapsulation efficiency could be reached at the operating conditions of 30 MPa, 338 K and 15% ethanol as cosolvent. The average size of the atractylone-containing liposomes was measured to be 506.5 nm [39].

The liposomal microencapsulation of rose essential oil was also conducted using the improved RESS system. Three surfactants, Tween 80, deoxycholic acid sodium (DAS) and Poloxamer 188, were evaluated for their stabilizing effects [40]. PC was mixed with cholesterol in a 3:1 ratio. Then the coating material was blended with rose essential oil in a 20:1 ratio. The PC / cholesterol / rose essential oil mixture was dissolved in ethanol and placed in the reactor. SC-CO_2 was then introduced into the reactor. Two hours of phase equilibrium were required for this microencapsulation. SC-CO_2 containing the lipid mixture was sprayed into the PBS buffer (pH 7.2) containing the three surfactants, respectively. For the optimal pre-expansion conditions, it was found that 30 MPa, 338 K and 15% ethanol as cosolvent contributed to 70.33% of the highest encapsulation efficiency. The results showed that Poloxamer 188 (5% w/w) could improve the encapsulation efficiency up to 89.46% with 94 nm of average liposomal size [40].

1.4.2.3. Supercritical reverse phase evaporation (SCRPE)

SCRPE is similar to the REV method for liposomal microencapsulation. The only difference is that SC-CO_2 is substituted for the organic solvent as the solution medium. It is a batch process and SC-CO_2 is used as the sole phospholipid-dissolving agent [41]. The microencapsulation system of SCRPE is depicted in Figure 1.7. In this process, the phospholipids were sealed in the volume-variable view cell followed by the SC-CO_2 pressurization until the desired pressure was reached between 12 and 30 MPa. The operating temperature was set at 60 ^{o}C. After 20 minutes of

phase equilibrium, the adequate amount of the aqueous D-(+)-glucose solution (0.2 M) was slowly introduced into the view cell via a HPLC pump at 0.05 ml per minute. SC-CO_2 was then rapidly released to produce a homogenous liposomal dispersion.

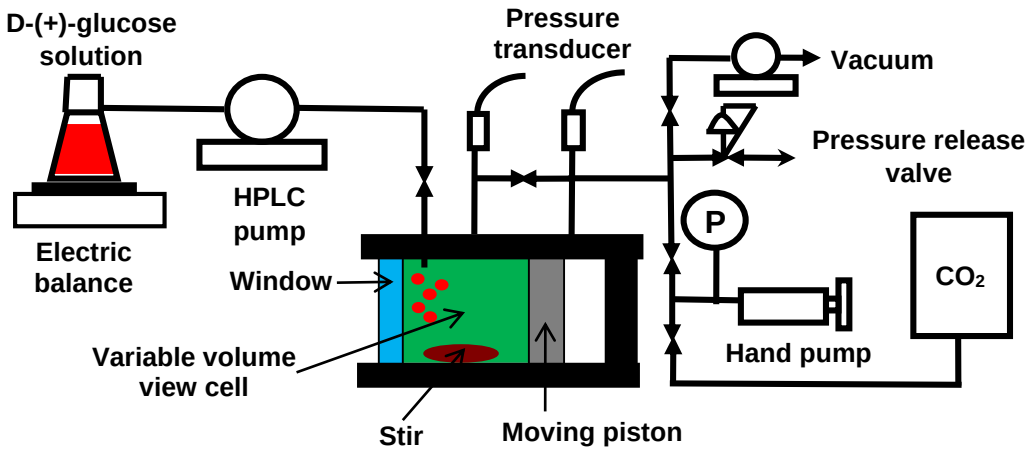

Figure 1.7. Schematic diagram of the SCRPE liposomal microencapsulation process (Otake et al., 2001). P: pressure gauge

Under a transmission electron microscope (TEM), the soy lecithin containing 95% of PC formed large unilamellar vesicles (LUVs) with the liposomal size ranging from 0.2 to 1.2 μm. Using lecithin containing 32% of PC produced the small multilamellar liposomes within 0.1 to 0.25 μm of size distribution. 6.5% of ethanol addition in SC-CO_2 as cosolvent enhanced the solubility of phospholipids, mainly PC, resulting in higher encapsulation efficiency up to 10%. In their study on liposomes produced with L-α-dipalmitoylphosphatidylcholine (DPPC) and L-α-dioleoylphosphatidylcholine (DOPC), varying the operating pressure had a significant influence on the liposomal size distributions of the final emulsions. The heterogeneous phase of the glucose solution / SC-CO_2 / phospholipid system below 20 MPa created larger water / CO_2 droplet before the phospholipid microencapsulation than the homogenous phase above 20 MPa. As a result, it was found that the droplet size of the liposomes prepared at pressures below 20 MPa was larger

than those above 20 MPa [42]. A depressurization rate of SC-CO_2 below c.a. 1 MPa per min assured larger liposomal size and higher encapsulation efficiency [21].

Liposomal microencapsulation with SCRPE was also investigated in regard to the molecular structural effect of various phospholipid combinations from soybean lecithin. It was found that the zwitterionic structure of PC can form a bulky structure of the phospholipid bilayer compared to the denser bilayer formed by phosphatidylethanolamine (PE), phosphatidylinositol (PI) and phosphatidic acid (PA). This feature of PC contributed to the efficient formation of LUVs and a higher encapsulation efficiency for hydrophilic substances [37]**.**

1.4.2.4. Depressurization of an expanded solution into aqueous media) process for bulk production of liposomes (DESAM)

DESAM was developed for bulk liposomal microencapsulation featuring the reduced solvent residue of less than 4% (v/v) and moderate operating pressure between 4 and 5.5 MPa [22]. As shown in Figure 1.8, the DESAM system mainly consists of the expansion and vesicle-generating vessels. 1,2-Distearoyl-sn-glycero-3-phosphatidylcholine (DSPC) and cholesterol in the ratio of 9 to 1 were dissolved in ethanol or chloroform with 20 mg / ml of the solutes' concentrations. The DSPC / cholesterol solution was then injected into the expansion chamber followed by pressurization of CO_2 up to 4 and 5.5 MPa at 22 ^oC for chloroform and ethanol, respectively. During this step, the solution in the chamber was expanded with rising pressure. 10 minutes were required for the ternary phase equilibrium of the lipids, CO_2 and solvent. 50 ml of the aqueous medium containing pure water or TRIS-buffered saline solution (20 mM TRIS, 0.9% NaCl and pH 7.4) was placed in the vesicle formation chamber (VFC) and heated up to 75 ^oC for liposomal formation. In each run, the lipid-laden CO_2 was carried from the expansion chamber to VFC

through a stainless tubing nozzle (0.9 cm length and 178 μm I.D.) by opening the metering valve between the chambers. The DSPC / cholesterol mixture was then bubbled into and mixed with the aqueous medium to form liposomes in VFC.

It was found that the liposomes produced from the ethanol solution had average effective diameters ranging from 119 to 207 nm. The average liposomal diameter increased to 387 nm from the chloroform solution. As shown in Figure 1.9, it was observed that most of the liposomes had the unilamellar structure and spherical shape under TEM visualization. After eight months of storage at 5 ^{o}C, the liposomal emulsion was still stable with the average effective diameter and polydispersity increasing by only 13% and 7%, respectively.

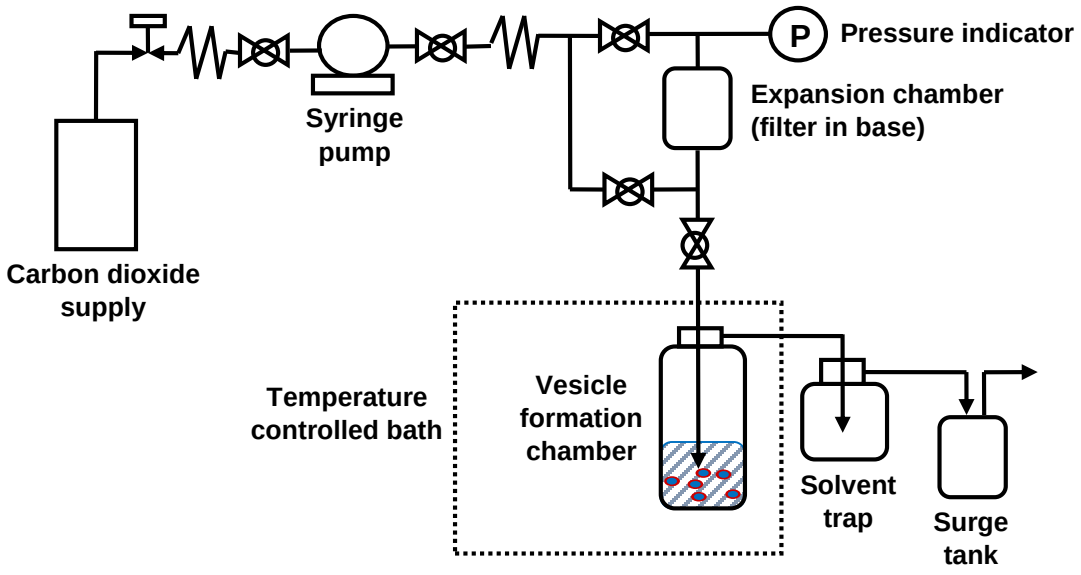

Figure 1.8. Schematic diagram of the DESAM process (Meure et al., 2009).

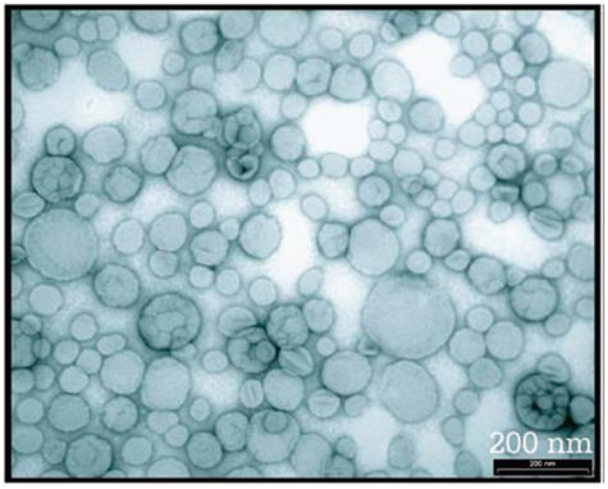

Figure 1.9. TEM image of liposomes produced in the DESAM process (Meure et al., 2009).

1.4.2.5. The critical fluid nanosome (CFN) process

The injection and decompression techniques were the first two methods in success of liposomal microencapsulation using supercritical fluid [16]. In the injection technique, a mixture of phospholipids, organic cosolvent and compressed gas was injected through a nozzle into an aqueous solution. In the decompression process, phospholipids, organic cosolvent, compressed gas and aqueous solution were mixed and then depressurized through a nozzle to form liposomes. In the injection method, the compressed phase was sprayed into the aqueous solution. Whereas in the decompression method, the aqueous phase was incorporated in the compressed phase and sprayed into the air. The major difference between these two processes was the incorporation of aqueous medium. The rate of depressurization had an influential effect on the liposomal size. It was reported that the injection and decompression methods were able to produce sterile and pharmaceutical grade liposomes with a narrow size distribution between 100 and 300 nm.

The critical fluid nanosome (CFN) process combined the injection and decompression techniques [19]. As shown in Figure 1.10, the critical fluid nanosome (CFN) process is composed of the high-pressure mixing and low-pressure trapping assemblies. The phospholipids, cholesterol

and other lipophilic compounds were loaded in the solid chambers 1 and 2. The co-solvent, such as ethanol, was introduced into SC-CO_2 through the injection port. The SC-CO_2 / ethanol fluid was then mixed with the coating materials in the solid chambers by the circulation pump with sufficient equilibrium time at 28 MPa and 60 ^{o}C for ensuring good mixing among the fluid and coating materials. The resulting fluidic mixture was then decompressed via a back pressure regulator (BPR) and tubing nozzle (0.5 ~ 0.06 mm I.D.) dipped in the phosphate-buffered saline or other biocompatible solution, such as cytochrome-C and paclitaxel. Nanosomes (nano-sized liposomes) were formed when the phospholipid-laden SC-CO_2 bubbled into the aqueous medium.

The results suggested that the size distribution of the nanosomes varied from 100 nm to 4 μm. The majority of the nanosomes was less than 300 nm. The photomicrograph of the phospholipid nanosomes encapsulating cytochrome-C is shown in Figure 1.11. No significant size change and bacterial growth were observed for the nanosomes made of egg yolk phosphatidylcholine (EPC) after six months of storage at 4 ^{o}C. The latter observation might reflect the capability of the CFN process to impart end-product sterility.

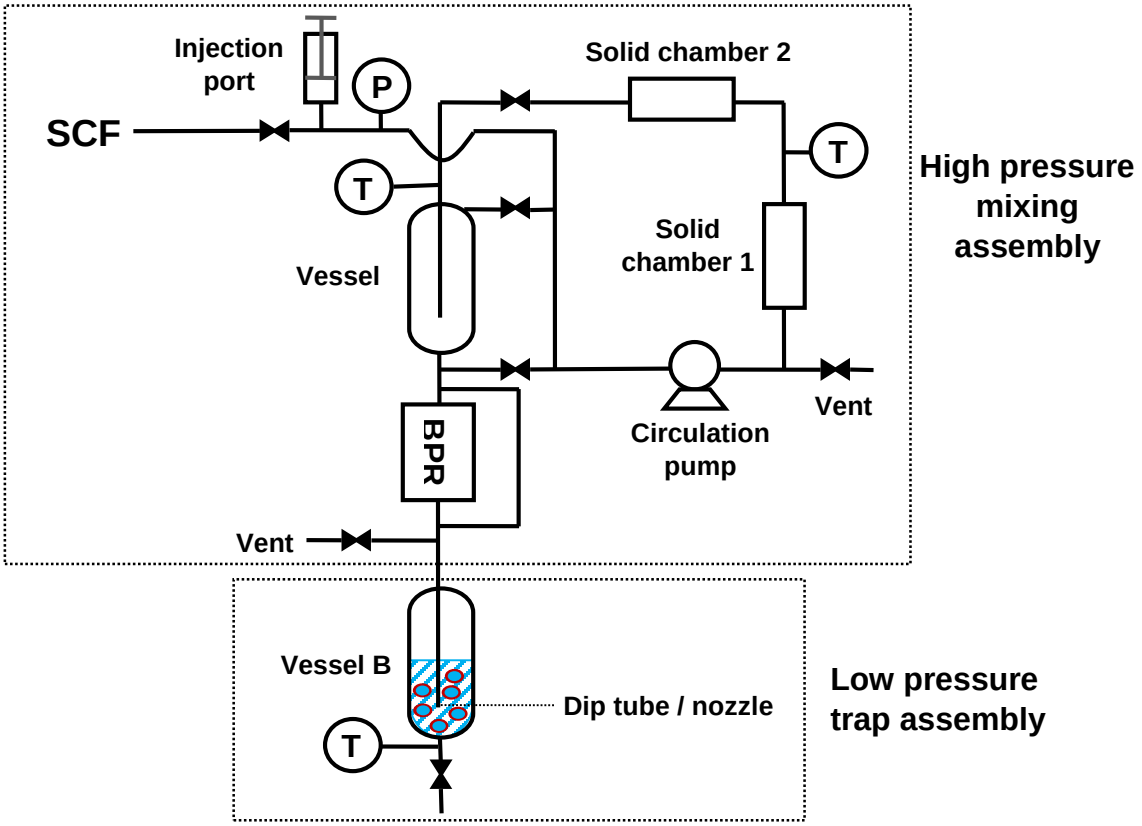

Figure 1.10. Schematic diagram of the critical fluid nanosome (CFN) apparatus (Castor, 2005).

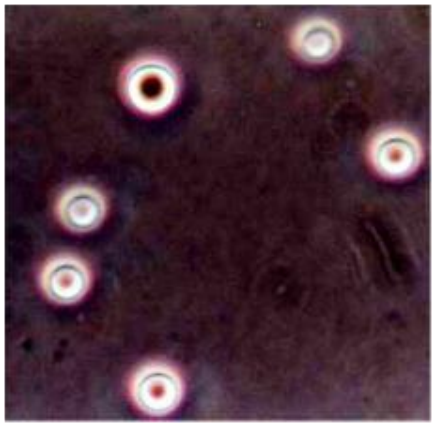

Figure 1.11. Photomicrograph of phospholipid nanosomes encapsulating cytochrome-C (Castor, 2005).

1.4.2.6. The supercritical antisolvent (SAS) process

The SAS process was first introduced for the micronization of soy lecithin [43], followed by the advanced application of liposomal microencapsulation [44]. The SAS process involved spraying of the phospholipid-dissolved organic solvent into a continuous phase of SC-CO_2, which was used as an antisolvent for phospholipid precipitation, but as a solvent for the organic solvent. In the process, SC-CO_2 instantaneously diffuses into the liquid phospholipid-laden phase and breaks the liquid phase into small droplets. Simultaneously, the organic solvent evaporates from the liquid droplets into the SC-CO_2 phase. This mass transfer phenomenon between the two phases induces a supersaturation of phospholipids in the liquid droplets followed by the precipitation of fine phospholipid particles, which will form liposomes by hydration with an aqueous cargo solution.

The experimental system for SAS semi-continuous precipitation is shown in Figure 1.12. In this study of micronized lecithin particles, the material was the modified soy lecithin S75, mainly containing 71% PC and 10% PE. CO_2 was pumped into the precipitation vessel up to a pressure between 8 and 11 MPa at 35 ^{o}C. The lecithin dissolved in ethanol with a concentration ranging from 2 to 16.5 wt. % was then injected into the vessel via another high pressure pump at a flow rate of 10 to 28 ml per hour. The CO_2 flow rate on the vent was maintained at 400 g per hour.

Fine phospholipid particles were formed when the lecithin-laden ethanol solution was introduced into the precipitation vessel where SC-CO_2 was filled. The particles fell to the bottom of the vessel and were directly collected for the analyses of size distribution and morphology. The results indicated that the size distribution of the SAS lecithin particles varied from 1 to 40 µm. As shown in Figure 1.13, the aggregated spherical and amorphous lecithin particles were observed

under the SEM visualization. The fine particles formed with different lecithin types were found to present similar size distribution and morphology [43].

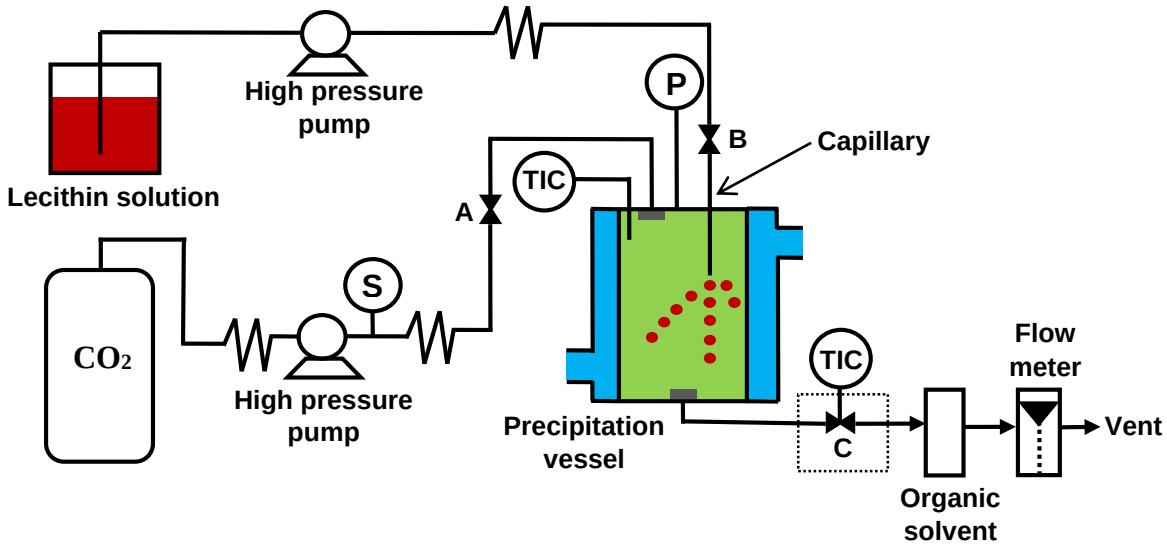

Figure 1.12. The SAS apparatus for formation of micronized lecithin particles (Badens et al., 2001). TIC: temperature indicator controllers; P: pressure gauge; A, B, C: metering valves.

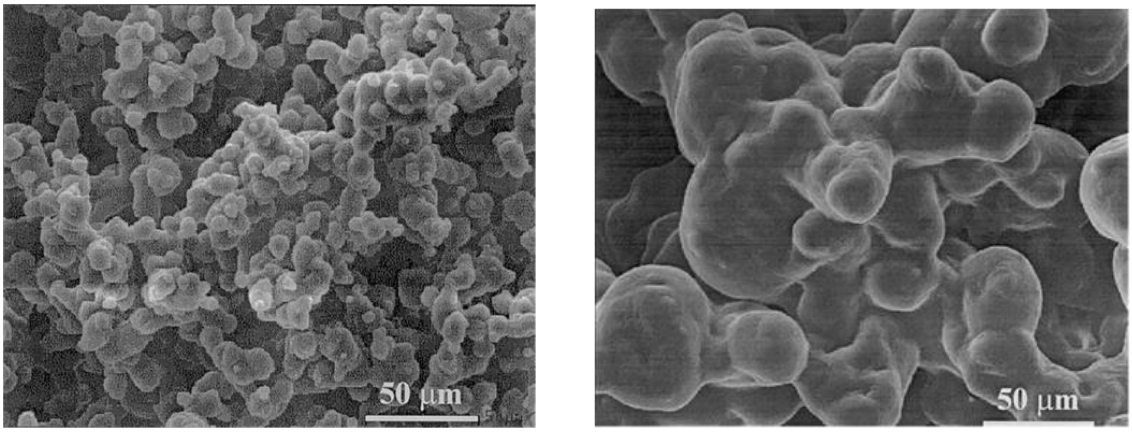

(A) The spherical **(B) The amorphous particles**

Figure 1.13. Phospholipid particles precipitated from the SAS process (Badens et al., 2001).

A continuous anti-solvent process (CAS) was established for the formation of liposomes [44]. As shown in Figure 1.14, CAS mainly consists of a CO_2 pump, organic solvent pump, water pump and autoclave vessel. Initially, 150 g of water was injected into the autoclave vessel. CO_2 was then introduced into the vessel with heating until the desired conditions were reached. The aqueous phase was stirred during the whole process at 225 rpm for efficient mixing. Phospholipids and cholesterol were first dissolved in the ethanol and sprayed into the autoclave filled with binary CO_2 and aqueous phases. When the aqueous phase became homogeneous and cloudy, the metering valve (No.10) was then opened to recover the liposomal emulsion. CO_2 and water were continuously filled into the autoclave to maintain the steady-state condition.

It was found that the optimal process parameters were 9 MPa of operating pressure, 308 K of operating temperature, 300 g / h, 240 ml / h and 180 ml / h of CO_2, ethanol and water flow rates, respectively. As shown in Figure 1.15, the liposomes formed at the above conditions were observed to be spherical and multilamellar with the size distribution between 10 and 100 μm.

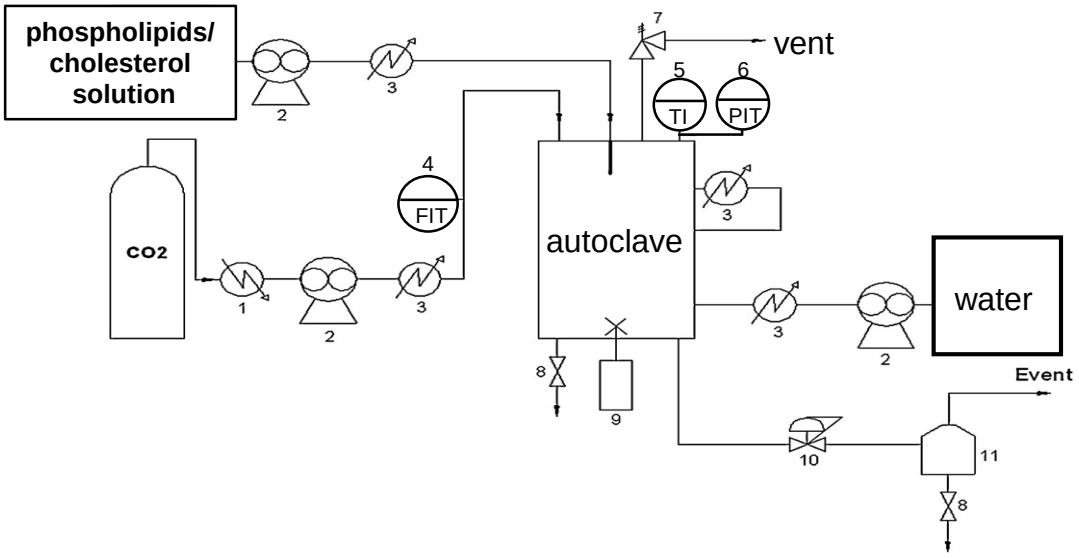

Figure 1.14. Schematic diagram of the continuous anti-solvent (CAS) process (Lesoin et al., 2011).

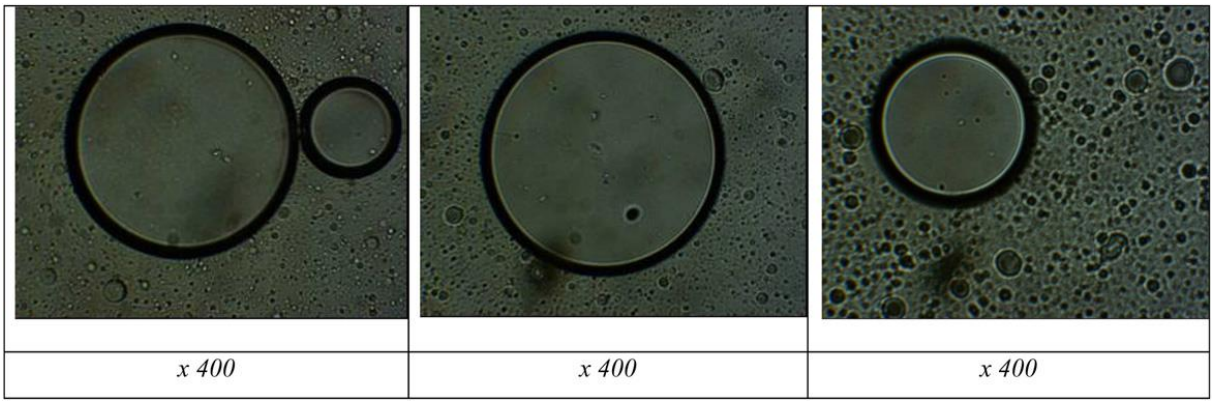

Figure 1.15. Phase contrast microscope images of liposomes formed in the CAS process (Lesoin et al., 2011).

1.4.2.7. Particles from gas saturated solutions (PGSS)

PGSS was initially designed for producing polymeric particles or encapsulating active compounds in polymeric capsules [45]. In this process, polymers and targeted active compounds are first dissolved in a solution in an autoclave at a given temperature. SC-CO_2 is then introduced into the solution until the saturated concentration is reached. The SC-CO_2 saturated solution containing polymers and active compounds is subsequently sprayed through a nozzle into a precipitation chamber. The microcapsules are formed and dried due to the intense cooling effect and solvent evaporation during the rapid depressurization of SC-CO_2.

PGSS was successfully developed for the liposomal microencapsulation of β-carotene [46]. Soy lecithin was dissolved in 50 ^{o}C water at a concentration of 62 g per liter. 0.13 g of β-carotene was first dissolved in 20 ml of dichloromethane and then added to 400 ml of the lecithin solution. The dichloromethane was removed by rotary evaporation. The aqueous dispersion of β-carotene and lecithin was saturated with SC-CO_2 at temperature ranging from 102 to 132 ^{o}C and pressure varying from 8 to 10 MPa. Solid capsules were formed by spraying the SC-CO_2 saturated dispersion through the nozzle (500 μm I.D). The capsule sizes varied from 10 to 500 μm with up to 60% of microencapsulation efficiency. By rehydration of these capsules, multilamellar liposomes

were formed within 1 to 5 μm of the size distribution. β-carotene encapsulated in the phospholipid bilayers of the liposomes shows the red-orange color in Figure 1.16.

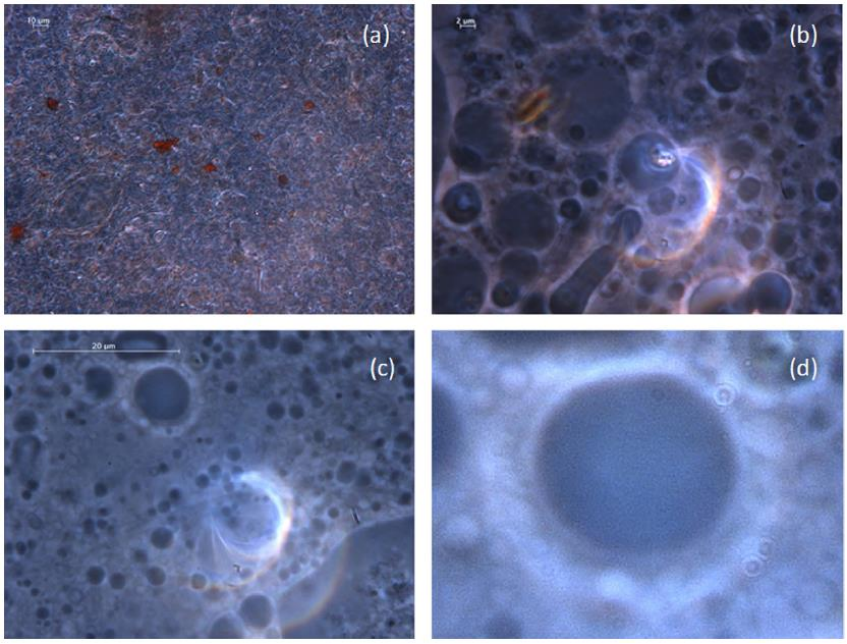

Figure 1.16. Microscopic images of rehydrated liposomes (Paz et al., 2012): (a) experiment 1; (b) experiment 2; (c) experiment 10; (d) enlargement of a liposome.

1.4.2.8. Depressurization of an expanded liquid organic solution-suspension (DELOS-SUSP)

SUV liposomes were synthesized using DELOS-SUSP [47]. The schematic diagram of liposomal microencapsulation is shown in Figure 1.17. Cholesterol, DPPC or poly(ethylene glycol) cholesteryl ethers (CHOL_PEGs) were dissolved in ethanol with 1.4 mg / ml of the lipid concentration and loaded in a high-pressure autoclave.

The solution was pressurized by SC-CO_2 up to 10 MPa at 35 ^oC. During the depressurization of SC-CO_2 through a nozzle at the base of the autoclave, the lipid mixture was simultaneously blended with the aqueous cargo solution to form the liposomes. Evaporation of CO_2 from the expanded organic solution caused fast cooling, which in turn resulted in a homogenous distribution of unilamellar SUV with the size ranging from 100 to150 nm and zeta-potential varying from 10

to 30 mV. It was also reported that DELOS-SUSP was scalable from 27 ml to 1.3 L while the size distributions of SUV liposomes were found to be unchanged.

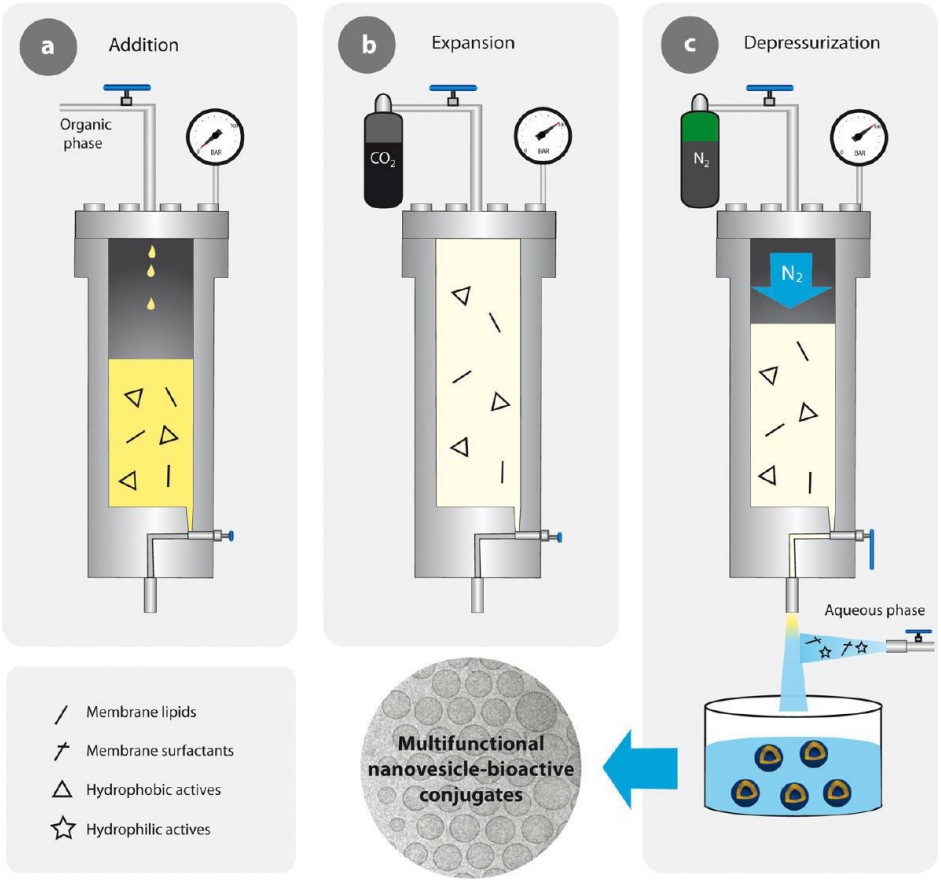

Figure 1.17. Schematic diagram of the DELOS-SUSP system for preparation of multifunctional nanovesicle-bioactive conjugates (Cabrera et al., 2013).

1.5. Latest developemts in liposomal micronecapsualtion using the dens gas techniques

A hydrophilic polymer can be incorporated on the liposomal surface in order to decrease the uptake of liposomes by the body defense systems, especially the mononuclear phagocyte system (MPS). As a result, the blood circulation time of liposomes is prolonged for efficient targeted therapy on tumors. Poly(ethylene glycols) (PEG's) have been extensively chosen as the membrane modifier on the liposomal surface due to its high biocompatibility and low cytotoxicity, low immunogenicity and good excretion kinetics [48-51].

The PEGylated liposomes (stealth liposomes) were successively formulated using supercritical antisolvent (SAS) technique for the microencapsulation of docetaxel [52]. Disteroyl glycerol phosphatidylethanolamine PEG_{2000} (DSPE-PEG_{2000}) was selected for the liposomal membrane modification. The best composition of hydrogenated soya phosphatidylcholine (HSPC), DSPE-PEG_{2000}, soya phosphatidylcholine (SPC) and cholesterol was determined in the ratio of 7 : 6 : 3 : 1 for 79.2% of optimal encapsulation efficiency (EE). Docetaxel, and the lipids / DSPE-PEG_{2000} mixture were blended in the ratio of 1 to 20 and dissolved in chloroform / ethanol solvents (2:1) followed by spraying the solution into the high pressure chamber filled with SC-CO_2. Supersaturation of the lipids / DSPE-PEG_{2000} / docetaxel was reached and stated to co-precipitate to form the PEGylated liposomes. The liposomes produced at 22 MPa, 40 ^{o}C and 120 g / min of CO_2 flow rate were found to be the ideal condition for the 255.2 nm of minimum liposomal size and 67.5 % of yield rate. The PEGylated liposomes also showed good stability for the 3-month storage at 2 to 8 and 30 ^{o}C respectively with the variation of size and EE less than 3 %.

1.6. Conclusion

Supercritical fluid processes for liposomal microencapsulation have drawn significant attention because the usage of organic solvent is substantially reduced or avoided, which results in less or even no pollution to the environment. More importantly, this green technology provides pure encapsulated bioactives to consumers with no harm of toxicity. This review provided an overview of the conventional and innovative techniques of liposomal microencapsulation. The differences and features of the main microencapsulation techniques were carefully described and compared. The results of this review are expected to be an aid for the advanced developments in non-toxic liposomal microencapsulation. The supercritical fluid microencapsulation is

advantageous for food, cosmetic and pharmaceutical applications because SC-CO_2 enables aseptic operating conditions. The ultimate goal is to design a rapid, pure and continuous process of supercritical liposomal microencapsulation, which can be scaled up for industrial productions.

REFERENCES

[1] Arifin, D. R.; Palmer, A. F. Physical properties and stability mechanisms of poly(ethylene glycol) conjugated liposome encapsulated hemoglobin dispersions. *Artif Cell Blood Substit Biotechnol* 2005, 33, 137-162.

[2] Nii, T.; Ishii, F. Encapsulation efficiency of water-soluble and insoluble drugs in liposomes prepared by the microencapsulation vesicle method. *Int J Pharm* 2005, 298, 198-205.

[3] Xia, S.; Xu, S. Ferrous sulfate liposomes: preparation, stability and application in fluid milk. *Food Res Ind* 2005, 38, 289-296.

[4] Sharma, A.; Sharma, U. S. Liposomes in drug delivery: progress and limitations. *Int J Pharm* 1997, 154, 123-140.

[5] Kiwada, H.; Sato, J.; Yamada, S.; Kato, Y. Feasibility of magnetic lipsomes as a targeting device for drugs. *Chem Pharm Bull* 1986, 34, 4253-4258.

[6] Shieh, M. F.; Chu, I. M.; Lee, C. J.; Kan, P.; Hau, D. M.; Shieh, J. J. Liposomal delivery system for taxol. *J Ferment Bioeng* 1997, 83, 87-90.

[7] Wong, J. P.; Yang, H.; Blasetti, K. L.; Schnell, G.; Conley, J.; Schofiel, L. N. Liposome delivery of ciprofloxacin against intracellular Francisella tularensis infection. *J Control Release* 2003, 92, 265– 273.

[8] Decker, C.; Schubert, H.; May, S.; Fahr, A. Pharmacokinetics of temoporfin-loaded liposome formulations: Correlation of liposome and temoporfin blood concentration. *J Control Release* 2013, 166, 277-285.

[9] Fowler, R. A.; Fossheim, S. L.; Mestas, J. L.; Ngo, J.; Canet-Soulas, E.; Lafon, C. Non-invasive magnetic resonance imaging follow-up of sono-sensitive Liposome tumor delivery and controlled release after high-intensity focused ultrasound. *Ultrasound Med Biol* 2013, 39, 2342-2350.

[10] Keller, B. C. Liposomes in Nutrition. *Trends Food Sci Tech* 2001, 12, 25-31.

[11] Stone, W. L.; Smith, M. Therapeutic uses of antioxidant liposomes. *Mol Biotechnol* 2004, 27, 217-230.

[12] Gouin, S. Microencapsulation: industrial appraisal of existing technologies and trends. *Trends Food Sci Tech* 2004, 15, 330-347.

[13] Taylor, M. T.; Davidson, M. P.; Bruce, B. D.; Weiss, J. Liposomal nanocapsules in food science and agriculture. *Crit Rev Food Sci Nutr* 2005, 45, 587-605.

[14] Yokoyama, S.; Inagaki, A.; Tsuchiya, K.; Sakai, H.; Imura, T.; Ohkubo, T.; Tsubaki, N.; Abe, M. Stearylamine changes the liposomal shape from MLVs to LUVs. *J Oleo Sci* 2005, 54, 251-254.

[15] Jo, S. M.; Kim, J. C. Glucose-triggered release from liposomes incorporating poly(*N*-isopropylacrylamide-co-methacrylic acid-co-octadecylacrylate) and glucose oxidase. *Colliod Polym Sci* 2009, 287, 379-384.

[16] Castor, T. P.; Aphios Corporation. Methods and apparatus for making liposomes. United States patent US 5554382A. 1996.

[17] Frederiksen, L.; Anton, K.; Hoogevest, P. V.; Keller, H. R.; Leuenberger, H. Preparation of liposomes encapsulating water-soluble compounds using supercritical carbon dioxide. *J Pharm Sci* 1997, 86, 921-928.

[18] Magnan, C.; Badens, E.; Commenges, N.; Charbit, G. Soy lecithin micronization by precipitation with a compressed fluid antisolvent - influence of process parameters *J Supercrit Fluid* 2000, 19, 69-77.

[19] Castor, T. P. Phospholipid nanosomes. *Curr Drug Delivery* 2005, 2, 329-340.

[20] Utada, A. S.; Lorenceau, E.; Link, D. R.; Kaplan, P. D.; Stone, H. A.; Weitz, D. A. Monodisperse double emulsions generated from a microcapillary device. *Science* 2005, 308, 537-541.

[21] Otake, K.; Shimomura, T.; Goto, T.; Imura, T. Preparation of liposomes using an improved supercritical reverse phase evaporation method. *Langmuir* 2006, 22, 2543-2550.

[22] Meure, L. A.; Knott, R.; Foster, N. R.; Dehghani, F. The depressurization of an expanded solution into aqueous media for the bulk production. *Langmuir* 2009, 25, 326-337.

[23] Lopes, I. M. G.; Bernardo-Gil, M. G. Characterisation of acorn oils extracted by hexane and by supercritical carbon dioxide. *Eur J Lipid Sci Technol.* 2005, 107, 12-19.

[24] Shao, P.; Sun, P.; Ying, Y. Response surface optimization of wheat germ oil yield by supercritical carbon dioxide extraction. *Food and Bioprod Process* 2008, 86, 227-231.

[25] Bangham, A. D.; Standish, M. M.; Watkins, J. C. Diffusion of univalent ions across the lamellae of swollen phospholipids. *J Mol Biol* 1965, 13, 238-252.

[26] Batzri, S.; Korn, E. D. Single bilayer liposomes preapred with sonication. *Biochim Biophys Acta* 1973, 298, 1015-1019.

[27] Yokoyama, S.; Takeda, T.; Abe, M. Preparation of ganglioside Gm3 liposomes and their membrane properties. *Colloids Surf B* 2002, 27, 181-187.

[28] Szoka, F. C.; Papahadjopoulos, D. Procedure for preparation of liposomes with large internal aqueous space and high capture by reverse phase evaporation. *Proc Natl Acad Sci USA* 1978, 75, 4194-4198.

[29] Kim, J. M.; Kim, Y. J.; Jeong, J.; Kim, C.-J. Meat tenderizing effect of injecting encapsulated Ca^{2+} in liposome into rabbit before slaughter. *Biosci Biotechnol Biochem* 2006, 70, 2381-2386.

[30] Sada, E.; Katoh, S.; Terashima, M.; Tsukiyama, K.-I. Entrapment of an ion-dependant enzyme into reverse-phase vesicles. *Biotechnol Bioeng* 1988, 32, 826-830.

[31] Li, S.; Nickels, J.; Palmer, A. F. Liposome-encapsulated actin-hemoglobin (LEAcHb) artificial blood substitutes. *Biomaterials* 2005, 26, 3759-3769.

[32] Maulucci, G.; Spirito, M. D.; Arcovito, G.; Boffi, F.; Castellano, A. C.; Brigantiy, G. Particle size distribution in DMPC vesicles solutions undergoing different sonication times. *Biophys J* 2005, 88, 3545-3550.

[33] Dua, J. S.; Rana, A. C.; Bhandari, A. K. Liposome: methods of preparation and applications. *Int J Pharm Stud Res* 2012, 3, 14-20.

[34] Yamaguchi, T.; Nomura, M.; Matsuoka, T.; Koda, S. Effects of frequency and power of ultrasound on the size reduction of liposome. *Chem Phys Lipids* 2009, 160, 58-62.

[35] Shum, H. C.; Lee, D.; Yoon, I.; Kodger, T.; Weitz, D. A. Double emulsion templated monodisperse phospholipid vesicles. *Langmuir* 2008, 24, 7651-7653.

[36] Castor, T. P.; Chu, L.; Aphios corporation. Methods and apparatus for making lipsomes containing hydrophobic drugs. United States patent US 5776486A. 1998.

[37] Imura, T.; Otake, K.; Hashimoto, S.; Gotoh, T.; Yuasa, M.; Yokoyama, S.; Sakai, H.; Rathman, J. F.; Abe, M. Preparation and physicochemical properties of variuos soybean lecithin liposomes using supercritical reverse phase evaporation method. *Colloids Surf B* 2002, 27, 133-140.

[38] Wen, Z.; You, X.; Liu, B.; Zheng, Z.; Pu, Y.; Li, Q., Application of an improved RESS process for Atractylodes macrocephala Koidz volatile oil liposomes production, in 4th International Conference on Bioinformatics and Biomedical Engineering, IEEE Computer Society, Chengdu, China, 2010.

[39] Wen, Z.; Liu, B.; Zheng, Z.; You, X.; Pu, Y.; Li, Q. Preparation of liposome particle of atractylone by supercritical carbon dioxide process. *Adv Mat Res* 2010, 92, 177-182.

[40] Wen, Z.; You, X.; Jiang, L.; Liu, B.; Zheng, Z.; Pu, Y.; Cheng, B. Liposomal incorporation of rose essential oil by a supercritical process. *Flavour Frag J* 2011, 26, 27-33.

[41] Otake, K.; Imura, T.; Sakai, H.; Abe, M. Development of a new preparation method of liposomes using supercritical carbon dioxide. *Langmuir* 2001, 17, 3898-3901.

[42] Imura, T.; Gotoh, T.; Otake, K.; Yoda, S.; Takebayashi, Y.; Yokoyama, S.; Takebayashi, H.; Sakai, H.; Yuasa, M.; Abe, M. Cortrol of physicochemical properties of liposomes using a supercritical reverse pahse evaporation method. *Langmuir* 2003, 19, 2021-2025.

[43] Badens, E.; Magnan, C.; Charbit, G. Microparticles of soy lecithin formed by supercritical processes. *Biotechnol Bioeng* 2001, 72, 194-204.

[44] Lesoin, L.; Crampon, C.; Boutin, O.; Badens, E. Development of a continuous dense gas process for the production of liposomes. *J Supercrit Fluids* 2011, 60, 51-62.

[45] Cocero, M. J.; Martín, Á.; Mattea, F.; Varona, S. Encapsulation and co-precipitation processes with supercritical fluids: Fundamentals and applications. *J Supercrit Fluid* 2009, 47, 546-555.

[46] Paz, E. d.; Martín, Á.; Cocero, M. J. Formulation of β-carotene with soybean lecithin by PGSS (particles from gas saturated solutions)-drying. *J Supercrit Fluids* 2012, 72, 125-133.

[47] Cabrera, I.; Elizondo, E.; Esteban, O.; Corchero, J. L.; Melgarejo, M.; Pulido, D.; Córdoba, A.; Moreno, E.; Unzueta, U.; Vazquez, E.; Abasolo, I.; Simó Schwartz, J.; Villaverde, A.; Albericio, F.; Royo, M.; García-Parajo, M. F.; Ventosa, N.; Veciana, J. Multifunctional nanovesicle-bioactive conjugates prepared by a one-step scalable method using CO2-expanded solvents. *Nano lett* 2013, 13, 3766-3774.

[48] Luo, D.; Haverstick, K.; Belcheva, N.; Han, E.; Saltzman, W. M. Poly(ethylene glycol)-conjugated PAMAM dendrimer for biocompatible, high-efficiency DNA delivery. *Macromolecules* 2002, 35, 3456-3462.

[49] Mao, S.; Shuai, X.; Unger, F.; Wittmar, M.; Xie, X.; Kissel, T. Synthesis, characterization and cytotoxicity of poly(ethylene glycol)-graft-trimethyl chitosan block copolymers. *Biomaterials* 2005, 26, 6343–6356.

[50] Dreborg, S.; Akerblom, E. B. Immunotherapy with monomethoxypolyethylene glycol modified allergens *Crit Rev Ther Drug Carr Syst* 1990, 6, 315-365.

[51] Yamaoka, T.; Tabata, Y.; Ikada, Y. Distribution and tissue uptake of poly(ethylene glycol) with different molecular weights after intravenous administration to mice. *J Pharm Sci* 1994, 83, 601-606.

[52] Naik, S.; Patel, D.; Surti, N.; Misra, A. Preparation of PEGylated liposomes of docetaxel using supercritical fluid technology. *J Supercrit Fluids* 2010, 54, 110-119.

Chapter 2: Development of a novel supercritical fluid process for liposomal microencapsulation

2.1. Abstract

A supercritical fluid (SCF)-based process, consisting of supercritical fluid extraction and rapid expansion of a supercritical solution, was successfully developed for advanced SCF applications. A vacuum-driven cargo loading setup was invented for introducing the targeted compounds into the SCF system without additional energy input. This novel SCF process was proven to be suitable to the liposomal microencapsulation of liquid-phase cargos. Supercritical carbon dioxide (SC-CO_2) was used as the sole phospholipid-dissolving agent and an environmentally friendly substitute for organic solvents. The SCF technique of microencapsulation was designed to be a nontoxic and continuous process with the capacity for bulk production of the bioactive-encapsulated phospholipid vesicles.

Keywords: supercritical fluid, microencapsulation, liposome, rapid expansion of a supercritical solution, Bernoulli's principle, continuity equation

2.2. Establishment of a supercritical fluid microencapsulation system

2.2.1. Conceptualization

Supercritical carbon dioxide (SC-CO_2) is a density-adjustable fluid with solvent behavior similar to hexane [1]. Its moderate critical pressure (7.4 MPa) and low critical temperature (31.1 ^oC) make it an ideal candidate for biomaterial processing. SC-CO_2 has been widely used for the extraction of bioactive compounds and removal of toxic compounds within the past three decades. In addition to being nontoxic, environmentally friendly, and economical, complete evaporation of SC-CO_2 from the final product is the most special feature to supercritical fluid (SCF) applications. Rapid expansion of a supercritical solution (RESS) is a new attempt to form nanoscale particles using the SCF technology. Therefore, developing an advanced SCF process based on the RESS technique was set as the goal of my doctoral research.

2.2.2. Construction of the SFC system

In the initial stage, the SCF system was first established. It consisted of three main parts: a high pressure pump, a mixing vessel, and an expansion nozzle. The schematic diagram is presented in Figure 2.1. After the preliminary tests of different pumps for effective CO_2 pressurization, a high-capacity diaphragm pump was chosen because of its high efficiency of fluid transfer and low maintenance cost. To maintain constant pressure in the mixing vessel, a back pressure regulator (BPR) was installed to recirculate the excessive CO_2 back to the pump, as shown in the red arrows. The mixing vessel was equipped for loading and dissolving coating materials in SC-CO_2.

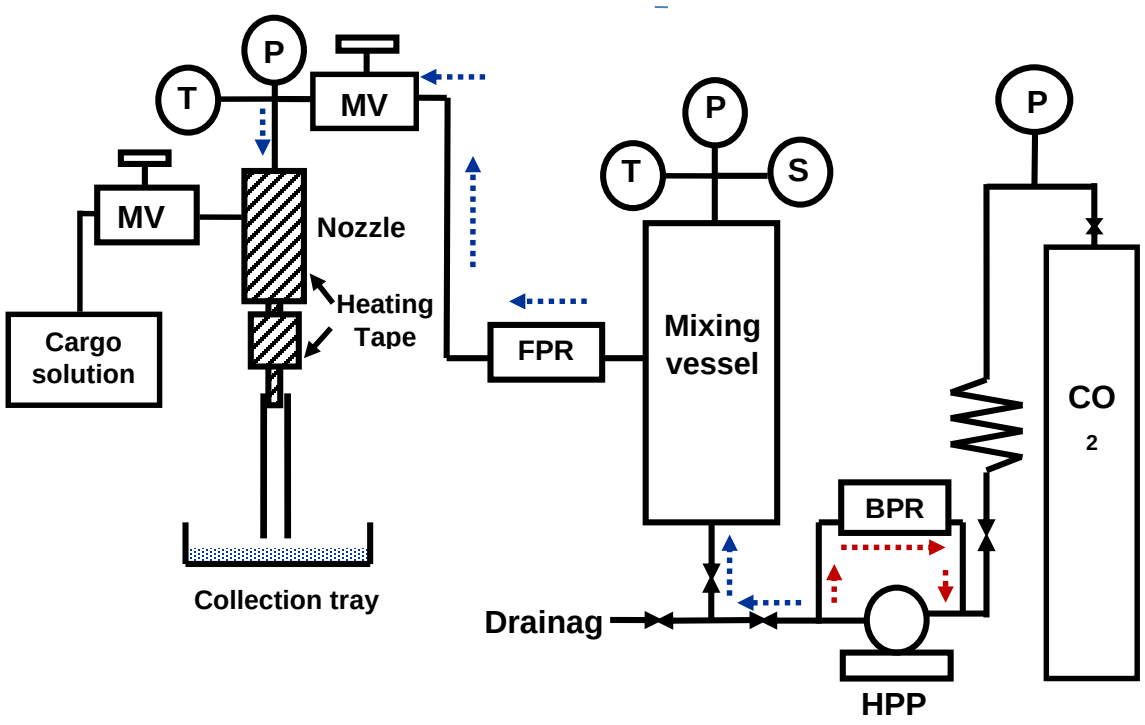

Figure 2.1. Schematic diagram of the SCF microencapsulation system.
BPR: back pressure regulator, HPP: high pressure pump, FPR: forward pressure regulator, MV: metering valves, P: pressure indicators, T: temperature indicators, S: safety valve

When SC-CO_2 was driven from the mixing vessel and passed through a small orifice, rapid depressurization occurred in the expansion nozzle. Tiny particles of targeted compounds started to nucleate and were carried into the nozzle. The pathway of SC-CO_2 in the SCF system is shown as the blue, dashed arrows in Figure 2.1. A forward pressure regulator (FPR) was installed to maintain a constant pressure of SC-CO_2 in the section before the expansion nozzle. The maximum pressures of the mixing vessel and expansion nozzle were 42 MPa and 20 MPa, respectively, for a broad range of tests. Different regions of the SCF system were heated by glass wool tapes in a range of 50 to 95 ^{o}C. Efficient and consistent heat transfer was provided to avoid the Joule-Thomas effect during rapid SC-CO_2 expansion. 316 stainless-steel tubing with 6.35mm O.D. and 4.57 mm I.D.

was successfully tested and installed in the system for optimal performance. Finally, the prototype of the SCF system was successfully built and tested for operation and safety.

2.2.3. Research direction-microencapsulation or fine particle formation?

Based on a comprehensive literature research, fine particle formation using the RESS technique was already studied in a certain number of research papers [2-6], while the RESS process for microencapsulation was still in an early stage [7, 8]. This was due to the limited choices of coating materials, toxicity of organic solvents used as cosolvents, time consuming process, and low encapsulation efficiency. My research objective thus became the creation of a nontoxic and continuous process of microencapsulation advancing from existing SCF technology.

2.2.4. Feasibility study

To evaluate the feasibility of the SCF process of microencapsulation, the coating of red chili oil on whey protein powder was first attempted. Paprika powder was load in the SCF system at 60 ^{o}C and 20.68 MPa with two hours of phase equilibrium. Red chili oil was extracted from paprika powder by SC-CO_2 and carried into the expansion nozzle. Whey protein concentrate (WPC, 500-1000 micron of particle size) was loaded into the nozzle by gravity and simultaneously mixed with the red paprika oil. As shown in Figure 2.2, WPC was successfully coated with paprika oil and showed darker color intensity compared to the original WPC, indicating that the continuous SCF process of microencapsulation was practically feasible. The next step was to decide what types of coating and core materials were suitable for the success of this study.

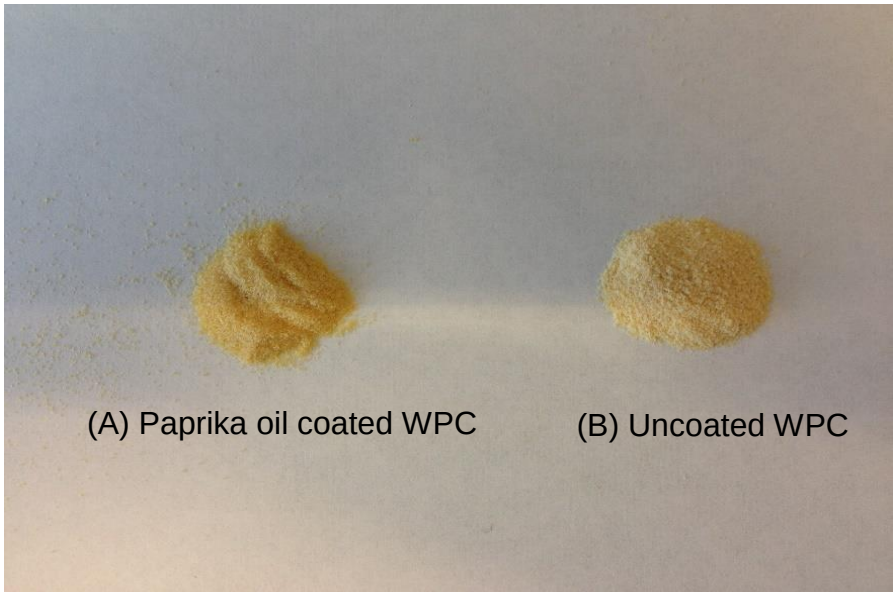

Figure 2.2. Red chili oil coating on whey protein concentrate (WPC) using the SCF process of microencapsulation.

2.3. Implementation of liposomal microencapsulation

2.3.1. Searching for suitable coating materials

Polyethylene glycol (PEG), alginate, polylactic acid (PLA), and soy lecithin were chosen as the coating materials and tested for SCF microencapsulation. SC-CO_2 is a nonpolar fluid with a solvent behavior similar to hexane [1]. Hence, non-polar and lipophilic compounds will be more soluble in SC-CO_2. PEG, alginate, and PLA are polar polymers with very limited solubilities in SC-CO_2. The phospholipids in soy lecithin are amphiphilic molecules, due to the polar phosphate head and nonpolar fatty acids. They act as the emulsifiers and form a water/oil/water emulsion called liposomes [9, 10]. These liposomes are versatile and encapsulate hydrophilic compounds in their aqueous core and lipophilic compounds inside one or multiple phospholipid bilayers [11, 12].

In addition, soy lecithin is the most economical material compared to the other purified and modified phospholipids. The solubility of soy phospholipids in SC-CO_2 is reported to be approximately 0.1 %, which is sufficient for liposomal microencapsulation [13]. Based on the results of our preliminary experiments, soy phospholipids were successfully extracted from lecithin by SC-CO_2 in the mixing vessel, followed by the generation of liposomes in the expansion nozzle of the SCF process

2.3.2. Process design

2.3.2.1. Cargo loading

Cargo loading by gravity for the SCF microencapsulation was first tested on aqueous samples. The challenges were the inconsistent loading rate and unfavorable backflow occurring in the loading tube. Sonication for cargo loading was then conducted. The cargo solution was sonicated to form mist and directed into the expansion nozzle for liposomal microencapsulation. However, low loading efficiency was a major disadvantage for this SCF process.

Vacuum-driven cargo loading was attempted for its feasibility. 3 to 5 mmHg of vacuum was built up in the expansion nozzle from the high speed of the SC-CO_2 stream flowing through an orifice during its rapid expansion (the vena contracta effect). The cargo solution was introduced into the nozzle by vacuum with no additional energy input. The cargo loading rate was controlled by a metering valve and vacuum force. This innovative setup for cargo loading was applied for liposome microencapsulation using the novel SCF process.

2.3.2.2. Nozzle configuration

The diameter of nozzle controls the size of final liposomal emulsion. The nozzles with 500, 1000, and 1500 microns were tested. It was found that the resistance built up in the 500-micron nozzle was too strong, resulting in very slow SC-CO_2 stream flowing into the nozzle. As a result, the vacuum was not well established, and the cargo solution was not drawn into the nozzle. On the other hand, depressurization of SC-CO_2 through the 1500-micron nozzle was too fast. Soy phospholipids dissolved in SC-CO_2 quickly precipitated and formed big lipid particles before mixing with the cargo droplets in the nozzle. Serious aggregation was observed in the liposomal emulsion. Thus, it was found that the desired vacuum (3 to 5 mmHg) was best established in the nozzle with the 1000-micron I.D. The fine phospholipid particles slowly nucleated and were well mixed with the cargo droplets. The liposomes were well generated in this nozzle configuration.

2.3.2.3. Mixing directions of cargo and soy phospholipids in expansion nozzle

Perpendicular and concentric mixing of cargo and soy phospholipids were tested for SCF microencapsulation. As shown in Figure 2.3, perpendicular mixing means that the cargo and phospholipids were blended at a 90 degree angle. The impact of the SC-CO_2 stream was completely exerted on the vacuum-driven cargo solution. As a result, the tiny cargo droplets were formed and encapsulated by soy phospholipids to produce liposomes. Concentric mixing means the SC-CO_2 stream was directed in the same direction as the cargo solution. Concentric mixing was found to be less efficient than perpendicular mixing. Therefore, the perpendicular nozzle configuration was chosen and used in the SCF system of microencapsulation.

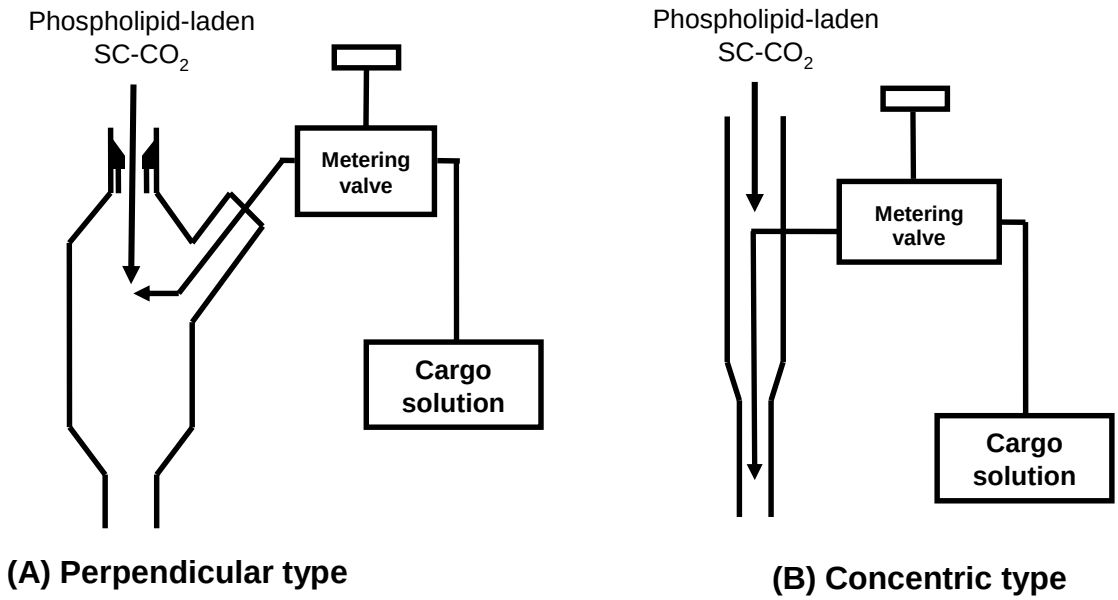

Figure 2.3. Two types of expansion nozzles used in the SCF microencapsulation process.

2.3.2.4. Loading distance between nozzle orifice and loading tube

The cargo solution was introduced into the nozzle by the vacuum created by the high-speed SC-CO_2 stream through a 1000-micron nozzle (the vena contracta effect). The vacuum was only located at a small area between the nozzle and cargo loading tube. Determining this vacuum area was crucial to the success of this SCF liposomal microencapsulation. After a number of tests for vacuum creation, 3 to 5 mmHg of vacuum was measured when the cargo loading tube was installed at 10 mm below the nozzle. The detailed configuration of the nozzle is depicted with the vena contracta area in Figure 2.4.

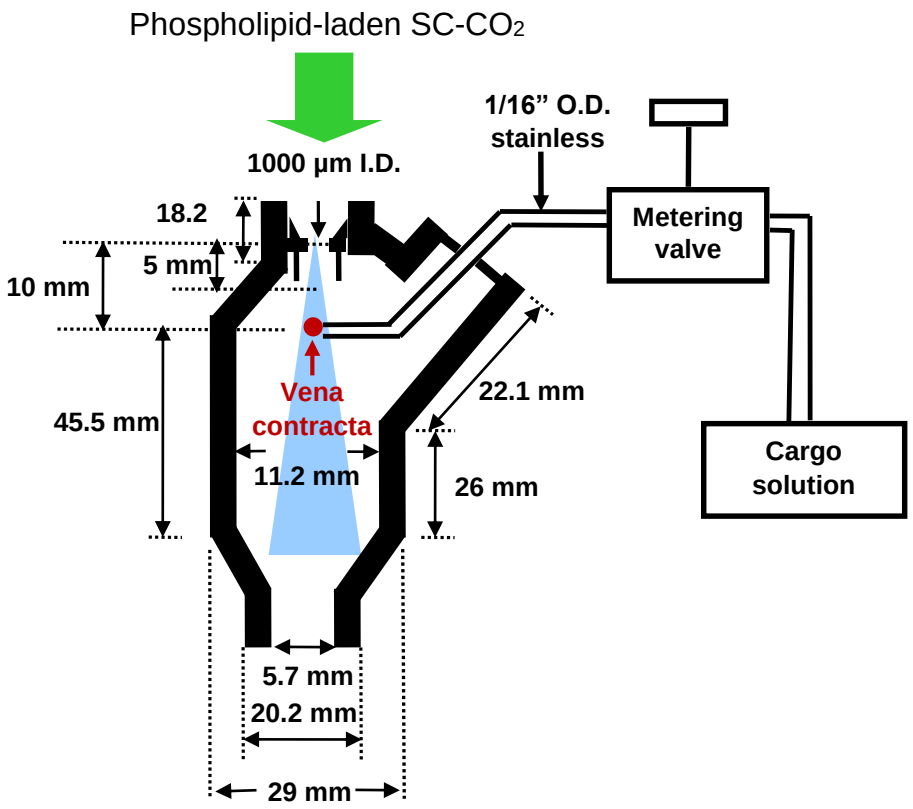

Figure 2.4. Configuration of the expansion nozzle.

2.4. Theoretical study

Fluid dynamics well describes the relationship of pressure and velocity of SC-CO_2 in the SCF process for liposomal microencapsulation. The theoretical explanation of this SCF process is based on the principles of energy and mass balance, and proposed using Bernoulli's equation and the continuity equation for simplified estimation of the optimal operating condition.

Bernoulli's equation

Energy per unit volume before = Energy per unit volume after

$$P_1 + (1/2)\cdot\rho\cdot V_1^2 + \rho\cdot g\cdot h_1 = P_2 + (1/2)\cdot\rho\cdot V_2^2 + \rho\cdot g\cdot h^2 \quad \text{.....(1)}$$

Pressure energy	Kinetic energy per unit volume	Potential energy per unit volume

Continuity Equation

$$Q = A_1 \cdot V_1 = A_2 \cdot V_2 \quad \text{.....(3)}$$

where Q is volumetric flow rate; $A_1 = 0.25 \cdot \pi \cdot d_1^2$; $A_2 = 0.25 \cdot \pi \cdot d_2^2$.

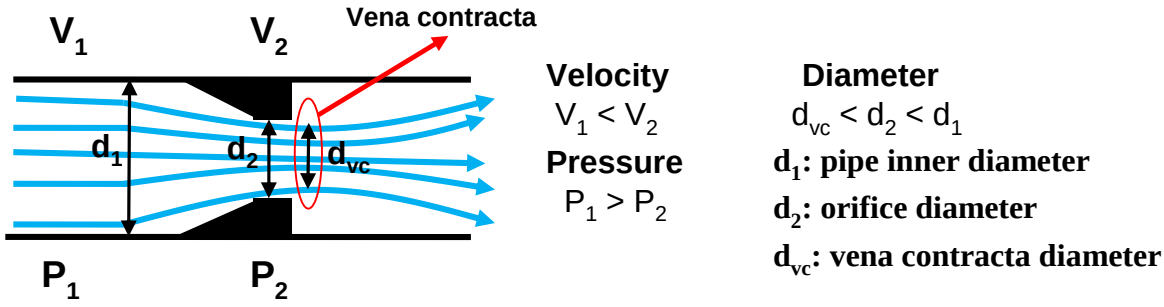

Figure 2.5. Illustration of the vena contracta effect for a fluid flowing through a circular nozzle.

The empirically estimated parameters for the SCF process of liposomal microencapsulation are listed in Table 2.1. The phospholipids' solubility in SC-CO_2 was reported to be 0.1 % (w/v) [13]. Therefore, the mass flow rate of the phospholipids carried by SC-CO_2 in the SCF process was calculated to be 0.011 g/s.

The water solubilization capacity (W_{soln}) was used as an indicator to evaluate the emulsification capacity of the phospholipid-based emulsion [14], which is defined as follows:

$$W_{soln} \equiv [\text{mole-}H_2O_{soln}] / [\text{mole-amphiphilic ipids}] \quad \text{.....(4)}$$

The molar ratios of water added to amphiphilic phospholipids between 20:1 and 50:1 presented the desirable water solubilization capacity [14]. Based on the above information, the loading rate of cargo solution can be estimated using Equation 5 for the optimal emulsification capacity.

$$\text{Cargo mass flow rate} = \text{calc. phospholipid mass flow rate} \cdot W_{soln} \quad \text{.....(5)}$$

The ideal cargo mass flow rates are expected to be in the range of 0.23 g/s to 0.57 g/s. Assuming the density of the aqueous cargo solution is approximately 1 g/cm^3, the volumetric cargo loading rate is estimated to be within 0.23 and 0.57 ml/s.

Table 2.1. Empirical and calculated parameters for the SCF process of microencapsulation

Empirical parameters		Calculated parameters	
Diameter of the inner tube (d_1)	4.65×10^{-3} m	**Area of the vena contracta (A_{vc})[4]**	1.20×10^{-7} m^2
Area of the orifice (A_1)[1]	1.70×10^{-5} m^2	**Volumetric flow rate of SC-CO_2 at the orifice[5]**	11.34 ml/s
Diameter of the orifice (d_2)	5×10^{-4} m	**Theoretical velocity of SC-CO_2 at the orifice[6]**	57.77 m/s
Area of the orifice (A_2)[1]	1.96×10^{-7} m^2	**Mass flow rate of soy phospholipids in SC-CO_2**	0.011 g/s
Vacumm[2]	54.38 (Kgf/m^3)	**Volumetric flow rate of cargo solution**	0.23-0.57 ml/s
CO_2 density[3]	283.16(kg/m^3)		

[1] Area (A) $= 0.25 \cdot \pi \cdot d^2$
[2] 4 mmHg = 54.38 Kgf / m^3
[3] Density at 12.41 MPa and 90 ^{o}C
[4] $A_{vc} = 0.611 \cdot A_2$
[5] $Q = C_c \cdot A_2 \cdot \{ 2 \cdot (p_1 - p_2) / [\rho \cdot (1 - (A_2 / A_1)^2] \}^{1/2}$
[6] $V = Q / A_2$

2.5. Liposomal microencapsulation

The SCF process for liposomal microencapsulation was tested for operation and inspected for safety. The suitable cargo materials were then determined for this microencapsulation process. Based on preliminary results, the operating parameters of the mixing vessel were set at 60 ^{o}C and 20.68 MPa. The parameters of the expansion nozzle were set at 90 ^{o}C and 12.41 MPa. Five solid and liquid cargos were selected and evaluated for the feasibility of liposomal microencapsulation.

2.5.1. Solid cargos

Iron powder

500-1000 nm of iron powder was selected. As shown in Figure 2.6 (A), the microencapsulated liposomes of iron were observed under an optical microscope with 10×40 amplification. One notch of the scale bar is equal to 2.5 microns. The iron was able to be encapsulated in the liposomes. The liposome size varied from 5 to 20 microns. However, the process was inefficient. Only 1 to 2 iron particles were found in the liposomes. The decomposition of liposomes occurred after 2 to 3 hours of storage at 4 ^{o}C due to the heavy density of iron.

Fluorescent microspheres

200 nm green-yellow fluorescent microspheres were then tested. In Figure 2.6 (B), the liposomes encapsulating fluorescent microspheres were visualized under a confocal laser scanning microscope (CLSM). The liposomes were found to be stable after 7 days of storage at 4 ^{o}C. However, the encapsulation efficiency was as low as in the test of iron particles.

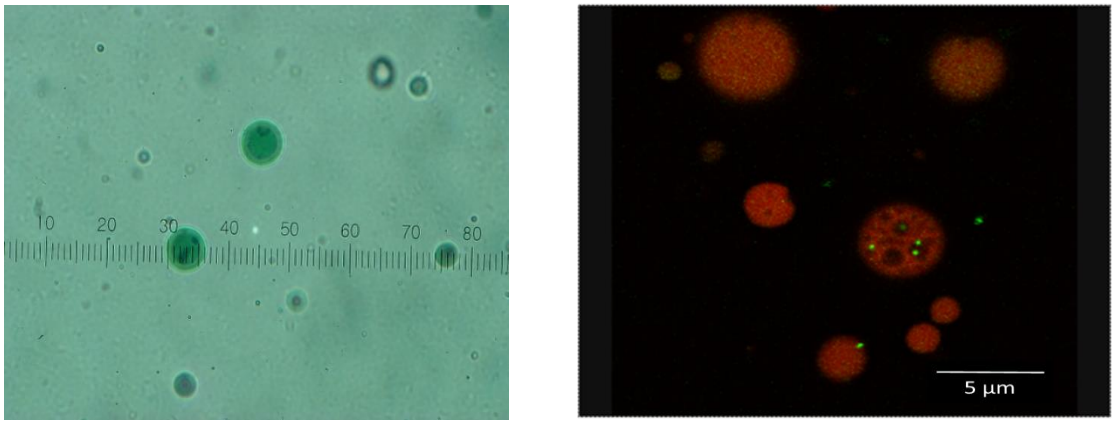

(A) Iron powder **(B) Fluorescent microspheres**

Figure 2.6. The SCF liposomes encapsulating solid cargos: (A) iron powder, observed under a 10×40 optical microscope; (B) 200 nm fluorescent microspheres, observed under a 10×63 confocal laser scanning microscope.

2.5.2. Liquid cargos

Liquid core materials were tested to improve the encapsulation efficiency of SCF liposomes, due to better miscibility of cargo and coating materials. Ferrous sulfate ($FeSO_4$) and ferric chloride ($FeCl_2$) were selected for a feasibility study. In Figure 2.7 (A), it was observed that free ferrous sulfate was deposited on the liposomal membrane. The aggregation of liposomes occurred within 12 hours of storage at 4 ^oC. Additionally, as shown in Figure 2.7 (B), ferrous chloride was successfully encapsulated in the liposomes and presented in a greenish color under an optical microscope. However, the $FeCl_2$-encapsualted liposomes lost their stability after 6 hours of storage at 4 ^oC. Ferrous sulfate and ferrous chloride were thus not suitable for this SCF microencapsulation process.

Fluorescein isothiocyanate (FITC) showed the most promising results for SCF microencapsulation. In Figure 2.7 (C), the liposomes encapsulating FITC presented bright green color in the core, surrounded by red phospholipid bilayers. The encapsulation efficiency of the SCF liposomes was improved and the emulsion was found to be stable for more than 7 days of storage at 4 ^oC. Thus, it was determined that FITC would be the targeted cargo on the SCF liposomal microencapsulation.

2.6. Process improvements

A static mixer was installed in the expansion nozzle to prolong the mixing time of the liquid cargo and soy phospholipids and to improve size uniformity and encapsulation efficiency. To automate this process, a solenoid valve was equipped above the expansion nozzle to upgrade the SCF operating system to a continuous process. It was successfully tested for practical operation. The novel SCF process for liposomal microencapsulation is shown in Figure 2.8.

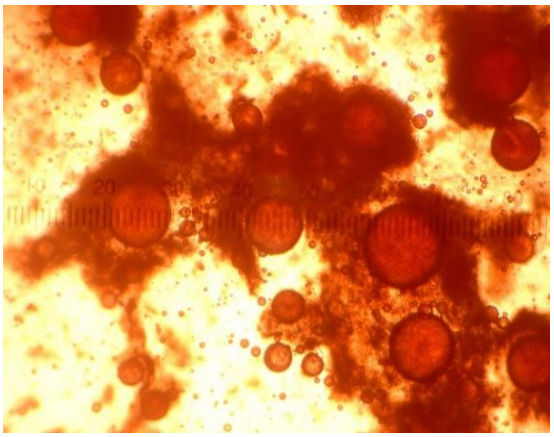

(A) Ferrous sulfate

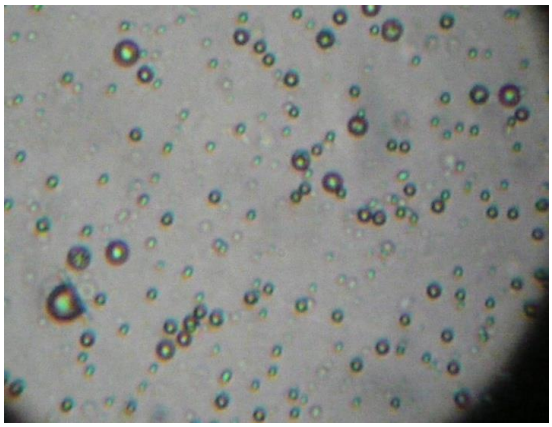

(B) Ferrous chloride

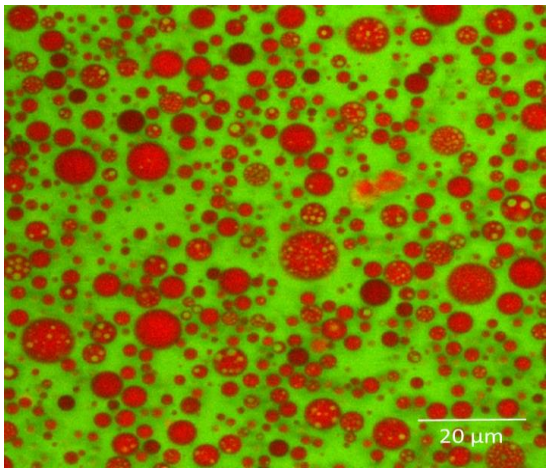

(C) FITC

Figure 2.7. The SCF liposomes encapsulating liquid cargos: (A) Ferrous sulfate and (B) Ferrous chloride, observed under an 10×40 optical microscope; (C) FITC, observed under a 10×63 confocal laser scanning microscope.

Figure 2.8. A continuous SCF process for liposomal microencapsulation.

2.7. Conclusions

From a concept to a well-functioning system, a novel SCF technique was successfully developed for liposomal microencapsulation. It aimed to be a nontoxic continuous process based on the flow-through design and without using any organic solvent. Vacuum-driven cargo loading was a significant innovation in this SCF microencapsulation system. The method provides an environmentally friendly solution for commercial production of liposomes in the food, pharmaceutical and cosmetic industries. In addition, using natural soy lecithin as the coating material drastically reduces the cost of the liposomal microencapsulation. Further characterization of the SCF liposomes under different operating conditions have been conducted for the completion of my doctoral research.

References

[1] Gupta, R. B.; Shim, J. J., Solubility in supercritical carbon dioxide. 2006, CRC Press; Taylor & Francis Group Florida, USA. pp. 3.

[2] Hezave, A. Z.; Aftab, S.; Esmaeilzadeh, F. Micronization of ketoprofen by the rapid expansion of supercritical solution process. *J Aerosol Sci* 2010, 41, 821-833.

[3] Hezave, A. Z.; Esmaeilzadeh, F. The effects of RESS parameters on the diclofenac particle size. *Adv Powder Technol* 2011, 22, 587-595.

[4] Huang, J.; Moriyoshi, T. Fabrication of fine powders by RESS with a clearance nozzle. *J Suprict Fluid* 2006, 37, 292-297.

[5] Tandya, A.; Dehghan, F.; Foster, N. R. Micronization of cyclosporine using dense gas techniques. *J Script Fluids* 2006, 37, 272-278.

[6] Kröber, H.; Teipel, U.; Krause, H. Manufacture of submicron particles via expansion of supercritical fluids. *Chem Eng Technol* 2000, 23, 763-765.

[7] Kim, J. H.; Paxton, T. E.; Tomasko, D. L. Microencapsulation of naproxen using rapid expansion of supercritical solutions. *Biotechnol Progr* 1996, 12, 650-661.

[8] Matsuyama, K.; Mishima, K.; Hayashi, K. I.; Ishikawa, H.; Matsuyama, H.; Harada, T. Formation of microcapsules of medicines by the rapid expansion of a supercritical solution with a nonsolvent. *J Appl Polym Sci* 2003, 89, 742-752.

[9] Bangham, A. D.; Standish, M. M.; Watkins, J. C. Diffusion of univalent ions across the lamellae of swollen phospholipids. *J Mol Biol* 1965, 13, 238-252.

[10] Frederiksen, L.; Anton, K.; Hoogevest, P. V.; Keller, H. R.; Leuenberger, H. Preparation of liposomes encapsulating water-soluble compounds using supercritical carbon dioxide. *J Pharm Sci* 1997, 86, 921-928.

[11] Márquez, M. M. A. L.; Wagner, J. R.; Alonso, S. d. V.; Chiaramoni, N. S. Liposomes as vehicles for vitamins E and C: an alternative to fortify orange juice and offer vitamin C protection after heat treatment. *Food Res Int* 2011, 44, 3039-3046.

[12] Mallick, S.; Choi, J. S. Liposomes: versatile and biocompatible nanovesicles for efficient biomolecules delivery. *J Nanosci Nanotechnol* 2014, 14, 755-765.

[13] Teberikler, L.; Koseoglu, S.; Akgerman, A. Selective extraction of phosphatidylcholine from lecithin by supercritical carbon dioxide/ethanol mixture. *J Am Oil Chem Soc* 2001, 78, 115-120.

[14] Yamazaki, K.; Imai, M.; Suzuki, I. Water solubilization capacity and mean emulsion size of phospholipid-based isooctane-alcohol W/O microemulsion. *Colloids Surf A* 2007, 293, 241-246.

Chapter 3: Solubility measurements of soy phospholipids in supercritical carbon dioxide using the dynamic technique

3.1. Abstract

Solubility of soy phospholipids in supercritical carbon dioxide (SC-CO_2) was determined using a dynamic equilibrium system. Three temperatures (60, 75, and 90 °C) and three pressures (12.41, 16.55, and 20.68 MPa) were used for the solubility measurements. The solubility of soy phospholipids in SC-CO_2 was observed to increase from 0.009 % to 0.14 % with the pressure rising from 12.41 MPa to 20.68 MPa at 60 ^oC. As expected, the solubility decreased from 0.14 % to 0.01 % when the temperature was increased from 60 ^oC to 90 ^oC at 20.68 MPa. The highest phospholipids solubility of 0.14 % was reached at the highest pressure of 20.68 MPa and lowest temperature of 60^oC. The increased SC-CO_2 density from 292.2 kg/m^3 to 710.6 kg/m^3 was the dominant factor for the enhanced solubility of soy phospholipids in SC-CO_2 when the pressure was increased from 12.41 to 20.68 MPa. The solubility data obtained with the dynamic technique were found to be in good agreement with the predictive models based on the Chrastil, del Valle-Aguilera, and Sparks equations. A linear relationship was observed between the solubility data of soy phospholipids and density of SC-CO_2. The solubility data of a targeted compound in SC-CO_2 is the first step to design an efficient system for advanced SC-CO_2 applications. The results obtained in this study were employed to design a novel nontoxic process for liposomal microencapsulation using natural soy lecithin as the coating material.

Keywords: dynamic solubility measurement, soy lecithin, phospholipids, supercritical carbon dioxide, semi-empirical models

3.2. Introduction

Lipids with two fatty acids and a phosphate group connected by ester linkages to a glycerol backbone are called phospholipids (PLs). PLs have both polar and nonpolar portions because the phosphate group can ionize. With this property, they can act as the emulsifiers for emulsion formation [1]. PLs have found their use in food, pharmaceutical and cosmetic applications, especially in liposome formation for controlled release and targeted therapies of bioactive compounds and drugs [2, 3]. PLs have also gained significant attention for their health benefits. For example, phosphatidylcholine (PC) is a major source of choline, which plays an important role in cardiovascular and liver health as well as in memory improvement [4].

Soy lecithin, a byproduct from the refining process of vegetable oil, is a major source of PC with some other PLs, such as phosphatidylethanolamine (PE) and phosphatidylinositol (PI), carbohydrates, glycolipids and some residual oil. It is a natural and economically affordable material for the microencapsulation of targeted compounds [5]. Currently, solvent extraction, such as ethanol or acetone, and centrifugation are adopted for commercial production of de-oiled lecithin with higher PL concentration. Solvent residue, high cost of solvent separation, and low separation efficiency of centrifugation are the main concerns regarding these processes.

Supercritical carbon dioxide (SC-CO_2) is a benign, environmentally friendly, inert and nonflammable fluid. SC-CO_2 extraction is an ideal alternative for the PL purification from crude lecithin without solvent residue. Selective extraction of the PLs from soy lecithin by adjusting SC-CO_2 density makes this technique commercially significant and promising. In the advanced applications, several techniques based on SC-CO_2 have been applied to design various processes for liposomal microencapsulation [6-11]. SC-CO_2 can partially or completely replace the organic solvents as the PL-dissolving medium. The solubility data of PLs in SC-CO_2 is the first step to

design an efficient system for advanced bioprocesses, such as extraction, fine particle formation, and microencapsulation. However, such data, with reasonable accuracy, are not readily available. Our objective was to measure the solubility of the PLs from soy lecithin in SC-CO_2 at different operating conditions. The data obtained in this study will be employed to design a novel eco-friendly SC-CO_2 process for liposomal microencapsulation using natural soy lecithin as the coating material.

3.3. Theoretical models

Generally, two types of mathematical models are used to explain the solubility behavior of a solute in a supercritical fluid (SCF): semi-empirical methods and equations of state (EOS). The solubility correlation using EOS is more challenging since it requires complex computations, and most physical property values are not immediately available in the literature. Semi-empirical models are often applied to predict a solute's solubility in SC-CO_2, due to their relative simplicity. The most common semi-empirical models are based on a correlation of the SCF density and the solute's solubility data. These density-based models can provide accurate predictions of solubility behaviors in SC-CO_2 for the compounds with higher molecular weights, such as triglycerides, lipids, and oils [12].

Chrastil developed a semi-empirical correlation to predict a compound's solubility in SC-CO_2 using the solvent density and the reciprocal of operating temperature as independent variables. A linear relationship between a solute's solubility and solvent density is thus [13]:

$$\ln C = k \cdot \ln \rho + c_1/T + c_0 \quad \text{……(1)}$$

where C is the solute's solubility (g/L), ρ is the solvent's density (g/L), and T is the operating temperature (K). The equation constants include k, c_1 and c_0, where k is an association number, c_1

is a function of enthalpy for solvation and vaporization, and c_0 is a function of association number and molecular weights of the solute and solvent.

Del Valle and Aguilera proposed a modified model to adjust for the change in the enthalpy of a solute during vaporization at different temperatures [14], as shown in Equation 2:

$$\ln C = k \cdot \ln \rho + c_1/T + c_2/T^2 + c_0 \quad \text{.....(2)}$$

The term ($1/T^2$) was introduced to improve the prediction accuracy of solubility of a solute in SC-CO_2.

As seen in Equation 3, the Sparks model introduced a linear function of SC-CO_2 density into the association number (k) of the Chrastil model [15]. This model is particularly useful for a solvent with reduced density of less than 1, and provides a more accurate prediction of solubility in SC-CO_2 for compounds with higher molecular weights.

$$\ln C = (c_3 + c_4 \cdot \rho) \cdot \ln \rho + c_1/T + c_0 \quad \text{.....(3)}$$

The goodness of fit for these models was evaluated by the absolute average relative deviation (AARD) presented in Equation 4.

$$\text{AARD (\%)} = \frac{1}{N} \sum_{N=1}^{N} \left[\frac{\left| S_{Cal} - S_{Exp} \right|}{S_{Exp}} \right] \times 100 \quad \text{.....(4)}$$

where S_{Cal} is the calculated solubility of a solute in SC-CO_2, S_{Exp} is the experimental solubility of a solute, and N is the number of data points.

3.4. Materials and methods

Dynamic solubility measurements of soy phospholipids in SC-CO_2 were adopted from our previous study [16]. The simplified schematic diagram of the SFT-250 SFE system (Supercritical

Fluid Technologies, Newark, Delaware) is shown in Figure 3.1. The system consisted of a high pressure pump (HPP), extraction vessel (EV), and separation vessel (SV) for sample collection. The SC-CO_2 flow rate was controlled by a restrictor and metering valve (MV). Performix^{TM} E soy lecithin was provided by Archer Daniels Midland Company (Minnesota, USA). Carbon dioxide (purity >999 g/kg), used as a supercritical solvent, was purchased from Airgas (Ithaca, NY, USA). The solubility measurements were conducted at three operating temperatures (60, 75 and 90 ^{o}C) and three pressures (12.41, 16.55 and 20.68 MPa).

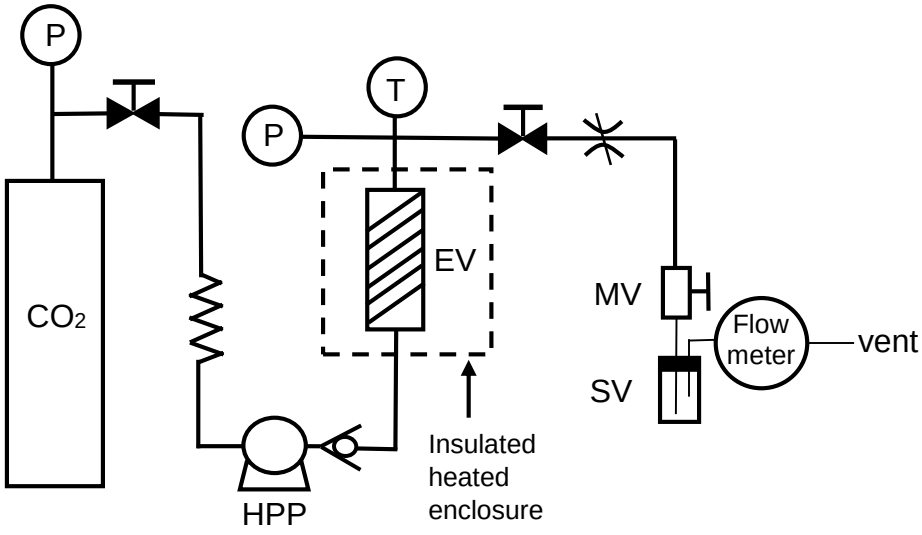

Figure 3.1. Schematic diagram of the SFT-250 SFE system used for dynamic solubility measurements of soy phospholipid in SC-CO_2. P: pressure indicators, T: temperature indicators, HPP: high pressure pump, MV: metering valve, EV: extraction vessel, SV: separation vessel.

3 grams of soy lecithin was loaded in the 100-ml EV and installed in the insulated chamber of the extraction unit. CO_2 was then introduced into the EV until the desired pressure was reached. After 30 minutes of phase equilibration, the MV was opened for the sample collection. The flow rate of SC-CO_2 was maintained at 0.67 g/minute, where the saturated solubility of a solute in SC-

CO_2 was ensured and observed to be independent of the flow-rate factor [17]. After two hours of SC-CO_2 extraction, the total amount of extracted phospholipids from soy lecithin were collected for analysis using a gravimetric method [18].

3.5. Results and discussion

As shown in Figure 3.2, the solubility of soy phospholipids in SC-CO_2 at 60, 75 and 90^oC increases with rising pressure. However, as expected, at the same pressure, the solubility decreases with the elevation of temperatures. Figure 3.3 shows the variation of SC-CO_2 density as a function of operating temperature and pressure. The SC-CO_2 density increases with rising pressure and decreases with increasing temperature. The loss of SC-CO_2 density, due to incremental changes in temperature, may cause a decline in the dissolving power of SC-CO_2. As a result, the solubility of soy phospholipids decreases with rising temperatures. The highest soy phospholipids' solubility of 0.14 % was reached at the highest operating pressure of 20.68 MPa and the lowest temperature of 60^oC in our study.

Similar solubility behavior of the phospholipids from a de-oiled soy lecithin by SC-CO_2 was reported for the dynamic solubility measurement [19]. Phosphatidylcholine (PC), phosphatidylethanolamine (PE) and phosphatidylinositol (PI) were selectively extracted from soy lecithin by SC-CO_2 at 17.2 MPa, 60 ^oC, and 2 ml/minute of SC-CO_2 flow rate. A 20:1:1 mass ratio for PC:PE:PI was measured as the composition of total phospholipid extracts. Increasing the pressure from 17.2 MPa to 20.7 MPa resulted in a larger amount of total phospholipid extracts. In contrast, it was observed that total phospholipid extracts were decreased by 70 % with the temperature rising from 60^oC to 80^oC. This finding is attributed to a decline in SCF density, which led to the loss of solvent capacity of SC-CO_2.

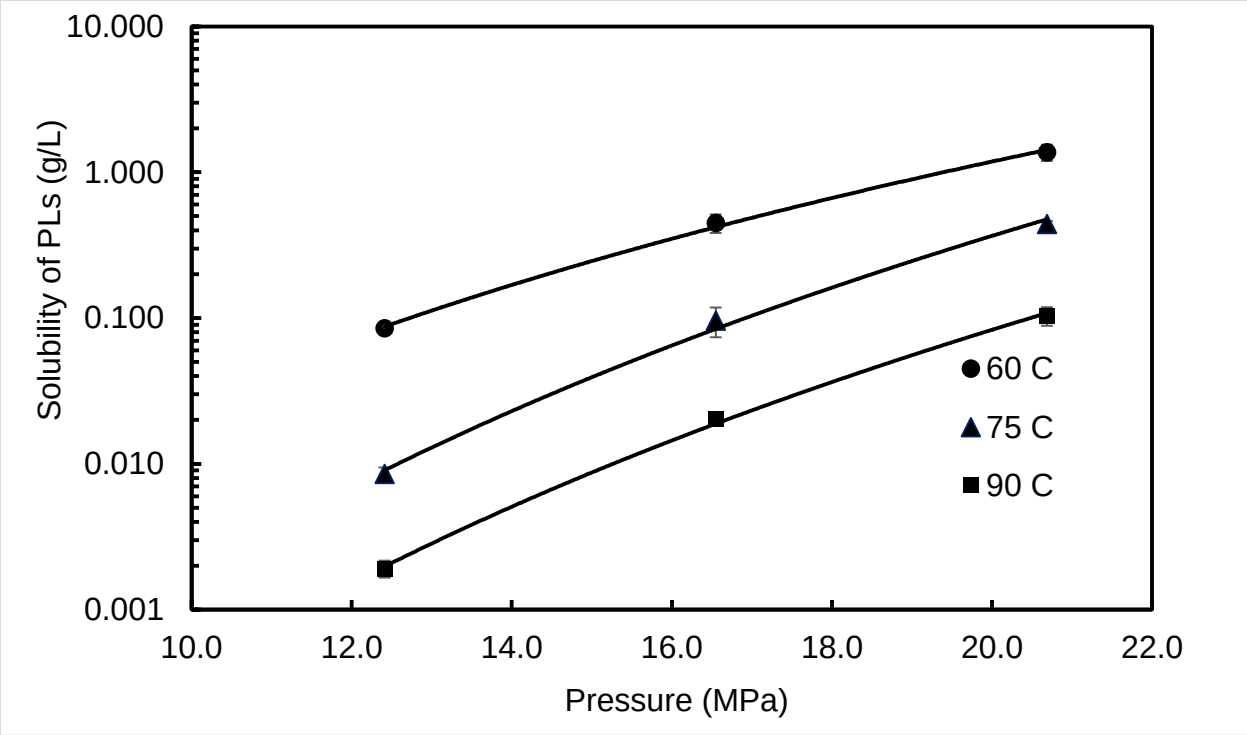

Figure 3.2. Solubility of the phospholipids from soy lecithin in SC-CO_2 as a function of operating temperature and pressure.

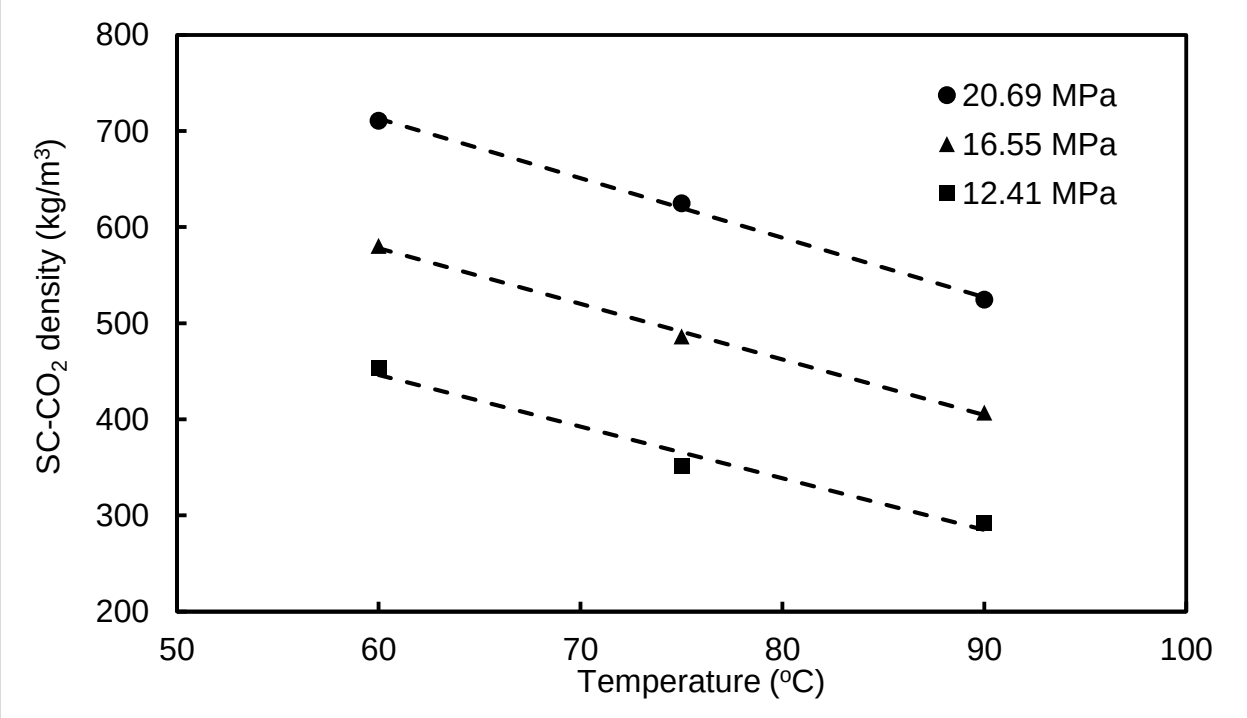

Figure 3.3. Variation of SC-CO_2 density as a function of operating temperature and pressure.

Composition of phospholipids extracts from defatted soybean flakes (DSF) using SC-CO_2 extraction has also been reported [20]. An enrichment of PC, which made up to 80 % of the total extracted phospholipids, was obtained at 23.9 MPa between 60 ^oC and 70^oC. Total extracts increased from 0.7 mg/g DSF to 8.2 mg/g DSF when the pressure was increased from 23.9 MPa to 68.9 MPa at 60^oC.

Figure 3.4 shows the correlation of the dynamic solubility data of soy phospholipids with SC-CO_2 density using the semi-empirical equations of (A) Chrastil, (B) del Valle-Aguilera, and (C) Sparks. The isotherms represent the calculated solubilities of soy phospholipids at 60, 75 and 90 ◦C, respectively. The calculated parameters of these three models are listed in Table 1. The Chrastil model is based on the assumption that the molecules of a solute associate with the molecules of a fluid to form a solvato complex, which is in equilibrium with the fluid [13]. The del Valle-Aguilera model was modified from the Chrastil model to compensate for the variation in enthalpy of a solute's vaporization with temperature. This model was verified to be well fitted with the solubility correlation of vegetable oils in SC-CO_2 [14]. In the Sparks model, a linear function of SC-CO_2 density was introduced into the association number (k) to account for the SC-CO_2 density variation on the solubility behavior of a solute in SC-CO_2. This model is particularly suitable to a solvent with reduced density of less than 1 when high pressure is applied in the process [15].

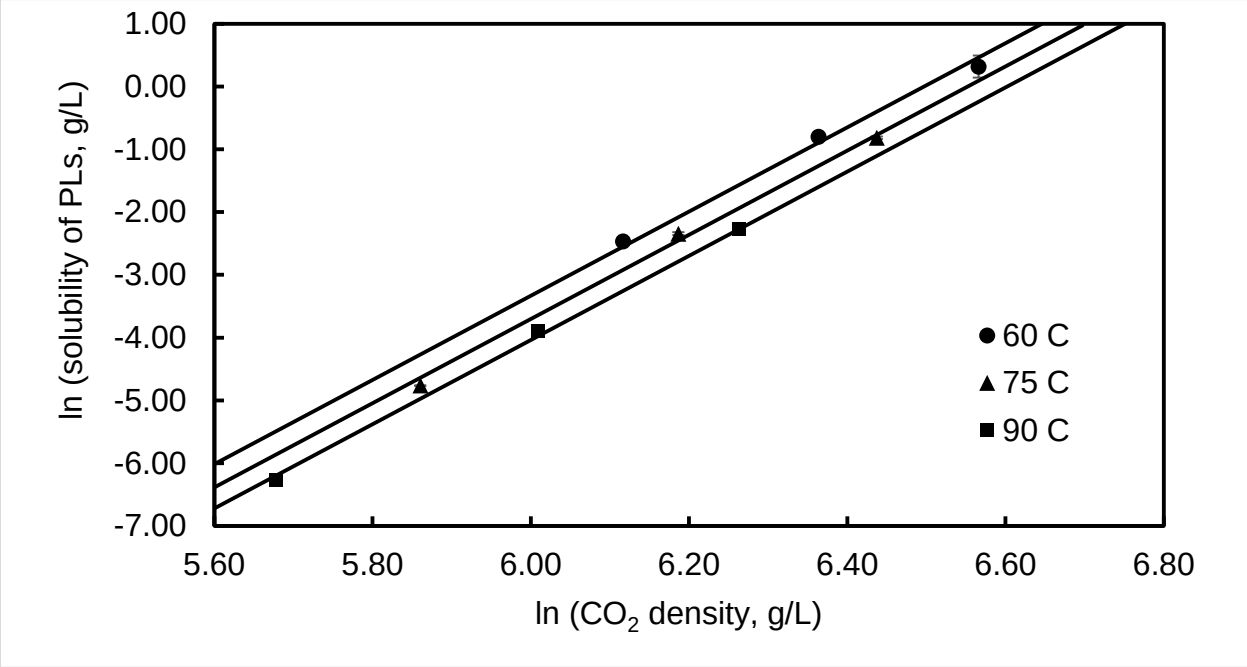

(A) The Chrastil model

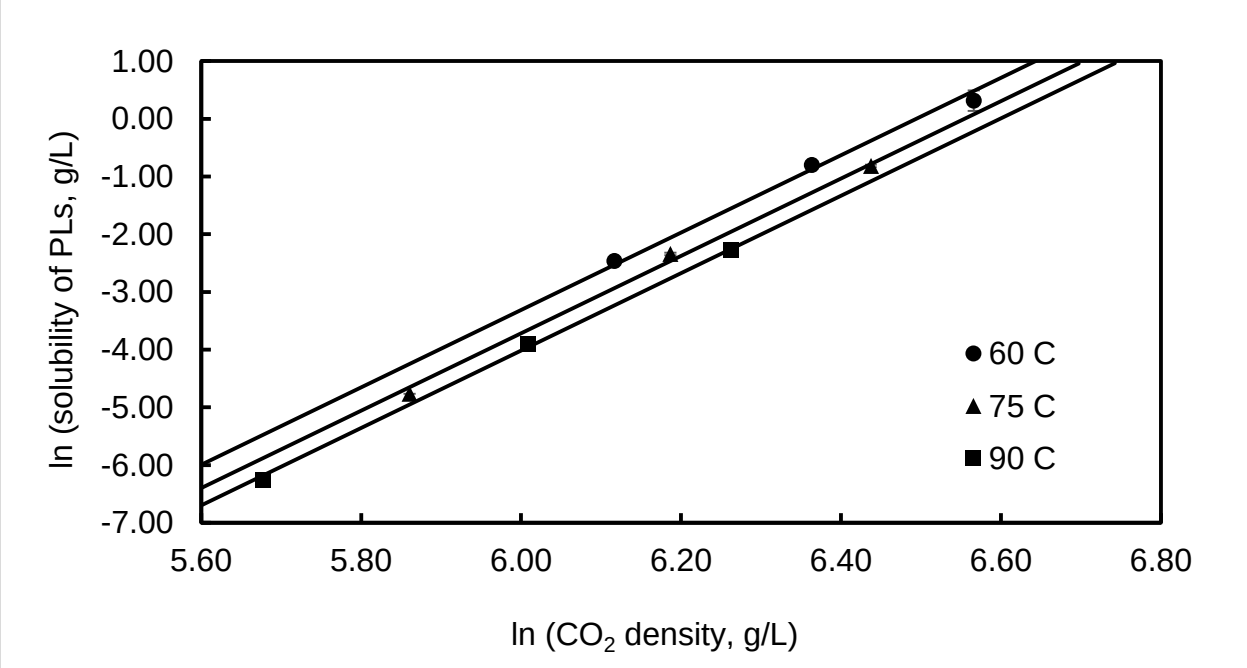

(B) The del Valle-Aguilera model

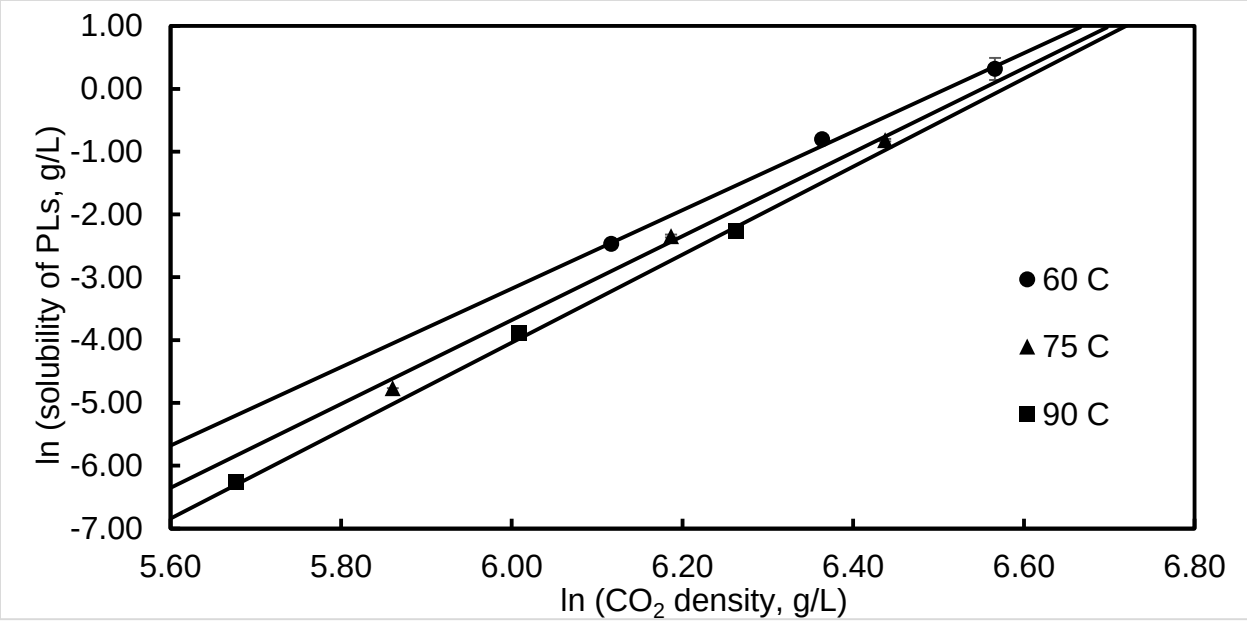

(C) The Sparks model

Figure 3.4. Correlation of soy phospholipids' solubility with SC-CO_2 density at different temperatures and pressures: (A) the Chrastil model; (B) the del Valle-Aguilera model; (C) the Sparks model.

Table 3.1. Calculated parameters for the semi-empirical solubility models

Models	Parameters						R^2
	k	c_0	c_1	c_2	c_3	c_4	
Chrastil[a]	6.7	-52.1	2843				0.99
Del Valle-Aguilera[b]	6.7	-33.2	-1.03×10^4	2.28×10^6			0.99
Sparks[c]			2.9×10^3		8.46	-5.3×10^{-4}	0.99

[a] $\ln C = k \ln \rho + c_1/T + c_0$
[b] $\ln C = k \ln \rho + c_1 / T + c_2 / T^2 + c_0$
[c] $\ln C=(c_3+c_4 * \rho)*\ln \rho + c_1 / T+c_0$

As the results show, a linear relationship was observed between the solubility data of soy phospholipids and the density of SC-CO_2 in the three models of solubility correlation. The solubility data were in good agreement with the predictive models within the range of temperatures and pressures investigated. The R^2 values were each 0.99. The association numbers were found to be 6.7 in the Chrastil and del Valle-Aguilera models, meaning more CO_2 molecules were required

to form a solvato complex for dissolution of soy phospholipids [16]. The increased SC-CO_2 density from 292.2 kg/m^3 to 710.6 kg/m^3 was the main factor for the enhanced solubility of soy phospholipids in SC-CO_2 when the pressure was increased from 12.41 to 20.68 MPa.

Table 3.2 shows the deviations of the solubility prediction of the phospholipids from soy lecithin in SC-CO_2 using the Chrastil, del Valle-Aguilera, and Sparks models. The average values of absolute average relative deviation (AARD) are 8.5 %, 8.2 %, and 4.2 %, respectively, for these three models. Most of the AARD values are less than 10 % and within the acceptable level (less than 20 %) [14, 15, 21], indicating that the accurate prediction of soy phospholipids' solubility in SC-CO_2 was well established using these density-based models. The Sparks model presented the best fit of solubility correlation with the lowest AARD values.

Table 3.2. Deviation of the predicted solubilities of soy phospholipids in SC-CO_2 using the Chrastil, del Valle-Aguilera, and Sparks equations

Model	**Pressure (MPa)**	**Temperature (°C)**		
Chrastil		**60**	**75**	**90**
	12.41	8.48	13.28	5.68
	16.55	9.14	10.28	8.26
	20.69	15.38	4.7	1.33
	***AARD (%)**	**8.5**		
Del Valle-Aguillera		**60**	**75**	**90**
	12.41	6.44	11.88	8.14
	16.55	7.12	11.40	6.12
	20.69	17.95	3.40	0.97
	***AARD (%)**	**8.2**		
Sparks		**60**	**75**	**90**
	12.41	0.59	13.55	6.00
	16.55	6.30	3.53	3.64
	20.69	1.68	2.43	6.89
	***AARD (%)**	**4.6**		

*Absolute Average Relative Deviation

3.6. Conclusions

Solubility of the phospholipids from soy lecithin in SC-CO_2 was found to increase as pressure was raised from 12.41 to 20.68 MPa and as temperature was decreased from 90 to 60 ^oC. The highest solubility of 0.14 % was reached at 20.68 MPa and 60^oC, the highest operating pressure and lowest temperature at which the solubility was tested, in the dynamic solubility measurements. A linear relationship between the solubility data and SC-CO_2 density indicated good agreement with the Chrastil, del Valle-Aguilera and Sparks models. These three semi-empirical models provided accurate solubility prediction of soy phospholipids in SC-CO_2. The lowest AARD value of 4.6 % was found in the Sparks model. Based on the results, the SC-CO_2 density is an influential factor to the solubility behavior of soy phospholipids in SC-CO_2.

References

[1] Weete, J. D.; Betageri, S.; Griffith, G. L. Improvement of lecithin as an emulsifier for water-in-oil emulsions by thermalization. *JAOCS* 1994, 71, 731-737.

[2] Torchilin, V. P. Recent advances with liposomes as pharmaceutical carriers. *Nat Rev Drug Dsicov* 2005, 4, 145-160.

[3] Verma, D. D.; Verma, S.; Blume, G.; Fahr, A. Particle size of liposomes influences dermal delivery of substances into skin. *Int J Pharm* 2003, 258, 141-151.

[4] Canty, D. J.; Zeisel, S. H. Lecithin and choline in human health and disease. *Nutr Rev* 52, 327-339.

[5] Cano-Salazar, L. F.; Juárez-Ordáz, A. J.; Gregorio-Jáuregui, K. M.; Martínez-Hernández, J. L.; Rodríguez-Martínez, J.; Ilyina, A. Thermodynamics of chitinase partitioning in soy lecithin liposomes and their storage stability. *Appl Biochem Biotechnol* 2011, 165, 1611-1627.

[6] Frederiksen, L.; Anton, K.; Hoogevest, P. V.; Keller, H. R.; Leuenberger, H. Preparation of liposomes encapsulating water-soluble compounds using supercritical carbon dioxide. *J Pharm Sci* 1997, 86, 921-928.

[7] Otake, K.; Imura, T.; Sakai, H.; Abe, M. Development of a new preparation method of liposomes using supercritical carbon dioxide. *Langmuir* 2001, 17, 3898-3901.

[8] Imura, T.; Gotoh, T.; Otake, K.; Yoda, S.; Takebayashi, Y.; Yokoyama, S.; Takebayashi, H.; Sakai, H.; Yuasa, M.; Abe, M. Cortrol of physicochemical properties of liposomes using a supercritical reverse pahse evaporation method. *Langmuir* 2003, 19, 2021-2025.

[9] Castor, T. P. Phospholipid nanosomes. *Curr Drug Delivery* 2005, 2, 329-340.

[10] Lesoin, L.; Crampon, C.; Boutin, O.; Badens, E. Development of a continuous dense gas process for the production of liposomes. *J Supercrit Fluids* 2011, 60, 51-62.

[11] Cabrera, I.; Elizondo, E.; Esteban, O.; Corchero, J. L.; Melgarejo, M.; Pulido, D.; Córdoba, A.; Moreno, E.; Unzueta, U.; Vazquez, E.; Abasolo, I.; Simó Schwartz, J.; Villaverde, A.; Albericio, F.; Royo, M.; García-Parajo, M. F.; Ventosa, N.; Veciana, J. Multifunctional

nanovesicle-bioactive conjugates prepared by a one-step scalable method using CO_2-expanded solvents. *Nano lett* 2013, 13, 3766-3774.

[12] Yu Z. R.; Bhajmohan Singh; Rizvi, S. S. H. Solubilities of fatty acids, fatty acid esters, triglycerides, and fats and oils in supercritical carbon dioxide. *J Supercrit Fluids* 1994, 7, 51-59.

[13] Chrastil, J. Solubility of solids and liquids in supercritical gases. *J Phys Chem* 1982, 86, 3016-3021.

[14] Valle, J. M. d.; Aguilera, J. M. An improved equation for predicting the solubilityof vegetable oils in supercritical CO_2. *Ind Eng Chem Res* 1988, 27, 1551-1553.

[15] Sparks, D. L.; Hernandez, R.; Estevez, L. A. Evaluation of density-based models for the solubility of solids in supercritical carbon dioxide and formulation of a new model. *Chem Eng Sci* 2008, 63, 4292-4430.

[16] Tsai, W. C.; Ruan, Y.; Rizvi, S. S. Solubility measurement of methyl anthranilate in supercritical carbon dioxide using dynamic and static equilibrium systems. *J Sci Food Agric* 2006, 86, 2083–2091.

[17] Salgın, U.; Salgın, S. Effect of main process parameters on extraction of pine kernel lipid using supercritical green solvents: solubility models and lipid profiles. *J Supercrit Fluids* 2013, 73, 18-27.

[18] Tejera-Garcia, R.; Connell, L.; Shaw, W. A.; Kinnunen, P. K. J. Gravimetric determination of phospholipid concentration. *Chem Phys Lipids* 2012, 165, 689-695.

[19] Teberikler, L.; Koseoglu, S.; Akgerman, A. Selective extraction of phosphatidylcholine from lecithin by supercritical carbon dioxide/ethanol mixture. *J Am Oil Chem Soc* 2001, 78, 115-120.

[20] Montanari, L.; Fantozzi, P.; Snyder, J. M.; King, J. W. Selective extraction of phospholipids from soybeans with supercritical carbon dioxide and ethanol. *J Supercrit Fluids* 1999, 14, 87-93.

[21] Salgın, U. G.; Salgın, S. Effect of main process parameters on extraction of pine kernel lipid using supercritical green solvents: solubility models and lipid profiles. *J Supercrit Fluids* 2013, 73, 18-27.

Chapter 4: Synthesis of liposomal vesicles by a novel supercritical fluid process

4.1. Abstract

A new technique of liposomal microencapsulation, composed of supercritical fluid (SCF) extraction, rapid expansion of a supercritical solution, and vacuum-driven cargo loading, was successfully developed. It aims to be a non-toxic continuous process based on the flow-through design and without usage of any organic solvent. Liposomal microencapsulation using the SCF process was conducted at three pressures (8.27, 12.41, 16.55 MPa), three temperatures (75, 83 and 90 ^{o}C) and two cargo loading rates (0.25 ml/second and 0.5 ml/second). Liposome size, zeta-potential, and encapsulation efficiency were characterized as functions of the operating parameters. The average liposome size varied from 400-500 nm to 900-1200 nm as the pressure was increased. For the liposomal microencapsulation of 0.2 M glucose solution, it was found that the highest encapsulation efficiency of 31.6 % was reached at the following condition: the middle expansion pressure of 12.41 MPa, highest expansion temperature of 90 ^{o}C, and lowest cargo loading rate of 0.25 ml/second. Under a confocal laser scanning microscope, the large unilamellar vesicles (LUVs) and multivesicular vesicles (MVVs) were observed to be a majority of the liposomal emulsion produced by this novel SCF technique.

Keywords: supercritical carbon dioxide, rapid expansion of supercritical solutions, microencapsulation, liposome, size, zeta potential, non-toxic, morphology

4.2. Introduction

Liposomes are the self-assembled spherical vesicles with one or more phospholipid bilayers separating an inner aqueous environment from the outer aqueous medium. They have long been used as models for the studies on biological membranes due to their similarity to real cell membranes. The compound of interest is securely encapsulated in the inner aqueous core protected by one or more phospholipid bilayers. Based on the size and lamellarity, liposomes can be categorized into four types: small unilamellar vesicles (SUVs), large unilamellar vesicles (LUVs), multilamellar vesicles (MLVs) and multivesicular vesicles (MVVs). The liposome size of SUVs varies from 20 to approximately 100 nm, whereas the sizes of LUVs, MLVs, and MVVs range from a few hundred nanometers to microns. The thickness of one phospholipid bilayer is approximately 4 to 5 nm [1].

Liposomal microencapsulation has drawn significant interest in the pharmaceutical industry. This technique can enhance the functionality of certain pharmaceuticals, such as the solubility improvement, controlled release and targeted delivery [2-4]. With this method evolved, it has started recently to be applied in the food industry for microencapsulation of antioxidants, enzymes, and nutraceuticals [5-7]. LUV is always preferred in the food industry due to its higher encapsulation efficiency, simpler process, and better stability [8]. Adding cholesterol, surfactants, or carbohydrate into the phospholipid bilayer can modify the rigidity, fluidity, and permeability of the liposomal membrane for specific purposes [9-11].

Traditionally, liposomes are prepared by thin film hydration (TFH), reverse phase evaporation (REV), and membrane extrusion. In recent years, due to the concern of organic solvent toxicity, several new techniques have been attempted to reduce or even completely avoid the use of organic solvents in the liposomal microencapsulation, including microfluidics, rapid expansion

of supercritical solutions (RESS), supercritical reverse phase evaporation (SCRPE) and several dense gas processes [12-18].

When the pressure and temperature are increased above the critical point of a gas or liquid, the vaporization line of the compound disappears. The homogenous phase is created and called the supercritical fluid (SCF) state. It exhibits some advantageous properties: low viscosity, enhanced solvating power, flexible density, optimal diffusivity, and better mass transfer rate. A number of compounds, such as carbon dioxide, ethanol, nitrogen, and propane, have been used in their supercritical state. Carbon dioxide is the most preferable candidate for the food industry due to its nontoxicity, environmentally friendly attributes, and economical cost. Supercritical carbon dioxide (SC-CO_2) is a density-adjustable fluid with solvent behavior similar to hexane. Its moderate critical pressure (7.4 MPa) and low critical temperature (31.1 ^oC) make SC-CO_2 an ideal candidate for biomaterial processing, including extraction of heat labile compounds, nonthermal pasteurization, and enzyme-catalyzed reactions [19-21]. The SCF microencapsulation is a novel concept and more studies are needed to determine its practicability. Different SCF processes for liposomal microencapsulation are briefly described below.

4.2.1. Rapid expansion of a supercritical solution (RESS)

The RESS technique was tested for liposomal microencapsulation of the hydrophilic FITC-dextran [13]. 1-palmitoyl-2-oleoylphosphatidylcholine (POPC) and cholesterol in a 7:3 molar ratio were weighed and loaded in the cartridge guard column. The column was installed in the high pressure recycling system. SC-CO_2 was introduced into the recycling system up to 25 MPa at 60 ^oC, with 4.8 % (v/v) addition of absolute ethanol as co-solvent. Ethanol and SC-CO_2 were homogenously mixed by the dynamic mixer before entering the recycling system. Without the

addition of ethanol, it was observed that no liposome was formed due to very low solubility of POPC in SC-CO_2. Thirty minutes of recycling was required to reach the saturated solubilities of POPC and cholesterol in SC-CO_2. The POPC and cholesterol-laden SC-CO_2 was then introduced into a encapsulation capillary (0.5 mm I.D.) by a back pressure regulator (BPR) controlling the flow rate at 5 ml/minute. The FITC-dextran solution was pumped into the encapsulation capillary at 40 µl/minute. The encapsulation efficiency was significantly raised from 1% to 15 % with the capillary inner diameter reducing from 0.5 mm to 0.25 mm. A static mixer was inserted between the capillary and collection flask to suppress foam formation while the final liposomal emulsion in the expansion system was recirculated to completely recover all liposomes. The size of multilamellar liposomes produced in this condition were found to be between 180 and 200 nm, with medium polydispersity.

4.4.2. Supercritical reverse phase evaporation (SCREP)

This technique is similar to the reverse phase evaporation method for liposomal microencapsulation, only with the substitution of SC-CO_2 for the organic solvent. The practicability of SCREP was first established by Otake et al., 2001 [22]. In this process, the soy phospholipids were sealed in the view cell followed by introducing SC-CO_2 up to the desired pressure between 12 and 30 MPa. The operating temperature was set at 60 ^{o}C. After the phase equilibrium was reached, 0.2 M D-(+)-glucose solution was introduced the view cell via a HPLC pump in the rate of 0.05 ml/minute. SC-CO_2 was then rapidly released to form large unilamellar vesicles (LUVs) with diameters of 0.1 to 1.2 µm. It was optional to add ethanol in the supercritical solution as cosolvent, which would enhance the encapsulation efficiency of the liposomes. Varying the operating pressure had a significant influence on the size distributions of the resultant

liposomes. The size of the liposomes prepared at the pressure below 20 MPa were found to be larger than that above 20 MPa [23]. Below 20 MPa, the encapsulation efficiency was higher with increasing SC-CO_2 pressure as well as SC-CO_2 density. A depressurization rate of SC-CO_2 less than 1 MPa/minute assured larger liposomal size and higher encapsulation efficiency [17]. The effect of molecular structures of various soy phospholipids on liposomal microencapsulation using SCREP was investigated. It was found that the zwitterionic structure of phosphatidylcholine (PC) contributed to an efficient formation of LUVs and a high encapsulation efficiency for hydrophilic compounds [24].

This study aimed to develop a novel SCF process for liposomal microencapsulation. This process consisted of the SCF extraction followed by rapid expansion of a supercritical solution, and vacuum-driven cargo loading. SC-CO_2 was chosen as the sole lecithin-dissolving medium to replace organic solvents used in traditional methods. The liposomal formation was an instant reaction requiring only 1 to 2 seconds for each run of microencapsulation. Liposome size, zeta potential, encapsulation efficiency (EE) were measured for the SCF liposomes produced at different combinations of pressures, temperatures, and cargo loading rates. The morphology of the liposomes was visualized under a confocal laser scanning microscope (CLSM). The effects of operating parameters were evaluated for their impacts on the formation of liposomes to determine the optimal operating condition.

4.3. Material and methods

Performix^{TM} E soy lecithin was provided by Archer Daniels Midland Company. Cholesterol (95% purity), a hexokinase assay kit, and fluorescent dyes, Nile Red and fluorescein isothiocyanate (FITC), were purchased from Sigma-Aldrich (St. Louis, MO 63103). Tris (hydroxylmethyl)

aminomethane (TRIS) was purchased from Bio-Rad (Hercules, CA 94547). D-glucose was purchased from Mallinckrodt Baker (Center Valley, PA 18034). Carbon dioxide (purity >999 g/kg), used as a supercritical solvent, was purchased from Airgas (Ithaca, NY, USA).

4.3.1. Preparation of fluorescent dyes

0.2 % (w/w) of Nile Red in ethanol was prepared by adding 40 mg of Nile Red to 20 grams of absolute ethanol, followed by vigorously mixing until the Nile Red was completely dissolved in ethanol. 5 mM FITC in pH 7.4 TRIS buffer was prepared as the liquid cargo solution.

4.3.2. Experimental design

The SCF liposomal microencapsulation was conducted at three pressures (8.27, 12.41, and 16.55 MPa), three temperatures (75, 83, and 90 ^{o}C), and two cargo loading rates (0.25 ml/second, 0.5 ml/second). The liposomes were characterized for their size distribution, zeta potential, encapsulation efficiency, and morphology.

4.3.3. Preparation of liposomal microencapsulation

2 grams of Performix E soy lecithin was well mixed with cholesterol in a 10:1 mass ratio. Adding cholesterol enhances the rigidity of the liposomal membrane by changing interactions between both the polar head groups and the hydrocarbon chain in the phospholipid layer. A decrease in the melting point and the transit enthalpy of the lecithin/cholesterol mixture was also observed [25]. The lecithin/cholesterol mixture was stored at 4 ^{o}C to be solidified for loading convenience.

The SCF microencapsulation system used for the preparation of liposomes has been described in Figure 2.1 (Chapter 2). The system consisted of three parts: a high pressure pump (HPP), a mixing vessel, and an expansion nozzle. Different areas of the SCF system were heated by glass wool heating tapes and controlled by Variable Autotransformers (Type 3PN1010, 120 V for input and 0-120V for output, Staco Energy Products, Co., Dayton, OH 45403). The detailed nozzle configuration has been illustrated in Figure 2.4 (Chapter 2). The perpendicular nozzle mixed the lecithin/cholesterol-laden SC-CO_2 with the cargo solution vertically for optimal blending condition.

The solidified lecithin/cholesterol mixture was loaded into the 1-L mixing vessel. CO_2 was then introduced by HPP up to 20.68 ± 0.3 MPa at 60 ± 1 ^oC. After at least two hours of phase equilibrium, the lecithin/cholesterol-laden SC-CO_2 was directed from the vessel to the expansion nozzle for liposomal microencapsulation. The nozzle pressure was maintained by a forward pressure regulator (FPR, Model 44-1124-24-131, 68.94 MPa for maximum input and 17.24 MPa for maximum output, TESCOM, Elk River, MN 55330) at 8.27, 12.41, and 16.55 MPa, respectively. The nozzle was maintained at 90 ± 2 ^oC to avoid the Joule-Thomas effect resulting from SC-CO_2 expansion [26]. During the entire operation, fresh CO_2 was continuously introduced into the mixing vessel where the pressure was maintained and excessive CO_2 was re-circulated by a back pressure regulator (BPR, Model L98377, 0.34-41.37 MPa for controlled pressure range, TESCOM, Elk River, MN 55330) as shown in the dashed arrows in Figure 2.1.

When SC-CO_2 expanded in the nozzle chamber, the phospholipid/cholesterol mixture began to nucleate as tiny particles, due to the decrease in pressure from high pressure to ambient pressure. Simultaneously, the vacuum was built up in the range of 3 to 5 mmHg due to the vena contracta effect when SC-CO_2 was passed through the 1000-micron perpendicular nozzle. The cargo

solution containing 0.02 mM pH 7.4 TRIS buffer or 0.2 M d-glucose solution was drawn into the chamber by this vacuum force and broken into small water droplets by the SC-CO_2 stream while shell material mixed with the core material. As a result, the liposomes were formed in a one-step process of approximately 1 to 2 seconds for each run. Fourteen to sixteen runs were conducted for one experiment. The emulsion containing liposomes in a pH 7.4 TRIS buffer was collected in the glass tray for further analysis.

4.4. Mechanism

The behavior of a fluid flowing through a small circular nozzle is illustrated in Figure 4.1. Based on the Bournelli principle, the fluid velocity increases around the section where the flow is contracted, which creates a vacuum in this contracted area. This vacuum point is called Vena Contracta. The mechanism of the supercritical fluid (SCF) process proposed for liposomal microencapsulation is described in Figure 4.1. When the phospholipid-laden SC-CO_2 flows through the nozzle, the cross section of the fluid decreases. The cargo solution would then be drawn into the nozzle chamber by the vacuum and broken into small droplets by strong impact of the SC-CO_2 stream. Simultaneously, rapid pressure drop in the expansion chamber would also trigger lecithin nucleation to form fine particles, because of drastic decrease of the phospholipids' solubility in SC-CO_2. As a result, when these tiny amphiphilic lipid particles are blended with cargo droplets inside the chamber, the phospholipid bilayer may assemble and surround around these aqueous droplets to form liposomes.

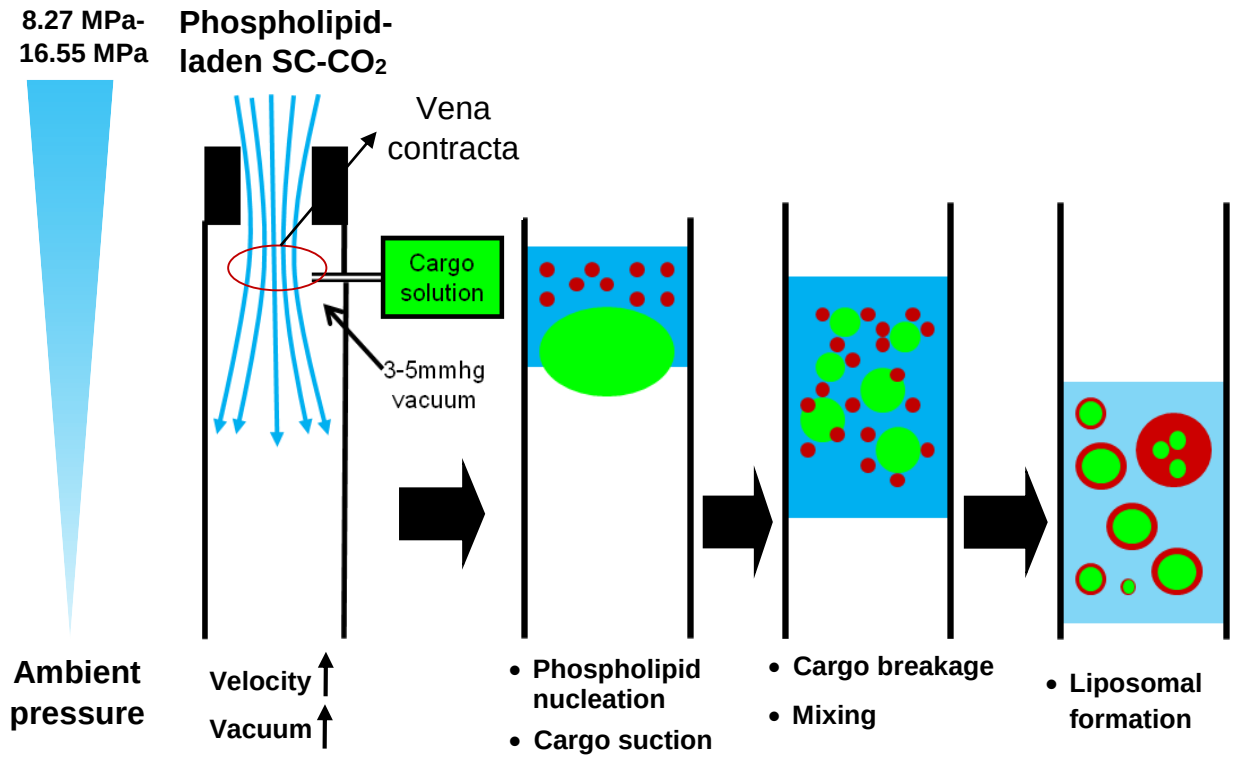

Figure 4.1. Mechanism of the SCF process for liposomal microencapsulation.

4.5. Characterization of liposomes

4.5.1. Size distribution

Size distribution of the liposomes was conducted using the 90 PLUS particle size analyzer (Brookhaven Instruments Corporation, Holtsville, NY 11742). 250 µl of liposomal emulsion was diluted with TRIS pH 7.4 buffer for to 10 ml of total volume. 3.5 ml of the diluted liposomal emulsion was poured in a 3.5-ml cuvette to evaluate the size distribution.

4.5.2. Zeta potential

Zeta potential of the liposomes was measured using the 90 PLUS particle size analyzer. 25 µl of liposomal emulsion was diluted with a TRIS pH 7.4 buffer for 10 ml of total volume. 1.2 to 1.5 ml of the diluted sample was analyzed for the surface charge of liposomes.

4.5.3. Encapsulation efficiency

The measurement of encapsulation efficiency (EE) for liposomal microencapsulation was modified from Manosroi et al. (2008) [27]. 0.5 ml of liposomal emulsion encapsulating 0.2 M D-glucose solution was loaded in the dialysis tube and dialyzed against 500 ml of 0.02 M TRIS pH 7.4 buffer for 12 hours to completely remove unencapsulated glucose. The temperature was maintained at 4 ^{o}C during dialysis. The buffer was changed every 3 hours. 120 µl of the purified liposomes was mixed with 880 µl of 4 % Triton solution, shaken, and left to settle for at least 3 minutes. 20 µl of the purified sample was analyzed using the hexokinase assay kit (Sigma-Aldrich) and measured spectrophotometrically at 340 nm for the optical density (OD) values. The EE of D-glucose in the SCF liposomes was calculated as a percentage according to the following equation.

EE (%) = (glucose concentration in dialyzed SCF liposomes / glucose concentration of the cargo solution) × 100

4.5.4. Morphology

1 ml of the liposomal emulsion was mixed with 3 to 4 drops of Nile Red in ethanol (0.2% w/w). After 1 minute of mild blending, 0.3 ml of the sample was put on a well slide and visualized under a Leica confocal laser scanning microscope (CLSM) with the 10× ocular lens and the 100× oil-phase objective lens for the morphology of SCF liposomes. The fluorescent emission wavelength of Nile Red was set at 558 to 635 nm and fluorescein isothiocyanate (FITC) was at 496-535 nm.

4.6. Results and discussion

4.6.1. Size distribution

Figure 4.2 shows the size distribution of liposomes produced using the novel SCF process under three pressures (8.27, 12.41, and 16.55 MPa) at 90 ^{o}C. A unimodal distribution of liposome size was observed within the pressure range studied. The liposome sizes at 12.41 and 16.55 MPa were found to be within 900 and 1700 nm, while the size distribution at 8.27 MPa was between 300 and 780 nm. Because of the unimodal size distribution, average liposome sizes were characterized as functions of operating pressure, temperature, and cargo loading rate.

Figure 4.3 shows the average sizes of the SCF liposomes measured at different pressures and temperatures. The isotherms represent 75, 83, and 90 ^{o}C, respectively. The cargo loading rate was set at 0.25 ml/second. The liposome size increased from approximately 400 nm to 1200 nm with the pressure rising from 8.27 MPa to 16.55 MPa. At the middle expansion pressure of 12.41 MPa, the smallest variation of the liposome size at different temperatures was observed, indicating that an efficient heat input minimized the breakage and aggregation of liposomes caused by the freezing effect during CO_2 expansion. In addition, the middle operating pressure provided a positive effort on mixing the cargo and phospholipids for liposomal microencapsulation during rapid expansion of SC-CO_2 in the nozzle.

For the 83 and 90 ^{o}C isotherms, the liposome size slightly decreased when the expansion pressure was increased from 12.41 MPa to 16.55 MPa. A similar trend has been reported for liposomal microencapsulation of sirolimus using the process of rapid expansion of a supercritical solution (RESS). The average liposome size slightly decreased from 500 nm to approximately 400 nm when the pressure was raised from 35 MPa to 40 MPa. As a small molecule, CO_2 may penetrate the membranes consisted of swollen phospholipid bilayers. The phospholipid bilayers are likely to

burst during rapid expansion of the SC-CO_2 solution, which decreased the vesicle size of liposomes [28].

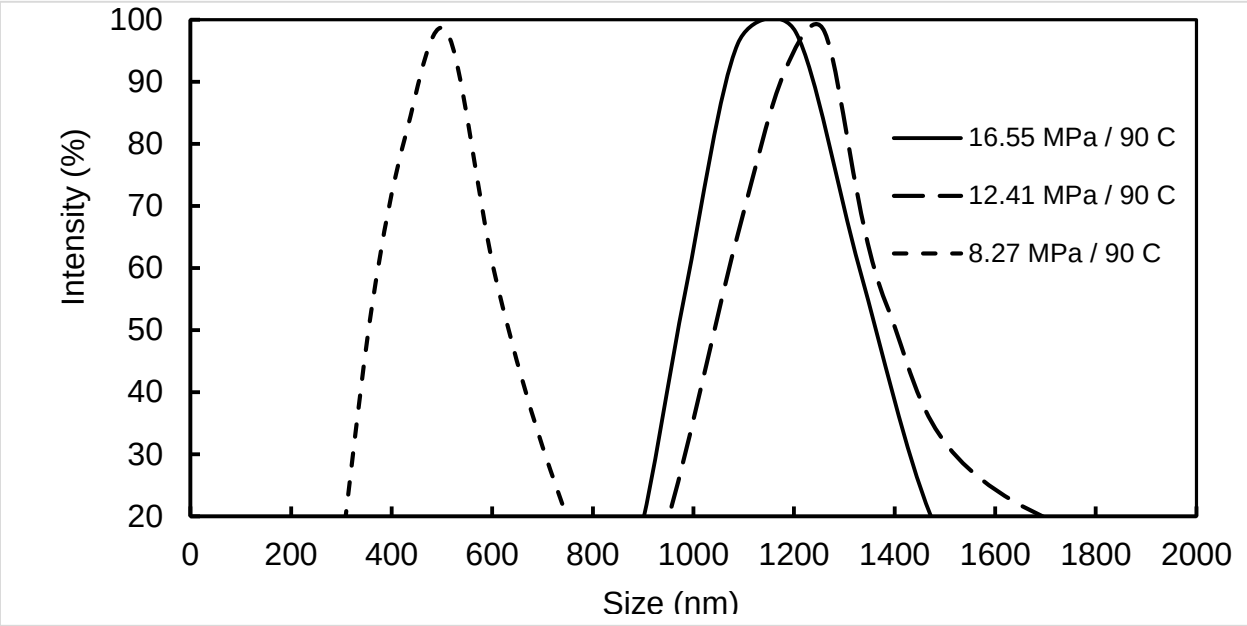

Figure 4.2. Size distribution of liposomes produced at 8.27, 12.41, 16.55 MPa, and 90 ºC.

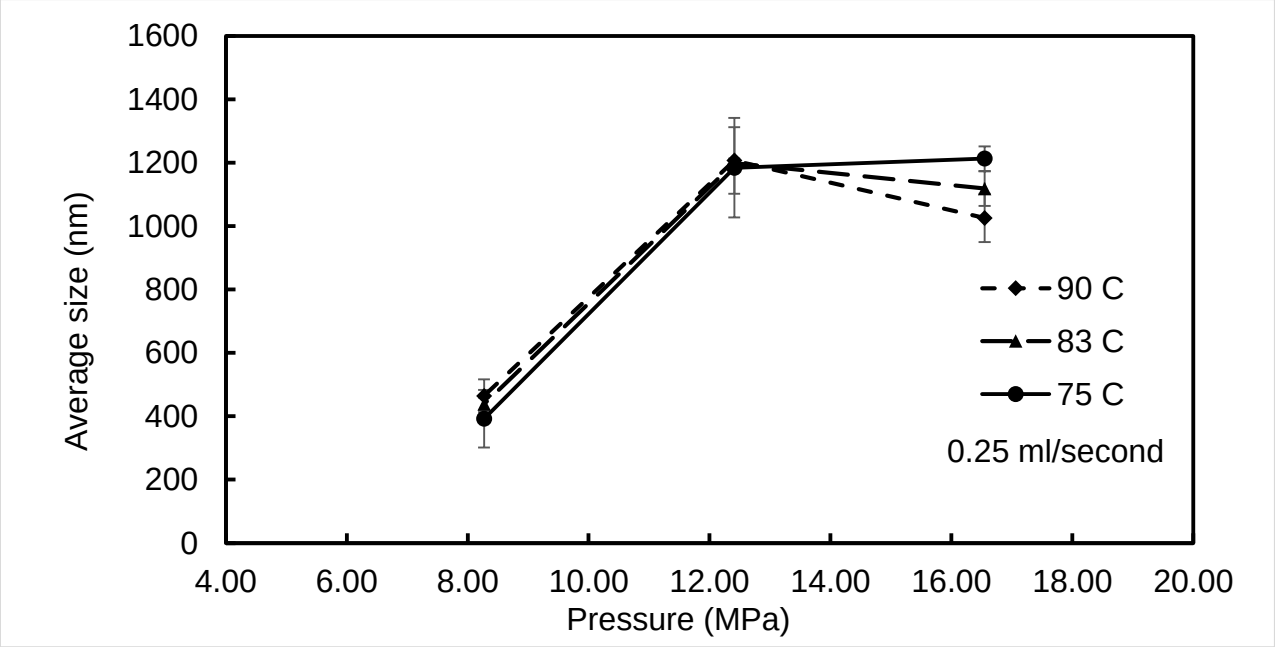

Figure 4.3. Size distribution of the liposomes produced using the SCF process at different temperatures and pressures. Cargo loading flow rate: 0.25 ml/second.

At 16.55 MPa, the average size of the liposomes produced at the lowest temperature (75 ^{o}C) was found to be larger than those at 83 and 90 ^{o}C. The Joule-Thomas effect during SC-CO_2 expansion occurred in the nozzle, and resulted in the damage and aggregation of the SCF liposomes generated at lower temperature.

Figure 4.4 shows a similar trend in the variation in average sizes of the liposomes produced at a cargo loading rate of 0.5 ml/second within the same range of expansion pressure and temperature. The liposome size was increased with rising pressure. At 16.55 MPa, the average sizes of liposomes produced at 83 and 90 ^{o}C were found to be smaller than that generated at 75 ^{o}C.

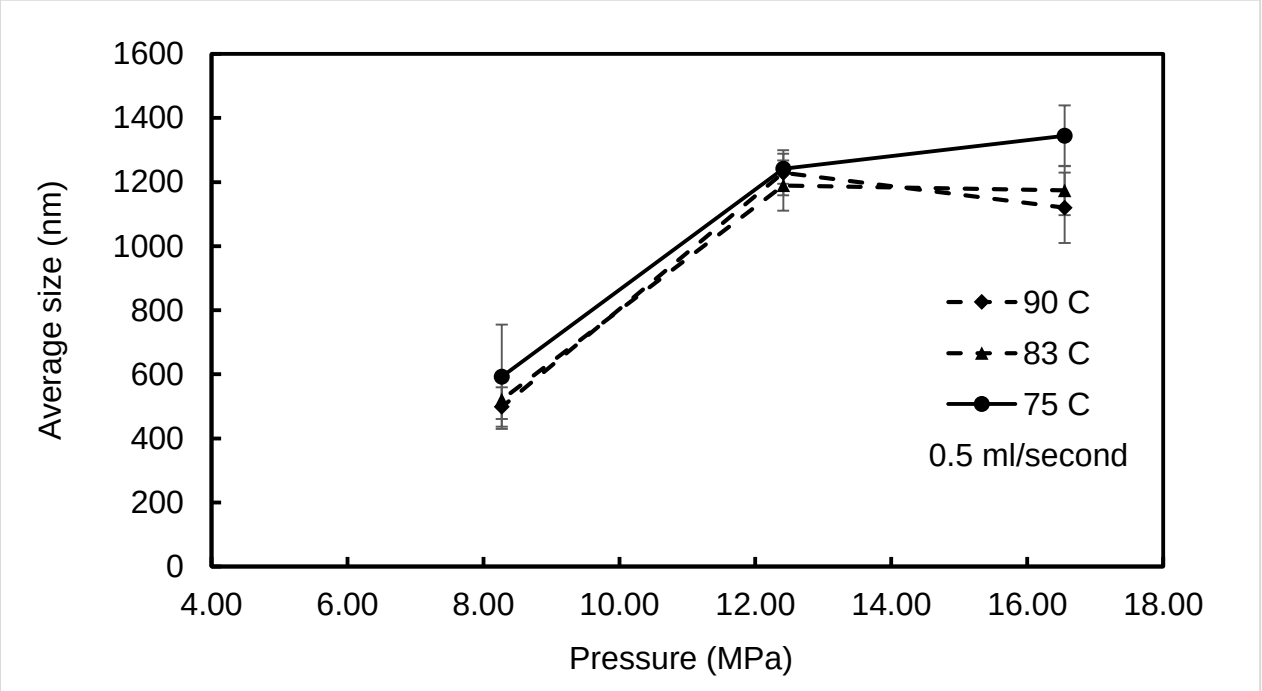

Figure 4.4. Size distribution of the liposomes produced using the SCF process at different temperatures and pressures. Cargo loading rate: 0.5 ml /sec

Expansion pressures and cargo loading rates of TRIS pH 7.4 buffer were evaluated for their effects on size variation of liposomes. Figure 4.5 shows the average liposome size measured at three expansion pressures, two cargo loading rates, and 90 ^{o}C. In this semi-logarithmic model, the liposome size increased from 464-498 nm to 1025-1228 nm when the pressure was raised from

8.27 MPa to 16.55 MPa. Based on these results, the cargo loading rates did not have a significant effect on the variation of liposome sizes. Expansion pressure accounted for the major influence on liposomal formation using the SCF process. In Figures 4.6 and 4.7, similar trends of size variation of SCF liposomes produced at 83 and 75 ^{o}C were observed.

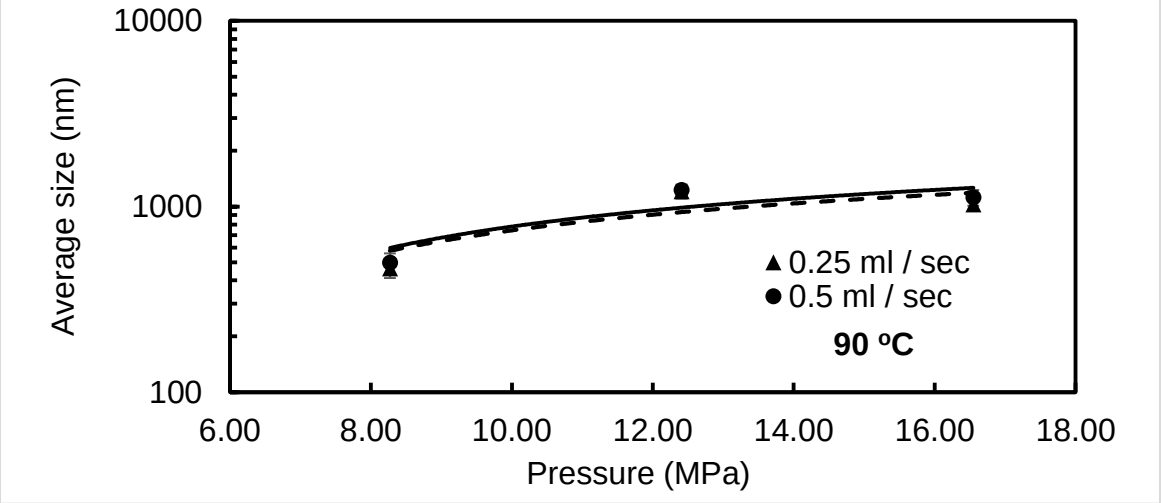

Figure 4.5. Size variation of the liposomes produced using the SCF process and characterized as function of cargo loading rate and pressure at 90 ^{o}C.

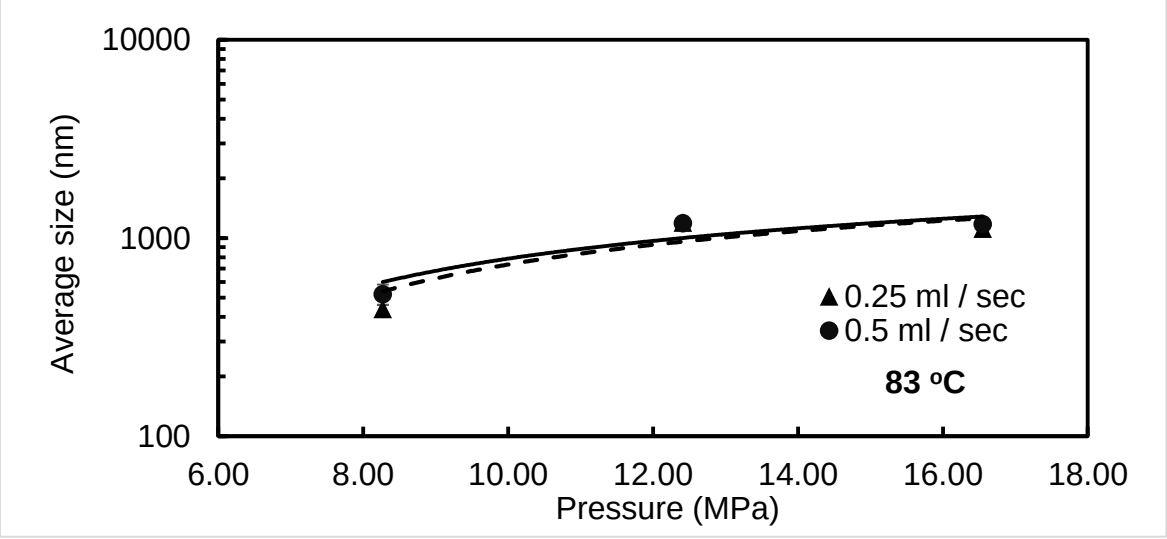

Figure 4.6. Size variation of the liposomes produced using the SCF process and characterized as function of cargo loading rate and pressure at 83 ^{o}C.

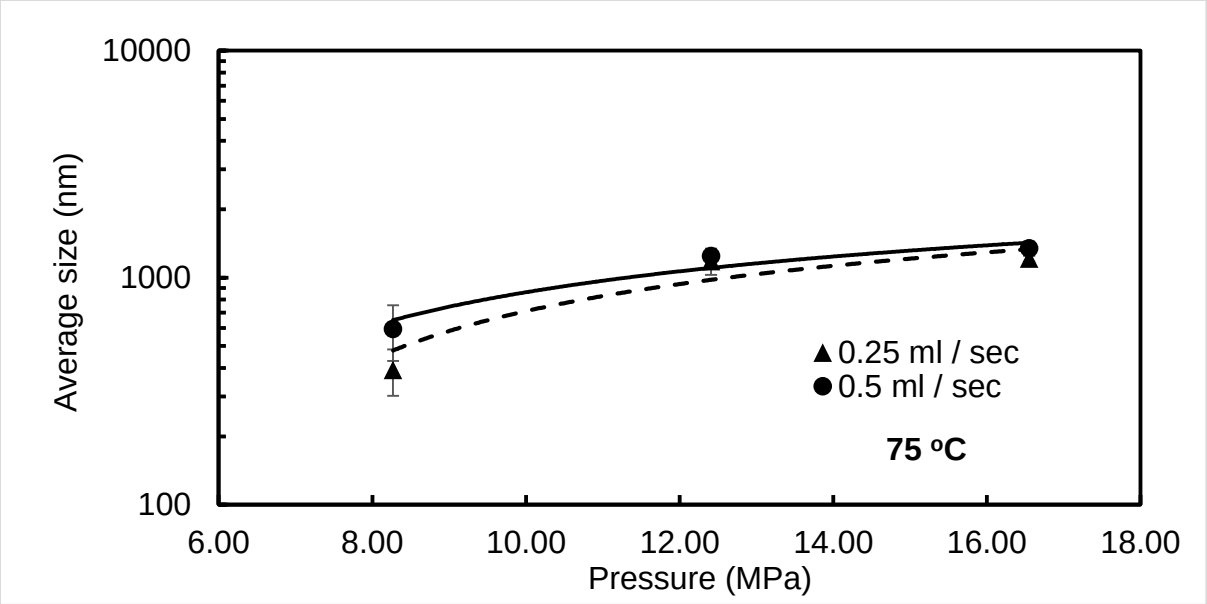

Figure 4.7. Size variation of the liposomes produced using the SCF process and characterized as function of cargo loading rate and pressure at 75 ºC.

4.6.2. Zeta potential

The surface charge provides the repulsive force for the stability of a colloidal system. Below -30 mV of zeta potential, the emulsion presents a good shelf-life stability [29]. Table 4.1 shows the zeta potential values of liposomes produced using the SCF process at different operating conditions. The zeta potential values of liposomal emulsions were found to vary between -47 and -54 mV, which indicates that good emulsion stability was sustained in the SCF liposomes. At different temperatures, the zeta potential values were observed to slightly increase as the pressure was raised from 8.27 MPa to 16.55 MPa. It has been reported that the solubilities of phosphatidylethanolamine (PE) and phosphatidylinositol (PI) in SC-CO_2 increased with pressure rising from 16.6 MPa to 68.9 MPa at 60 and 80 ºC, which increased the negative charge of phospholipid membranes [30].

Table 4.1. Zeta potential values of the liposomes produced using SCF microencapsulation process at different temperatures, pressures and cargo loading rates

0.25 ml/second	Zeta potentials (mV)		
Pressures (MPa)	**75**	**83**	**90**
16.55	-53.72±2.02	-54.72±1.29	-53.77±1.92
12.41	-51.66±1.96	-53.33±1.15	-53.46±1.22
8.27	-50.18±1.39	-52.56±0.75	-51.15±1.44

0.5 ml/second	Zeta potentials (mV)		
Pressures (MPa)	**75**	**83**	**90**
16.55	-50.62±1.72	-50.80±2.22	-50.1±1.94
12.41	-48.73±1.75	-50.16±2.00	-49.91±1.43
8.27	-47.59±2.46	-48.26±1.44	-47.35±1.93

4.6.3. Encapsulation efficiency

Encapsulation efficiency (EE) of 0.2 M D-glucose solution in the liposomes at different expansion temperatures and pressures are presented in Table 4.2. It was found that EE increased with the temperature rising from 75 to 90 ^{o}C in the pressure range of 8.27 MPa to 16.55 MPa. At the same temperature, the EE varied in the following descending order: 12.41 MPa, 16.55 MPa, and 8.27 MPa. The highest EE of 31.65 % was reached at 12.41 MPa and 90 ^{o}C with a glucose loading rate of 0.25 ml/second. Higher operating temperatures provides sufficient heat to minimize the damage and aggregation of the SCF liposomes in the expansion nozzle, due to the drastic freezing effect during rapid expansion of SC-CO_2. In addition, the phospholipids and aqueous cargo are thoroughly mixed when the operating temperature was raised above the phase transition temperature of soy phospholipids (40 to 42 ^{o}C). Therefore, the EE increased with the elevation of temperature. A similar trend of the temperature effect has been reported for liposomal microencapsulation of the Atractylodes oil using a modified RESS technique. The coating material

were phosphatidylcholine and cholesterol in a 3:1 mass ratio. The Atractylodes oil and lipid mixture were blended in a 1:20 mass ratio for the RESS microencapsulation. The results showed that the EE of the Atractylodes-oil-entrapped liposomes increased from 20 % to 80 % when the temperature was increased from 40 ^{o}C to 60 ^{o}C.

Table 4.2. Encapsulation efficiency of liposomes at different temperatures and pressures

	Encapsulation efficiency (%)		
Pressure (MPa)	**75**	**83**	**90**
16.55	13.04±0.03	15.62±0.01	17.77±0.02
12.41	16.52±0.01	23.86±0.02	31.65±0.03
8.27	2.26±0.01	4.55±0.03	6.37±0.01

Cargo loading rate: 0.25 ml/second

On the other hand, higher operating pressure enhances the solvating power of SC-CO_2 for more phospholipids dissolved in the supercritical solution. During rapid SC-CO_2 expansion in the nozzle, tiny phospholipid particles homogenously nucleate, instead of aggregating. Moreover, the stronger SC-CO_2 impact, resulting from the larger pressure drop, provides a higher energy for thoroughly mixing of tiny phospholipid particles and glucose solution. As a result, the liposomal microencapsulation were well conducted at higher pressure. The EE of the SCF liposomes produced at 12.41 MPa and 16.55 MPa was found to be higher than that at 8.27 MPa. Similar results has been reported in preparation of PEGylated liposomes using the supercritical antisolvent process [31]. The liposomes were formulated with hydrogenated soya phosphatidylcholine (HSPC), soya phosphatidylcholine (SPC) and cholesterol in a 7:3:1 mole ratio. Docetaxel was blended with the mixed lipids in a 1:20 mole ratio. The EE of the docetaxel-encapsulated liposomes increased from 51 % to 67 % when the operating pressure was raised from 10 MPa to 22 MPa.

The EE of the glucose-encapsulated liposomes generated at 12.41 MPa was found to be higher than those of the liposomes synthesized at 16.55 MPa. Higher expansion pressure may contributes too much SC-CO_2 stream impact on the liposomal formation in the nozzle, which caused the breakage of resultant liposomes. This explains why the EE of liposomes produced at 12.41 MPa was consistently higher than those at 16.55 MPa. A similar phenomenon was observed in a liposomal microencapsulation produced using a supercritical reverse phase evaporation method (SCREP) [32]. The EE of liposomes encapsulating 0.2 M glucose solution produced under 20 MPa was higher than that of the liposomes formulated above 20 MPa.

Table 4.3 shows the effect of cargo loading rate on the EE of liposomal microencapsulation using the SCF process. At the same expansion temperature and pressure, the EE of liposomes at 0.25 ml/second was found to be consistently higher than that at 0.5 ml/second. The diluting effect, due to higher cargo loading rate, resulted in the lower EE of the SCF liposomal microencapsulation.

4.6.4. Morphology

Figure 4.8 shows the morphology of the liposomes encapsulating FITC using the SCF process. The liposomes were produced at the optimal operating condition: 12.41 MPa, 90 ^{o}C, and 0.25 ml/second of the FTIC loading rate. The liposomal emulsion was visualized under a confocal laser scaning microscope (CLSM) with 10 × 100 amplification. It was observed that LUVs and MVVs made up for the majority of the SCF liposomes. The hydrophilic FITC showed yellow-green fluorescence under CLSM at the laser scanning wavelength between 496 and 535 nm. Nile Red was used to stain the phospholipid membranes and emitted red fluorescence at the scanning wavelength between 558 and 635 nm. If aqueous FITC droplets were encapsulated in liposomes,

they were surrounded by the red-colored phospholipid membranes. A clear view of the stereoscopic structure of the SCF liposomes would be provided by our supplementary videos.

Table 4.3 Encapsulation efficiency of liposomes at different flow rates and pressures at 90, 83 and 75 °C

90 °C	**Encapsulation efficiency (%)**	
Pressure (MPa)	**0.25 ml/second**	**0.5 ml/second**
16.55	17.77±0.02	10.96±0.02
12.41	31.65±0.03	16.91±0.02
8.27	6.37±0.01	3.20±0.01

83 °C	**Encapsulation efficiency (%)**	
Pressure (MPa)	**0.25 ml/second**	**0.5 ml/second**
16.55	15.62±0.01	8.80±0.04
12.41	23.86±0.02	10.25±0.03
8.27	4.55±0.03	2.27±0.02

75 °C	**Encapsulation efficiency (%)**	
Pressure (MPa)	**0.25 ml/second**	**0.5 ml/second**
16.55	13.04±0.03	8.24±0.01
12.41	16.52±0.01	5.98±0.01
8.27	2.26±0.01	1.86±0.01

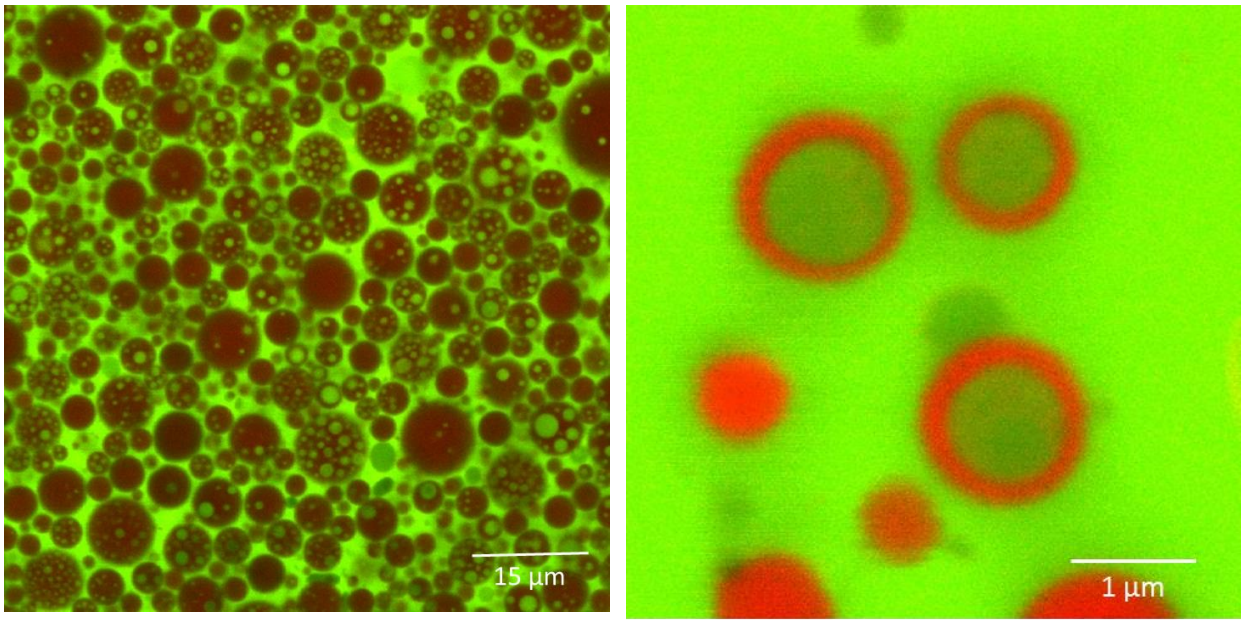

(A) 1× digital zooming

(B) 8 × digital zooming

Figure 4.8. CLSM visualization of SCF liposomes produced at 12.41 MPa, 90 ºC, and 0.25 ml/second of FITC loading rate:10×100 amplification.

4.7. Modeling

The size data of liposomes produced using the SCF microencapsulation method were correlated with expansion pressure, temperature and cargo loading rate using the empirical regression model. The quadratic equation shows the best fit of this correlation.

Liposomal size = $-0.00102 \cdot P^2 + 4.261 \cdot P - 5.98\ T + 255 \cdot F - 2764$……..….(1)

where P is expansion pressure (MPa), T is expansion temperature (^oC), and F is cargo loading rate (ml/second).

This model was proven to be within the significant level ($P<0.0001$). Normal distribution of the experimental data was observed. The R^2 value was 0.96. Table 4.4 shows the significant analyses of the parameters in Equation 1. It indicates that the expansion pressure had a significant effect on determining liposome size.

Figures 4.9 and 4.10 show the correlation of the SCF liposome size as functions of pressure and temperature at 0.25 and 0.5 ml/second of cargo loading rates. The symbols represent the average liposome sizes measured at 75, 83, and 90 ^{o}C. The solid and dashed lines represent the predicted liposome sizes calculated using Equation 1. The average AARD value is 8.26 %, indicating a good prediction model was well established. The expansion pressure is a dominant factor in determining the liposome size. The density of SC-CO_2 can be increased by rising pressure, which results in the higher solubility of phospholipids in SC-CO_2. Simultaneously, tiny phospholipid particles nucleate and are mixed thoroughly with the cargo solution by the stronger SC-CO_2 impact during rapid expansion of SC-CO_2 in the nozzle. As a result, better liposomal microencapsulation is performed with increasing liposome size in the novel SCF process.

As for the temperature effect on the SCF liposomal microencapsulation, the liposome size decreased with higher expansion temperatures at 83 and 90 ^{o}C. Sufficient heat was provided for liposomal microencapsulation in the expansion nozzle. The drastic freezing effect, due to rapid expansion of SC-CO_2, would be minimized to prevent the breakage and aggregation of the SCF liposomes.

Table 4.4. Parameter estimates on the size correlation of the SCF liposomes

Parameters	Coefficients	Stand errors of coefficients	T-values	p-values
Pressure^2	-0.001022	0.000086	-11.95	<0.0001
Pressure	4.261	0.309	13.77	<0.0001
Temperature	-5.98	2.37	-2.52	0.025
Flow rate	255	116	2.19	0.047
Constant	-2764	330	-8.37	<0.0001

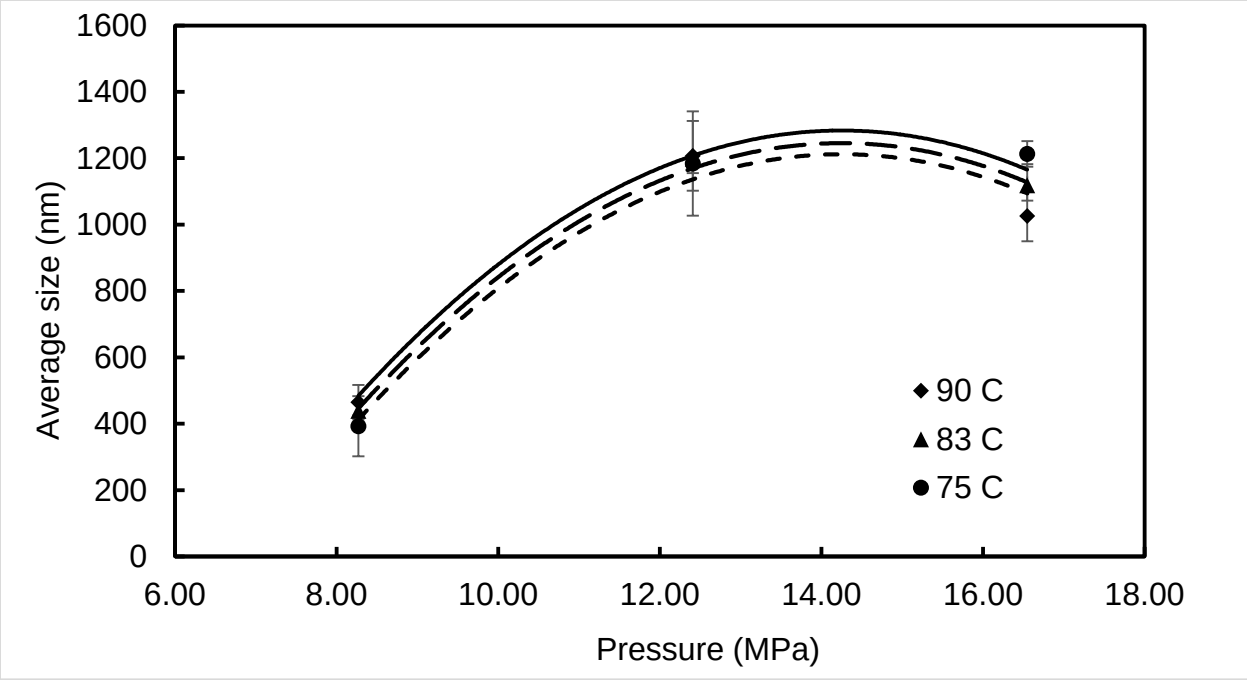

Figure 4.9. Correlation of the liposome-size data with expansion pressures and temperatures at 0.25 ml/second of cargo loading rate.

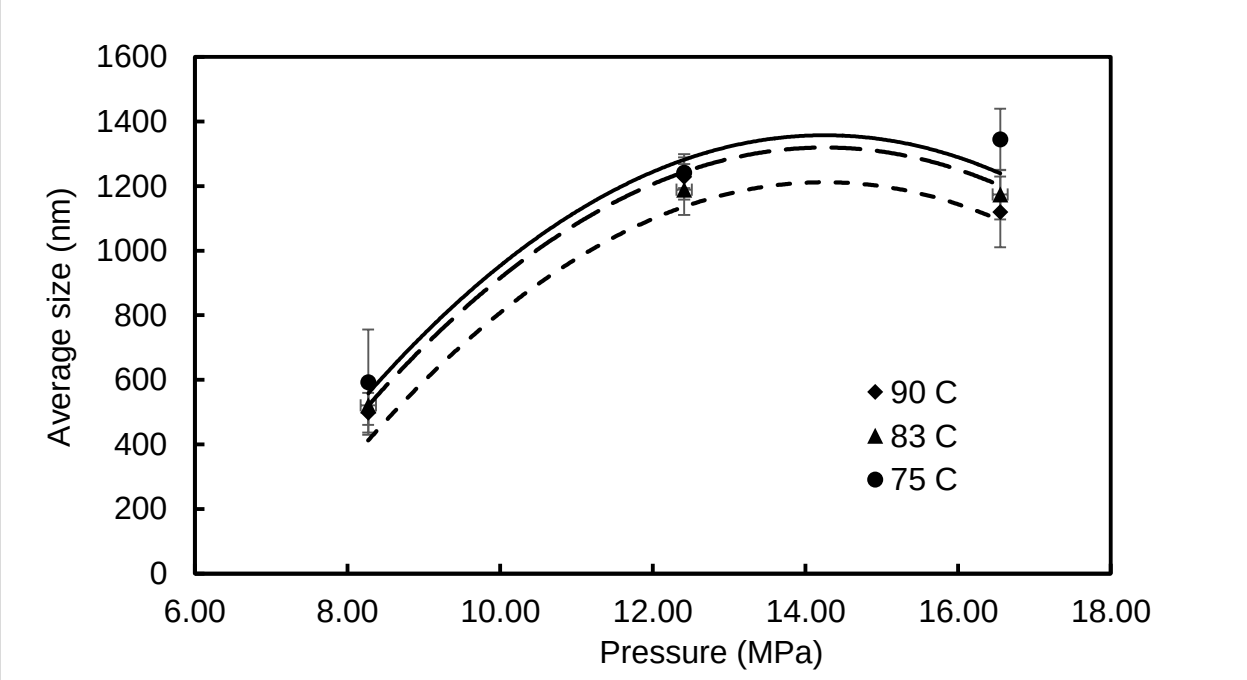

Figure 4.10. Correlation of the liposome-size data with expansion pressures and temperatures at 0.5 ml/second of cargo loading rate.

4.8. Advantages of this novel SCF process for liposomal microencapsulation

No organic solvent was involved in this new SCF process of liposomal microencapsulation. SC-CO_2 was used as the sole phospholipid-dissolving medium and instantly evaporated at ambient pressure. The cargo solution was drawn into the expansion nozzle with the vacuum created by the vena contracta effect. No additional energy was consumed in the SCF process for cargo loading. Our technique is a rapid and non-toxic process for bulk production of liposomes with the size ranging from sub-micron to 1-2 microns, which provides an ecofriendly alternative for generation and encapsulation of the versatile phospholipid vesicles.

4.9. Conclusions

The novel SCF process provided a rapid, benign and continuous method for liposomal microencapsulation. The size distribution of liposomes varied from 900 nm to 1400 nm in the pressure range of 12.41 MPa and 16.55 MPa. Zeta potential between -50 and -54 mV on the liposomal membranes suggested that good emulsion stability of the SCF liposomes was maintained. The highest encapsulation efficiency of 31.65% was reached at 12.41 MPa, 90 ^{o}C and 0.25 ml/second of 0.2 M cargo loading rate. The expansion pressure was found to be the most influential factor on determining liposome size. Large unilamellar vesicles (LUVs) and multivesicular vesicles (MVVs) accounted for the majority of liposomes produced by this novel technique of SCF microencapsualtion. An accurate model for predicting liposome size was well established as the function of expansion pressure, temperature, and cargo loading rate. This innovative SCF technique will be further evaluated for its capability to simultaneously microencapsulate hydrophilic and lipophilic bioactive compounds in one phospholipid vesicle.

References

[1] Sharma, A.; Sharma, U. S. Liposomes in drug delivery: progress and limitations. *Int J Pharm* 1997, 154, 123-140.

[2] Shieh, M. F.; Chu, I. M.; Lee, C. J.; Kan, P.; Hau, D. M.; Shieh, J. J. Liposomal delivery system for taxol. *J Ferment Bioeng* 1997, 83, 87-90.

[3] Wong, J. P.; Yang, H.; Blasetti, K. L.; Schnell, G.; Conley, J.; Schofiel, L. N. Liposome delivery of ciprofloxacin against intracellular Francisella tularensis infection. *J Controlled Release* 2003, 92, 265– 273.

[4] Kiwada, H.; Sato, J.; Yamada, S.; Kato, Y. Feasibility of magnetic lipsomes as a targeting device for drugs. *Chem Pharm Bull* 1986, 34, 4253-4258.

[5] Keller, B. C. Liposomes in Nutrition. *Trends Food Sci Tech* 2001, 12, 25-31.

[6] Stone, W. L.; Smith, M. Therapeutic uses of antioxidant liposomes. *Mol Biotechnol* 2004, 27, 217-230.

[7] Xia, S.; Xu, S. Ferrous sulfate liposomes: preparation, stability and application in fluid milk. *Food Res Ind* 2005, 38, 289-296.

[8] Gouin, S. Microencapsulation: industrial appraisal of existing technologies and trends. *Trends Food Sci Tech* 2004, 15, 330-347.

[9] Taylor, M. T.; Davidson, M. P.; Bruce, B. D.; Weiss, J. Liposomal nanocapsules in food science and agriculture. *Crit Rev Food Sci* 2005, 45, 587-605.

[10] Yokoyama, S.; Inagaki, A.; Tsuchiya, K.; Sakai, H.; Imura, T.; Ohkubo, T.; Tsubaki, N.; Abe, M. Stearylamine changes the liposomal shape from MLVs to LUVs. *J Oleo Sci* 2005, 54, 251-254.

[11] Jo, S. M.; Kim, J. C. Glucose-triggered release from liposomes incorporating poly(*N*-isopropylacrylamide-co-methacrylic acid-co-octadecylacrylate) and glucose oxidase. *Colloid and Polym Sci* 2009, 287, 379-384

[12] Castor, T. P.; Aphios Corporation. Methods and apparatus for making liposomes. USA Patent No: US5554382A. 1996.

[13] Frederiksen, L.; Anton, K.; Hoogevest, P. V.; Keller, H. R.; Leuenberger, H. Preparation of liposomes encapsulating water-soluble compounds using supercritical carbon dioxide. *J Pharm Sci* 1997, 86, 921-928.

[14] Magnan, C.; Badens, E.; Commenges, N.; Charbit, G. Soy lecithin micronization by precipitation with a compressed fluid antisolvent - influence of process parameters *J Supercrit Fluid* 2000, 19, 69-77.

[15] Castor, T. P. Phospholipid nanosomes. *Curr Drug Delivery* 2005, 2, 329-340.

[16] Utada, A. S.; Lorenceau, E.; Link, D. R.; Kaplan, P. D.; Stone, H. A.; Weitz, D. A. Monodisperse double emulsions generated from a microcapillary device. *Science* 2005, 308, 537-541.

[17] Otake, K.; Shimomura, T.; Goto, T.; Imura, T. Preparation of liposomes using an improved supercritical reverse phase evaporation method. *Langmuir* 2006, 22, 2543-2550.

[18] Meure, L. A.; Knott, R.; Foster, N. R.; Dehghani, F. The depressurization of an expanded solution into aqueous media for the bulk production. *Langmuir* 2009, 25, 326-337.

[19] Wimmer, Z.; Zarevúcka, M. A review on the effects of supercritical carbon dioxide on enzyme activity. *Int J Mol Sci* 2010, 11, 233-253.

[20] Yuk, H.-G.; Geveke, D. J. Nonthermal inactivation and sublethal injury of Lactobacillus plantarum in apple cider by a pilot plant scale continuous supercritical carbon dioxide system *Food Microbiol* 2011, 28, 337-383.

[21] Kraujalis, P.; Venskutonis, P. R. Supercritical carbon dioxide extraction of squalene and tocopherols from amaranth and assessment of extracts antioxidant activity. *J Supercrit Fluids* 2013, 80, 78-85.

[22] Otake, K.; Imura, T.; Sakai, H.; Abe, M. Development of a new preparation method of liposomes using supercritical carbon dioxide. *Langmuir* 2001, 17, 3898-3901.

[23] Matsuyama, K.; Mishima, K.; Hayashi, K.-I.; Ishikawa, H.; Matsuyama, H.; Harada, T. Formation of microcapsules of medicines by the rapid expansion of a supercritical solution with a nonsolvent. *J Appl Polym Sci* 2003, 89, 742-752.

[24] Imura, T.; Otake, K.; Hashimoto, S.; Gotoh, T.; Yuasa, M.; Yokoyama, S.; Sakai, H.; Rathman, J. F.; Abe, M. Preparation and physicochemical properties of variuos soybean lecithin liposomes using supercritical reverse phase evaporation method. *Colloids Surf B Biointerfaces* 2002, 27, 133-140.

[25] Taylor, T. M.; Weiss, J.; Davidson, P. M.; Bruce, B. D. Liposomal nanocapsules in food science and agriculture. *Crit Rev Food Sci* 2005, 45, 587-605.

[26] Henczka, M.; Bałdyga, J.; Shekunov, B. Y. Particle formation by turbulent mixing with supercritical antisolvent. *Chem Eng Sci* 2005, 60, 2193-2201.

[27] Manosroi, A.; Chutoprapat, R.; Abe, M.; Manosroi, J. Characteristics of niosomes prepared by supercritical carbon dioxide ($scCO_2$) fluid. *Int J Pharm* 2008, 352, 248-255.

[28] Zhang, W.; Sun, Y.; Li, Y.; Shen, R.; Ni, H.; Hu, D. Preparation and influencing factors of sirolimus liposome by supercritical fluid. *Artif Cells Blood Substit Immobil Biotechnol* 2012, 40, 62-65.

[29] Heurtault, B.; Saulnier, P.; Pech, B.; Proust, J. E.; Benoit, J. P. Physico-chemical stability of colloidal lipid particles. *Biomaterials* 2003, 24, 4283-4300.

[30] Montanari, L.; Fantozzi, P.; Snyder, J. M.; King, J. W. Selective extraction of phospholipids from soybeans with supercritical carbon dioxide and ethanol. *J Supercrit Fluids* 1999, 14, 87-93.

[31] Naik, S.; Patel, D.; Surti, N.; Misra, A. Preparation of PEGylated liposomes of docetaxel using supercritical fluid technology. *J Supercrit Fluids* 2010, 54, 110-119.

[32] Imura, T.; Gotoh, T.; Otake, K.; Yoda, S.; Takebayashi, Y.; Yokoyama, S.; Takebayashi, H.; Sakai, H.; Yuasa, M.; Abe, M. Cortrol of physicochemical properties of liposomes using a supercritical reverse pahse evaporation method. *Langmuir* 2003, 19, 2021-2025.

Chapter 5: Simultaneous microencapsulation of hydrophilic and lipophilic bioactives in liposomes produced by a novel supercritical fluid process

5.1. Abstract

Organic solvent residues are always a concern with the liposomes produced by traditional techniques. A nontoxic supercritical fluid (SCF) process has been previously reported for the production of integrated liposomes using a benign solvent. Our objectives were to encapsulate hydrophilic and lipophilic compounds in liposomes using this novel SCF process. Supercritical carbon dioxide (SC-CO_2) was chosen as the phospholipid-dissolving medium and an environmentally friendly substitute for organic solvents. The liposomal microencapsulation was conducted via a 1000-micron jetting nozzle at 12.41 MPa, 90 ^{o}C and 0.25 ml/second of cargo loading rate. Vitamins C and E were selected as model hydrophilic and lipophilic compounds encapsulated in integrated liposomes. The average vesicle size of vitamins C and E microencapsulated liposome was 951.02 nm with a zeta potential of -51.87 mV. The encapsulation efficiency (EE) was 32.97 % for vitamin C and 99.32 % for vitamin E. During 20 days of storage at 4 ^{o}C, the EE was found to slightly decrease by 1.76 % and 0.88 % for vitamins C and E, respectively. The versatile microencapsulation of hydrophilic and lipophilic compounds in the liposomes was successfully developed with this novel SCF process.

Keywords: liposomes, microencapsulation, supercritical carbon dioxide, vitamin C, vitamin E, hydrophilic, lipophilic, storage stability

5.2. Introduction

Liposomes are double emulsions with versatility in encapsulating hydrophilic compounds in the aqueous core and lipophilic compounds inside one or multiple phospholipid bilayers. With this special property, they have drawn the most attention through studies of controlled release, solubility improvements and targeted therapies in the food, cosmetic and pharmaceutical industries [1-4]. Based on their size and lamellarity, liposomes can be categorized into four types: small unilamellar vesicles (SUVs), large unilamellar vesicles (LUVs), multilamellar vesicles (MLVs) and multivesicular vesicles (MVVs). The liposomal size of SUVs varies from 20 to approximately 100 nm. The sizes of LUVs, MLVs, and MVVs range from a few hundred nanometers to microns. The thickness of one phospholipid bilayer has been reported to be approximately 4 to 5 nm [5]. Size, surface charge, and membrane composition can be changed simply by adding new ingredients to the lipid mixture before liposome preparation or by varying the preparation methods [6].

Traditionally, liposomes were prepared by thin film hydration, reverse phase evaporation vesicles (REV), membrane extrusion, and sonication. Nowadays, due to concerns about the toxicity of organic solvents, several new techniques have been developed to reduce or even completely avoid using organic solvents in liposomal microencapsulation, including microfluidics, rapid expansion of a supercritical solution (RESS), supercritical reverse phase evaporation (SC-RPE), and several dense gas processes [7-13]. Supercritical carbon dioxide (SC-CO_2) is a non-toxic density-adjustable fluid with solvent behavior similar to hexane [14, 15]. Its moderate critical pressure (7.4 MPa) and low critical temperature (31.1 ^{o}C) make it an ideal candidate for biomaterial processing.

Vitamin C (ascorbic acid) is a hydrophilic free-radical scavenger with strong antioxidant activity to clean all aggressive oxygen radicals. In addition, it can promote collagen synthesis, strengthen the body's immune system, and provide protection for our cardiovascular system. Vitamin E (tocopherol) is a lipophilic antioxidant that prevents on liver dysfunction, cancer, and heart disease. It has been reported that vitamins C and E perform a synergistic effect on their antioxidant activity to scavenge free radicals in human bodies. Vitamin E acts as the primary antioxidant and the resulting vitamin E radical then reacts with vitamin C to regenerate vitamin E [16, 17].

Our novel nontoxic supercritical fluid (SCF) process developed for liposomal microencapsulation and used in this study consisted of supercritical fluid extraction (SFE), rapid expansion of a supercritical solution, and vacuum-driven automatic cargo loading. SC-CO_2 was used as the sole phospholipid-dissolving medium with no involvement of organic solvents. Our objectives were to evaluate the simultaneous liposomal microencapsulation of hydrophilic and lipophilic molecules using this innovative SCF technique. Vitamins C and E were selected as model hydrophilic and lipophilic compounds for this study. Average liposome size, zeta potential, encapsulation efficiency (EE) were characterized for this double emulsion (W/O/W). The variations in average vesicle size, zeta potential and EE of the SCF liposomes were also evaluated for storage stability. The morphology of integrated liposomes was observed under a confocal laser scanning microscope (CLSM).

5.3. Materials and methods

Performix^{TM} E soy lecithin was provided by Archer Daniels Midland Company. Cholesterol with 95% purity, vitamins C and E, and protamine sulfate were purchased from Sigma Aldrich (St.

Louis, MO 63103). Carbon dioxide (purity >999 g/kg), used as a supercritical solvent, was purchased from Airgas (Ithaca, NY, USA). Tris (hydroxylmethyl) aminomethane (TRIS) was purchased from Bio-Rad (Hercules, CA 94547).

5.3.1. Preparation of liposomal microencapsulation

2 grams of Performix E soy lecithin was mixed thoroughly with cholesterol in a 10:1 mass ratio. The purpose of adding cholesterol is to enhance the rigidity of the liposomal membrane by changing interactions between both the polar head groups and the hydrocarbon chain in the phospholipid layer. A decrease in the melting point and phase-transit enthalpy of the lecithin/cholesterol mixture was also observed [18]. The lecithin/cholesterol mixture was stored at 4 ^{o}C to be solidified for loading convenience.

The SCF microencapsulation process for the preparation of liposomes has been described in Figure 2.1 (Chapter 2). The system mainly consisted of three parts: a high pressure pump (HPP), a mixing vessel, and a expansion nozzle. The temperatures of different areas in the SCF system were controlled by glass wool heating tapes and Variable Autotransformers (Type 3PN1010, 120 V for input and 0-120V for output, Staco Energy Products Company, Dayton, OH 45403). The perpendicular nozzle meant that SC-CO_2 was mixed with the cargo solution in the vertical angle.

The solidified lecithin/cholesterol mixture was loaded into the 1-L mixing vessel. Carbon dioxide (CO_2) was introduced by HPP up to 20.68 ± 0.3 MPa at 60 ± 1 ^{o}C. After at least two hours of phase equilibrium, the phospholipid/cholesterol-laden SC-CO_2 was controllably introduced into the expansion nozzle by a metering valve (MV, Type SS-4L-MH, Swagelock, Western NY Fluid System Technology, Rochester, NY 14467). The pre-expansion pressure in the nozzle was maintained at 12.41 ± 0.3 MPa by a forward pressure regulator (FPR, Model 44-1124-

24-131, 68.94 MPa for maximum input and 17.24 MPa for maximum output, TESCOM, Elk River, MN 55330). The nozzle temperature was maintained at 90 ± 2 ^{o}C to avoid drastic temperature drop below the phase transition temperature of the lipid mixture, approximately 40 ^{o}C, due to the Joule-Thomas effect happening in rapid SC-CO_2 expansion [19]. The cargo loading rate of vitamin C was set at 0.25 ml/second. During the entire operation, fresh CO_2 was continuously introduced into the mixing vessel where the pressure was maintained and excessive CO_2 was re-circulated by a back pressure regulator (BPR, Model L98377, 0.34-41.37 MPa for controlled pressure range, TESCOM, Elk River, MN 55330).

When SC-CO_2 expanded in the nozzle chamber, the phospholipid/cholesterol mixture began to nucleate as tiny particles due to pressure decreasing from 12.41 MPa to ambient pressure. Coincidentally, the vacuum was built up in the range of 3 to 5 mmHg of vacuum due to the vena contracta effect when SC-CO_2 was passed through a 1000-micron orifice in the expansion nozzle.

Soy lecithin, cholesterol, and vitamin E with a 10:1:1 mass ratio were thoroughly blended for liposomal microencapsulation of a lipophilic compound. The cargo solution containing 0.2 M vitamin C in TRIS pH 7.4 buffer was then drawn into the chamber with the vacuum force and broken into small aqueous droplets by the CO_2 stream impact while the lipid material was mixed with the cargo solution. As a result, the liposomes were formed in a one-step process taking within 1 to 2 seconds for each run. Fourteen to sixteen runs were conducted for one experiment. The emulsion containing liposomes in TRIS pH 7.4 buffer was directly collected in the glass tray for further analysis.

5.3.2. Characterization of the SCF liposomes

5.3.2.1. Size distribution

Size distribution of the liposomes was determined using a 90 PLUS particle size analyzer (Brookhaven Instruments Corporaton, Holtsville, NY 11742). 250 µl of liposomal emulsion was diluted with TRIS pH 7.4 buffer for 10 ml of total volume. 3.5 ml of the diluted liposomal emulsion was loaded in the 3.5-ml cuvette for the analysis of size distribution.

5.3.2.2. Zeta potential

Zeta potential of the liposomes was measured using a 90 PLUS particle size analyzer. 25 µl of liposomal emulsion diluted with TRIS pH 7.4 buffer for 10 ml of total volume. 1.2 to 1.5 ml of the diluted sample was measured for the surface charge of liposomes.

5.3.2.3. Encapsulation Efficiency

The Protamine aggregation method was adopted and modified for the purification of the liposomes encapsulating vitamins C and E. 0.1 ml of the liposomal emulsion was mixed with 0.1 ml protamine solution (10 mg/ml). The treated sample was left still for 3 minutes. 1.5 ml of saline solution (0.9 % w/v NaCl in TRIS pH 7.4 buffer) was added into the sample, followed by centrifugation at 2000 g for 25 minutes at 4 ^{o}C. The supernatant was removed from the liposomal sample. 0.6 ml of 10 % w/v Triton X-100 solution was added into the purified liposomes followed by agitation for at least 5 minutes to rupture the liposomes. Saline solution (0.9% w/v NaCl in TRIS pH 7.4 buffer) was then added up to 3.2 ml of the total volume. The optical density (OD) values of vitamins C and E were measured at 265 and 295 nm, respectively, using the UV-

spectrophotometer [20], and converted to the concentrations of both vitamins in the liposomes using the following equation [21].

$$EE\ (\%) = (\text{vitamin concentration in purified liposomes} / \text{vitamin concentration in the cargo}) \times 100$$

5.3.2.4. Morphology

1 ml of the liposomal emulsion was mixed with 3 to 4 drops of Nile Red in ethanol (0.2% w/w). After one minute of mild blending, 0.3 ml of the sample was set on a well slide and visualized under a Leica confocal laser scanning microscope with 10×100 amplification for the morphology of microencapsulated liposomes. The fluorescent emission wavelength of Nile Red was set at 558 to 635 nm.

5.3.2.5. Storage stability

The SCF liposomes, encapsulating TRIS pH 7.4 buffer (control), vitamin C, vitamin E, and vitamins C and E together, were stored at 4 ^{o}C in 20 or 21 days for the test of storage stability. The variations in average vesicle size, zeta potential, and EE were measured for the evaluation of emulsion stability during storage.

5.4. Results and discussion

5.4.1. Characterization of SCF liposomes

The size distribution, zeta potential, and EE were characterized for the liposomes encapsulating vitamins C and E. The liposomes encapsulating TRIS pH 7.4 buffer were chosen as the control. As shown in Table 5.1, the average size of the vitamin C-encapsulated liposomes (911.45 nm) is similar

to the control (909.20 nm). The average size of the vitamin E-encapsulated liposomes was determined to be 938.83 nm, slightly larger than the control and vitamin C-encapsulated liposomes. A similar phenomenon has been reported in the microencapsulation of vitamin E in Lipoid E-80 liposomes produced using membrane extrusion [22]. The encapsulation of vitamin E in liposomes increased the average vesicle size from 88 to 96 nm, due to the insertion of vitamin E in the phospholipid bilayers. This suggests that the solubility of lipophilic compounds in an aqueous medium can be improved by encapsulating these compounds in the hydrophobic domain of the phospholipid bilayers.

Table 5.1. Characterizations of liposomes encapsulating vitamin E and C produced at 12.41 MPa, 90 ºC and 0.25 ml/sec of cargo loading rate

Liposomal emulsion	Average liposomal size (nm)	Zeta potentials (mV)	Encapsulation efficiency (EE, %)
TRIS pH 7.4 buffer	909.20 ± 53.18	-52.21±1.27	
Vitamin C	911.45 ± 51.33	-52.19±1.21	32.68 ± 1.12
Vitamin E	938.83 ± 59.25	-52.14±1.59	99.20 ± 0.66

The surface charge provides the repulsive force for the stability of a colloidal system. Below -30 mV of zeta potential, the emulsion presents a good shelf-life stability [23]. The zeta potential values of these three samples were measured to be approximately -52 mV, indicating that good emulsion stability was sustained in these SCF liposomes [24]. These negative values could be attributed to the presence of negatively charged phospholipids, such as PE and PI, in the liposome membrane [22]. Table 5.1 indicates that the presence of vitamins C and E did not change the negative surface charge on the phospholipid membrane, suggesting that these two vitamins were successfully encapsulated in the liposomes without any interaction with the vesicle surface. The

measurement of zeta potential provides crucial information about the surface properties of the colloidal system and is useful to determine the type of association between active compounds and the dissolving media [25].

Encapsulation efficiency (EE) of vitamins C and E in the SCF liposomes were determined to be 32.68% and 99.20%, respectively. Vitamin E was almost entirely encapsulated in the liposomes. The high EE of vitamin E was probably due to its high lipophilicity [26]. Similar results have been reported for liposomal microencapsulation of vitamin E using the method of thin film hydration [20]. In that study, vitamin E was encapsulated in soy phosphatidylcholine (SPC)-based liposomes, and 99.15% to 99.73% EE of vitamin E in the liposomes was reached. 99.87 % EE of vitamin E in the liposomes has also been achieved by membrane extrusion [22]. Lipophilic compounds can be encapsulated more efficiently into the hydrophobic domains of phospholipid membranes if the vesicle is formed by multilamellar vesicles (MLVs) and multivesicular vesicles (MVVs) [27].

Encapsulation of vitamin C in liposomes was carried out by mixing the phospholipid/cholesterol-laden SC-CO_2 and vitamin C solution in the expansion nozzle. A loss of unencapsulated vitamin C happened during the SCF liposomal microencapsulation, which can be explained by the large interfacial tension between the aqueous cargo and soy phospholipids [28]. The EE of the other SC-CO_2 processes have been reported in the range of 10% to 20% for liposomal microencapsulation of hydrophilic compounds [8, 13, 29, 30]. This novel SCF process generated vitamin C-encapsulated liposomes with the highest EE (32.68%) to date.

5.4.2. Storage stability

Vesicle size is a direct indicator of emulsion stability since in most cases the vesicle size increases before macroscopic changes appear [31]. The variations of the average vesicle size, zeta

potential, and encapsulation efficiency in the SCF liposomes were evaluated over a storage period of 21 days at 4 ^{o}C.

The size variations in the microencapsulated liposomes during 21 days of storage at 4 ^{o}C are presented in Figure 5.1. On the 7th day, it was observed that the average vesicle size of the vitamin C-encapsulated liposomes increased from 911.45 nm to 1073.53 nm and remained nearly unchanged during the remainder of the study period. A similar trend was observed in the vitamin E- encapsulated liposomes, with the average vesicle size increasing from 938.83 nm to 1231.40 nm on the 7th day and remaining nearly unchanged for the remainder of the study period. The variation in zeta potential of the liposomes are presented in Table 5.2. During 21 days of the storage at 4 ^{o}C, the zeta potential values of the liposomes were found to be within the range of -52 to -49 mV, indicating that good emulsion stability was held during the entire storage period.

Figure 5.2 shows the variation in encapsulation efficiency (EE) of liposomes during 21 days of storage at 4 ^{o}C. The EE of vitamins C and E in liposomes were observed to only decrease by 1.35 % and 0.56 %, respectively, meaning vitamins C and E were well encapsulated in the liposomes with good protection from oxidation. To improve the emulsion stability of liposomes, some sterols or fatty acids can be added to phospholipid bilayers to strengthen their structure. In this study, addition of cholesterol to soy lecithin in the 10:1 mass ratio increases the arranging order and density of phospholipid bilayers, leading to an increase in thickness of liposome membranes. Moreover, the interactions such as hydrogen bonds between cholesterol and fatty acids improve the cohesiveness and mechanical strength of liposome bilayers, thus reducing the release of encapsulated compounds [32].

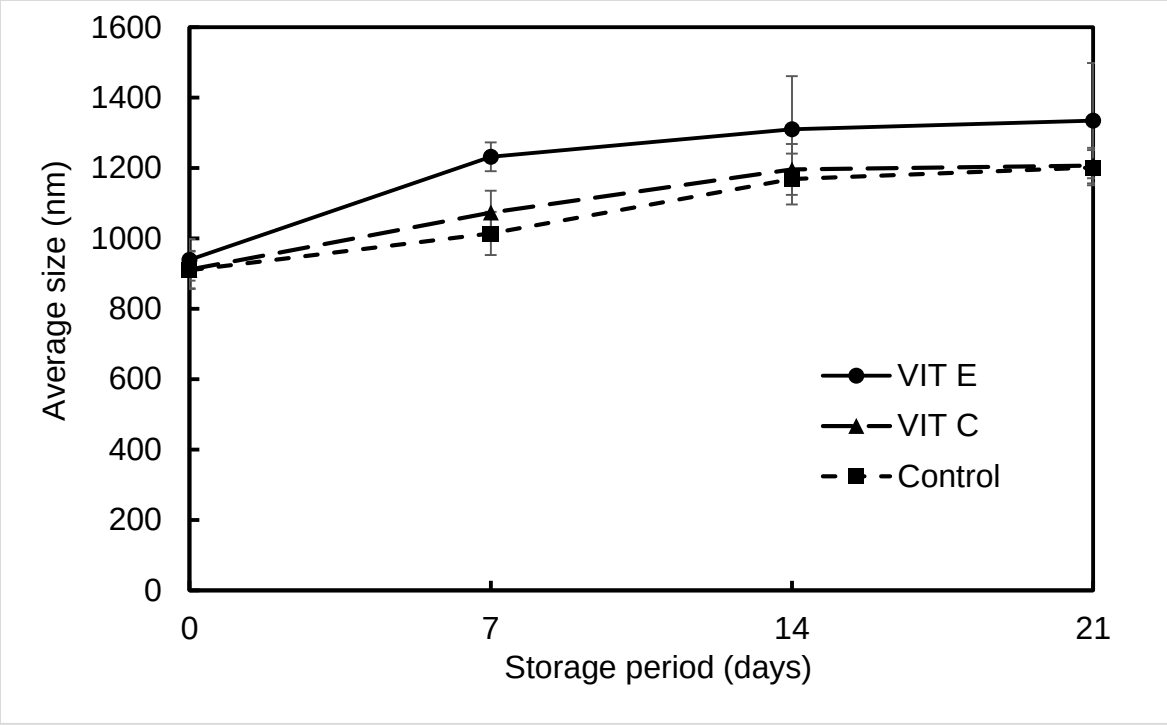

Figure 5.1. Size variation in the liposomes during 21 days of storage at 4 ºC.

Table 5.2. Variation in zeta potential in liposomes during 21 days of storage at 4 ºC

Encapsulating compound	Zeta potential (mV)			
	Days of the storage			
	0	7	14	21
Control	-52.14 ± 1.27	-49.52 ± 1.24	-49.22 ± 0.87	-49.34 ± 1.62
Vitamin C	-52.19 ± 2.21	-49.82 ± 1.38	-49.41 ± 1.53	-49.29 ± 1.10
Vitamin E*	-52.21 ± 1.59	-50.85 ± 2.20	-50.42 ± 1.72	-50.26 ± 2.57

*Phospholipids: cholesterol: vitamin E = 10:1:1

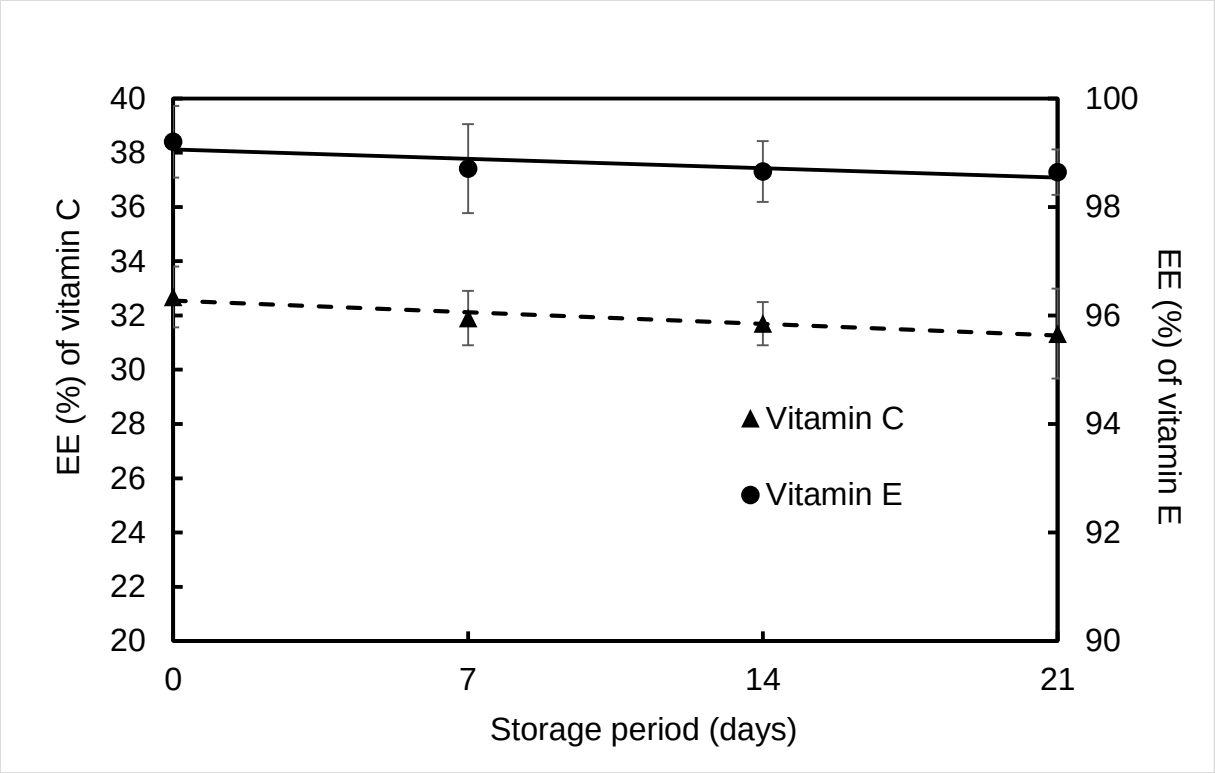

Figure 5.2. Variation in encapsulation efficiency of liposomes during 21 days of storage at 4 ^{o}C.

5.4.3 Simultaneous microencapsulation of vitamins C and E in the SCF liposomes

5.4.3.1. Characterization of the integrated liposomes

To evaluate the versatility of the SCF microencapsulation process, vitamins C and E were simultaneously encapsulated in liposomes to characterize their average vesicle size, zeta potential, encapsulation efficiency (EE) and morphology. The operating parameters in the expansion nozzle were set at 12.41 MPa, 90 ^{o}C, and 0.25 ml/second of cargo loading rate for optimal microencapsulation, determined by our previous study. Table 5.3 presents the characterizations of the SCF liposomes encapsulating vitamins C and E in either single or double microencapsulation. The average vesicle size and zeta potential of the double encapsulation were found to be similar to those of the single encapsulations. The EE of vitamin C in the double encapsulation was similar to that of the single encapsulation. A similar trend was observed in the SCF liposomal

microencapsulation of vitamin E. In summary, these results showed no interaction between vitamins C and E in the simultaneous liposomal microencapsulation.

Table 5.3. Characterization of SCF liposomes encapsulating vitamins C and E.

Model compounds	Vitamins C and E	Vitamin C	Vitamin E*
Average liposome size (nm)	951.02 ± 45.31	911.45 ± 51.33	938.83 ± 59.25
Zeta-potential (mV)	-51.87 ± 1.48	-52.19 ± 2.21	-52.21 ± 1.59
EE (%) of vitamin C	32.97 ± 1.86	32.68 ± 1.12	N.A.
EE (%) of vitamin E	99.32 ± 0.46	N.A.	99.20 ± 0.66

*Phospholipids: cholesterol : vitamin E= 10:1:1

5.4.3.2. Storage stability

The microencapsulated liposomes of vitamins C and E were evaluated for their stability during 20 days of storage at 4 ^{o}C. As shown in Figure 5.3, the average vesicle size of the SCF liposomes had increased from 951.02 nm to 1297.73 nm on the 10th day and remained nearly unchanged during the remainder of the storage period. The zeta potential of the SCF liposomes varied slightly within -51.87 and -48.17 mV, indicating that good emulsion stability was maintained in the entire storage period.

Figure 5.4 presents the EE variations of liposomes encapsulating vitamins C and E during 20 days of storage at 4 ^{o}C. The EEs of vitamins C and E in the liposomes were found to only decrease by 1.76 % and 0.88 %, respectively. In other words, vitamins C and E were well encapsulated in the liposomes with good protection from oxidation induced by the environment.

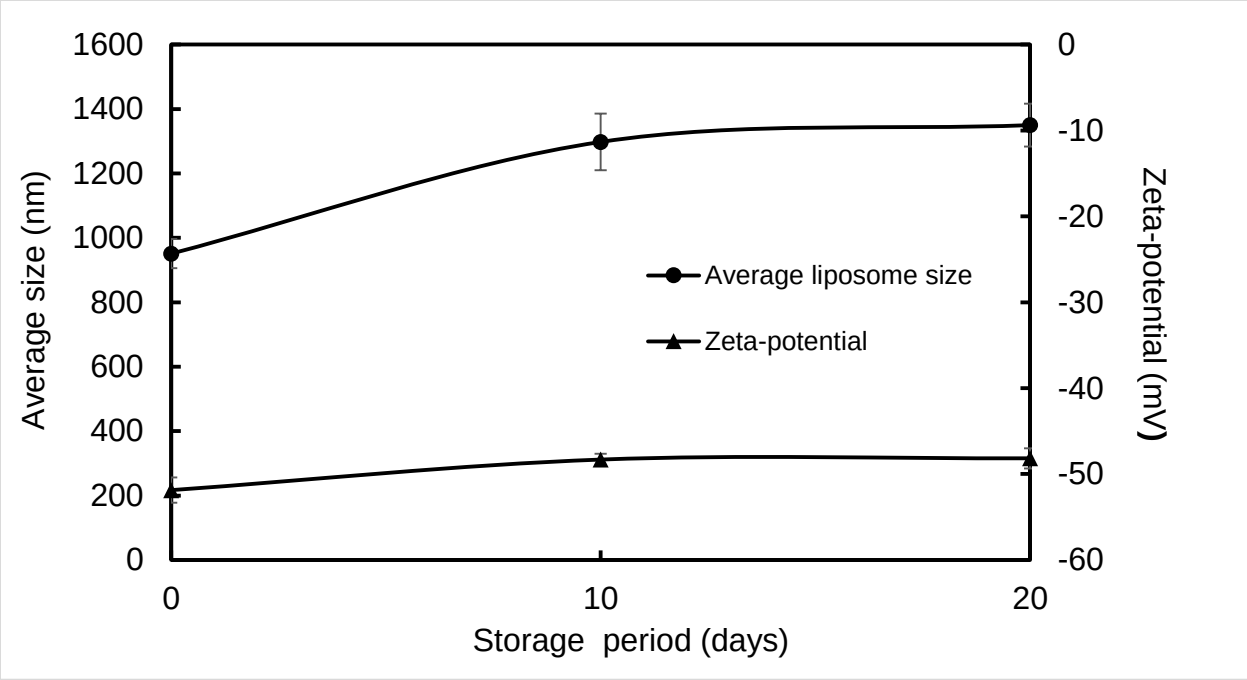

Figure 5.3. Variations in average size and zeta potential of the SCF liposomes encapsulating vitamins C and E during 20 days of storage at 4 ºC.

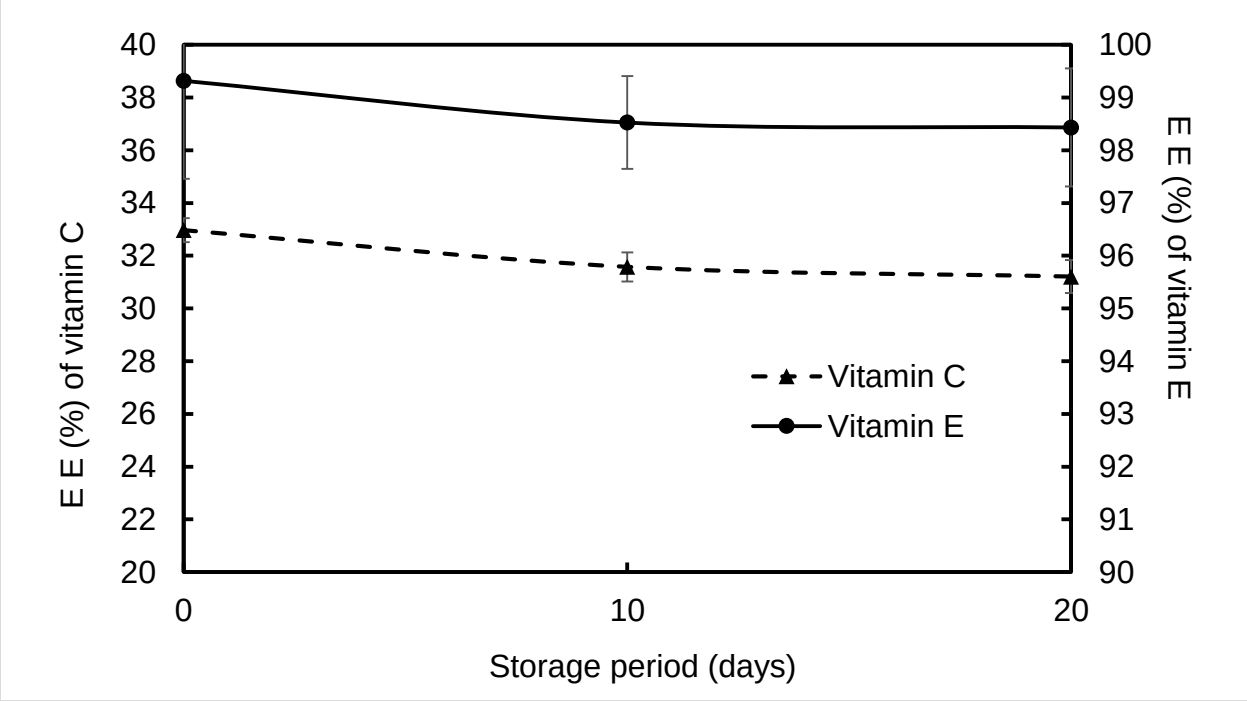

Figure 5.4. Variation in encapsulation efficiency of the SCF liposomes during 20 days of storage at 4 ºC.

5.4.3.3. Morphology

Figure 5.5 shows the morphology of the SCF liposomes encapsulating vitamins C and E using a confocal laser scanning microscopy with 10 × 100 amplification. The Nile Red stained phospholipid membrane, presented as red fluorescence under the scanning wavelength between 558 to 635 nm. Hydrophilic vitamin-C droplets were encapsulated in liposomes as dark cores, surrounded by the red-colored phospholipid membranes. It was observed that LUVs and MVVs accounted for the majority in this liposomal emulsion. LUVs contributed higher encapsualtion effeicney on aqueous cargo. MVVs were able to deliver multiple compounds with ideal controlled release rate [33].

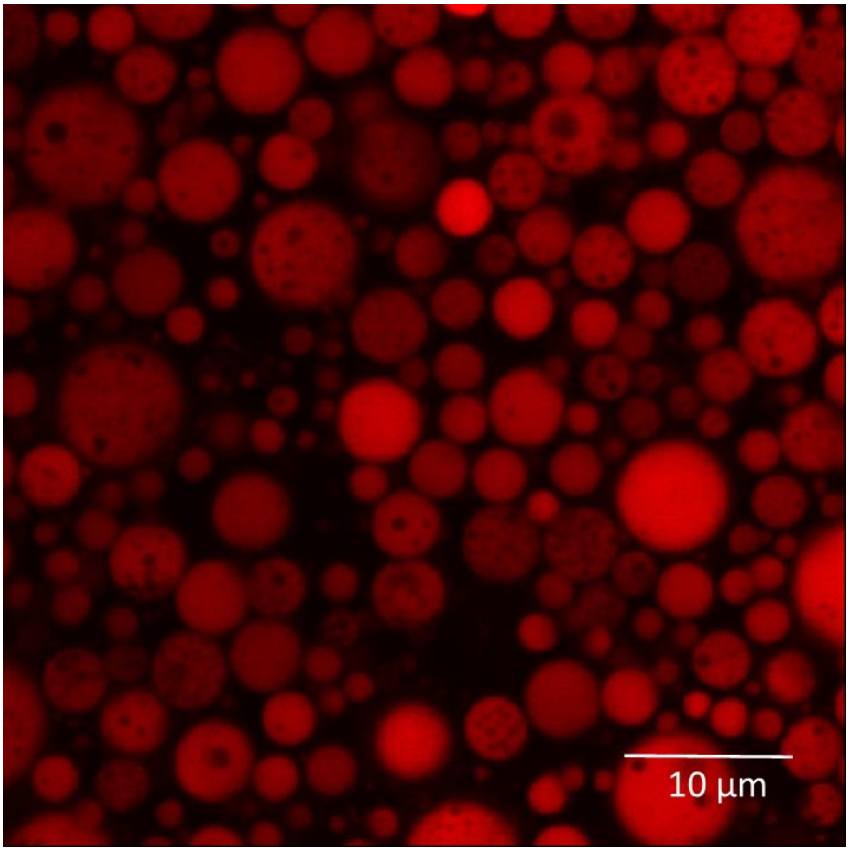

Figure 5.5. CLSM visualization of SCF liposomes produced at 12.41 MPa, 90 °C, and 0.25 ml/second of cargo loading rate: 10×100 amplification.

5.5. Conclusions

Simultaneous microencapsulation of vitamins C and E in liposomes was successfully achieved using the novel SCF process under 12.41 MPa, 60 ^{o}C, and 0.25 ml/second of cargo loading rate. The size of the SCF liposomes varied from 900 to 950 nm with approximately -52 mV of zeta potential. The encapsulation efficiencies of vitamins C and E were found to be 32.9 % and 99.3 %, respectively, in the liposomes produced with the simultaneous double microencapsulation. During 20 days of storage at 4 ^{o}C, good emulsion stability of the SCF liposomes was indicated based on average vesicle size, zeta potential, and EE. New methods of delivering bioactive macromolecules continue to be sought. The novel SCF process developed in this study offers a rapid, nontoxic and continuous technique for bulk production of integrated liposomes with a unique capability to microencapsulate a versatile group of bioactive compounds for food and pharmaceutical applications.

References

[1] Wang, T.; Deng, Y.; Geng, Y.; Gao, Z.; Zou, J.; Wang, Z. Preparation of submicron unilamellar liposomes by freeze-drying double emulsions. *BBA-Biomembranes* 2006, 1758, 222-231.

[2] Kiwada, H.; Sato, J.; Yamada, S.; Kato, Y. Feasibility of magnetic liposomes as a targeting device for drugs. *Chem Pharm Bull* 1986, 34, 4253-4258.

[3] Shieh, M. F.; Chu, I. M.; Lee, C. J.; Kan, P.; Hau, D. M. Liposomal delivery system for taxol. *J Ferment Bioeng* 1997, 83, 87-90.

[4] Wong, J. P.; Yang, H.; Blasetti, K. L.; Schnell, G.; Conley, J.; Schofield, L. N. Liposome delivery of ciprofloxacin against intracellular Francisella tularensis infection. *J Controlled Release* 2003, 92, 265-273.

[5] Amarnath Sharma; Sharma, U. S. Liposomes in drug delivery: progress and limitations. *Int J Pharm* 1997, 154, 123-140.

[6] Torchilin, V. P. Recent advances with liposomes as pharmaceutical carriers. *Nat Rev Drug Discov* 2005, 4, 145-160.

[7] Castor, T. P.; Aphios Corporation. Methods and apparatus for making liposomes. USA Patent No: US5554382A. 1996.

[8] Frederiksen, L.; Anton, K.; Hoogevest, P. V.; Keller, H. R.; Leuenberger, H. Preparation of liposomes encapsulating water-soluble compounds using supercritical carbon dioxide. *J Pharm Sci* 1997, 86, 921-928.

[9] Castor, T. P. Phospholipid nanosomes. *Curr Drug Delivery* 2005, 2, 329-340.

[10] Magnan, C.; Badens, E.; Commenges, N.; Charbit, G. Soy lecithin micronization by precipitation with a compressed fluid antisolvent - influence of process parameters *J Supercrit Fluid* 2000, 19, 69-77.

[11] Otake, K.; Shimomura, T.; Goto, T.; Imura, T. Preparation of liposomes using an improved supercritical reverse phase evaporation method. *Langmuir* 2006, 22, 2543-2550.

[12] Utada, A. S.; Lorenceau, E.; Link, D. R.; Kaplan, P. D.; Stone, H. A.; Weitz, D. A. Monodisperse double emulsions generated from a microcapillary device. *Science* 2005, 308, 537-541.

[13] Meure, L. A.; Knott, R.; Foster, N. R.; Dehghani, F. The depressurization of an expanded solution into aqueous media for the bulk production. *Langmuir* 2009, 25, 326-337.

[14] Shao, P.; Sun, P.; Ying, Y. Response surface optimization of wheat germ oil yield by supercritical carbon dioxide extraction. *Food and Bioprod Process* 2008, 86, 227-231.

[15] Lopes, I. M. G.; Bernardo-Gil, M. G. Characterisation of acorn oils extracted by hexane and by supercritical carbon dioxide. *Eur J Lipid Sci Technol.* 2005, 107, 12-19.

[16] Packer, J. E.; Slater, T. F.; Willson, R. L. Direct observation of a free radical interaction between vitamin E and vitamin C. *Nature* 1979, 278, 737-738.

[17] Tappel, A. L. Will antioxidant nutrients slow aging processes? *Geriatrics* 1968, 23, 97-105.

[18] Taylor, T. M.; Weiss, J.; Davidson, P. M.; Bruce, B. D. Liposomal nanocapsules in food science and agriculture. *Crit Rev Food Sci* 2005, 45, 587-605.

[19] Henczka, M.; Bałdyga, J.; Shekunov, B. Y. Particle formation by turbulent mixing with supercritical antisolvent. *Chem Eng Sci* 2005, 60, 2193-2201.

[20] Márquez, M. M. A. L.; Wagner, J. R.; Alonso, S. d. V.; Chiaramoni, N. S. Liposomes as vehicles for vitamins E and C: an alternative to fortify orange juice and offer vitamin C protection after heat treatment. *Food Res Int* 2011, 44, 3039-3046.

[21] Manosroi, A.; Chutoprapat, R.; Abe, M.; Manosroi, J. Characteristics of niosomes prepared by supercritical carbon dioxide (scCO2) fluid. *Int J Pharm* 2008, 352, 248-255.

[22] Laouini, A.; Charcosset, C.; Fessi, H.; Holdich, R. G.; Vladisavljević, G. T. Preparation of liposomes: a novel application of microengineered membranes - investigation of the process parameters and application to the encapsulation of vitamin E. *RSC Adv* 2013, 3, 4985-4994.

[23] Heurtault, B.; Saulnier, P.; Pech, B.; Proust, J. E.; Benoit, J. P. Physico-chemical stability of colloidal lipid particles. *Biomaterials* 2003, 24, 4283-4300.

[24] Mora-Huertas, C. E.; Fessi, H.; Elaissari, A. Polymer-based nanocapsules for drug delivery. *Int J Pharm* 2010, 385, 113-142.

[25] Barratt, G. Colloidal drug carriers: achievements and perspectives. *Cell Mol Life Sci* 2003, 60, 21-37.

[26] Afri, M.; Ehrenberg, B.; Talmon, Y.; Schmidt, J.; Cohen, Y.; Frimer, A. A. Active oxygen chemistry within the liposomal bilayer, part III: locating vitamin E, ubiquinol and ubiquinone and their derivatives in the lipid bilayer. *Chem Phys Lipids* 2004, 131, 107-121.

[27] Kulkarni, S. B.; Vargha-Butler, E. I. Study of liposomal drug delivery systems 2. Encapsulation efficiencies of some steroids in MLV liposomes. *Colloids Surf B Biointerfaces* 1995, 81, 77-85.

[28] Budai, L.; Kaszás, N.; Gróf, P.; Lenti, K.; Maghami, K.; Antal, I.; Klebovich, I.; Petrikovics, I.; Budai, M. Liposomes for topical use: a physico-chemical comparison of vesicles prepared from egg or soy lecithin. *Sci Pharm* 2013, 81, 1151-1166.

[29] Otake, K.; Imura, T.; Sakai, H.; Abe, M. Development of a new preparation method of liposomes using supercritical carbon dioxide. *Langmuir* 2001, 17, 3898-3901.

[30] Imura, T.; Gotoh, T.; Otake, K.; Yoda, S.; Takebayashi, Y.; Yokoyama, S.; Takebayashi, H.; Sakai, H.; Yuasa, M.; Abe, M. Cortrol of physicochemical properties of liposomes using a supercritical reverse pahse evaporation method. *Langmuir* 2003, 19, 2021-2025.

[31] Heurtault, B. e.; Saulnier, P.; Pech, B.; Proust, J. E.; Benoit, J. P. Physico-chemical stability of colloidal lipid particles. *Biomaterials* 2003, 24, 4283-4300.

[32] Gregoriadis, G.; Silva, H. d.; Florence, A. T. A procedure for the efficient entrapment of drugs in dehydration-rehydration liposomes (DRVs). *Int J Pharm* 1990, 65, 235-242.

[33] Meure, L. A.; Foster, N. R.; Dehghani, F. Conventional and dense gas techniques for the production of liposomes: a Review. *AAPS PharmSciTech* 2008, 9, 798-809.